Basic module
Physics of Nanostructures

Summer term 2026

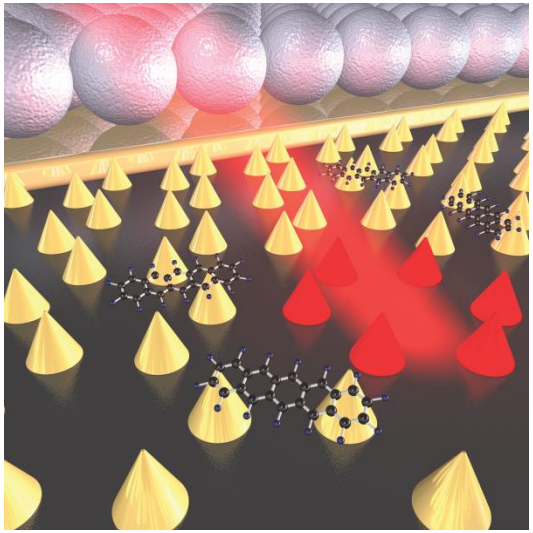

M. Fleischer, I. Zaluzhnyy,
Exercises: R. Löffler

How to see nanoobjects

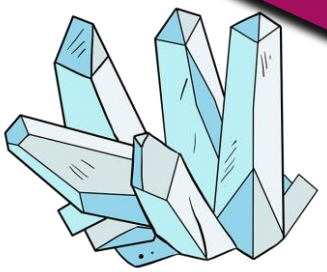

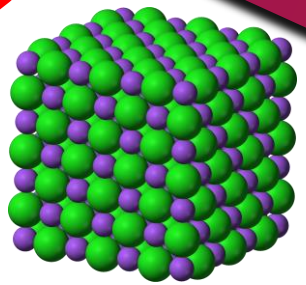

meters (m)

millimeters (10^{-3} m)

micrometers (10^{-6} m)

nanometers (10^{-9} m)

angstroms (10^{-10} m)

Optical resolution limit at

$$\sim\frac{\lambda}{2}\approx 0.2\ \mu\text{m}$$

Visible light:

wavelength: $\lambda = 380 - 850$ nm

energy: $E = 1.65 - 3.25$ eV

Light microscopy

Rayleigh criterion equation (resolution): $\Delta = k_1 \cdot \frac{\lambda}{NA} \sim \frac{\lambda}{n \cdot \sin\theta}$

Due to diffraction effects (Airy disc), the minimal distance between to objects is $\lambda/2$, so that the objects can be still resolved.

(a)

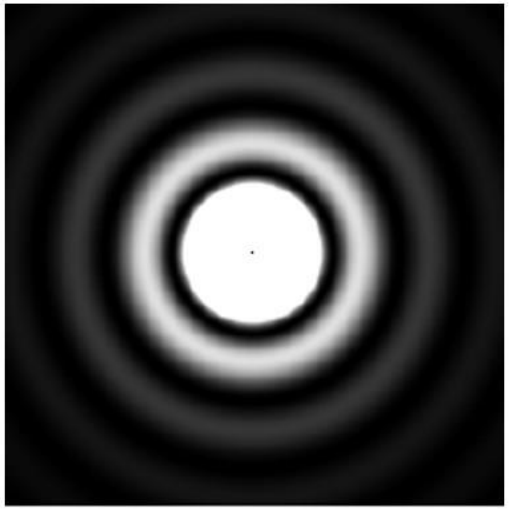

(b)

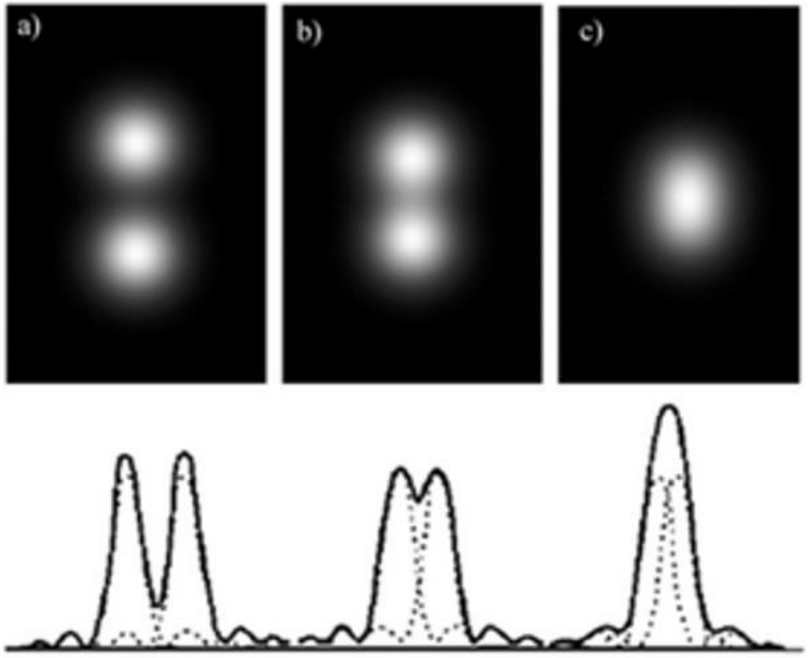

Dark field and phase contrast microscopy

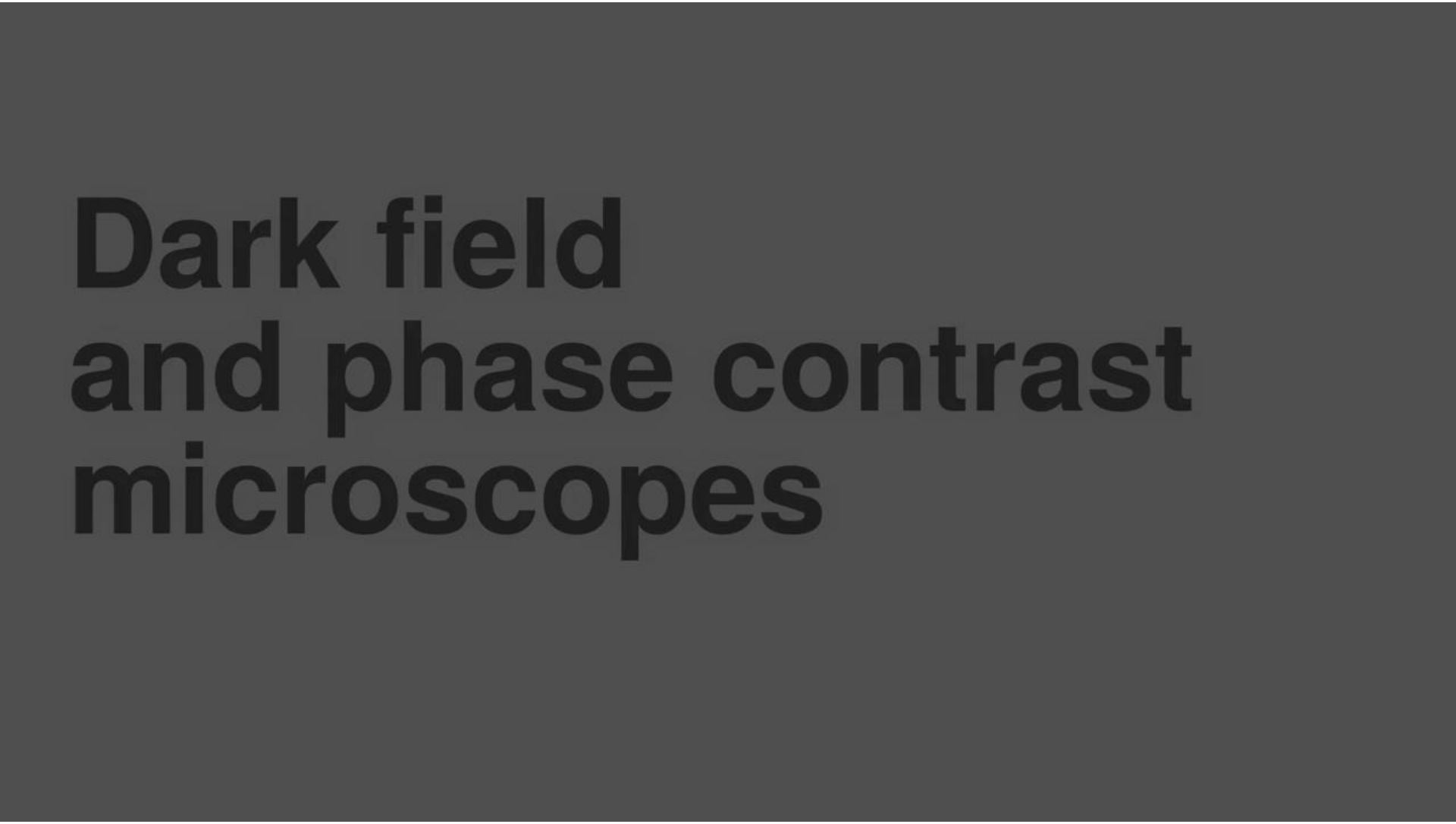

Comparison of some microscopy techniques

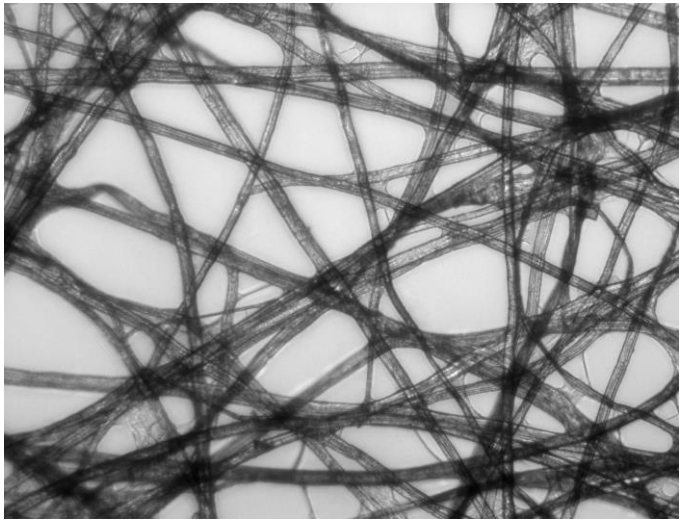

Bright-field illumination,
sample contrast comes from attenuation

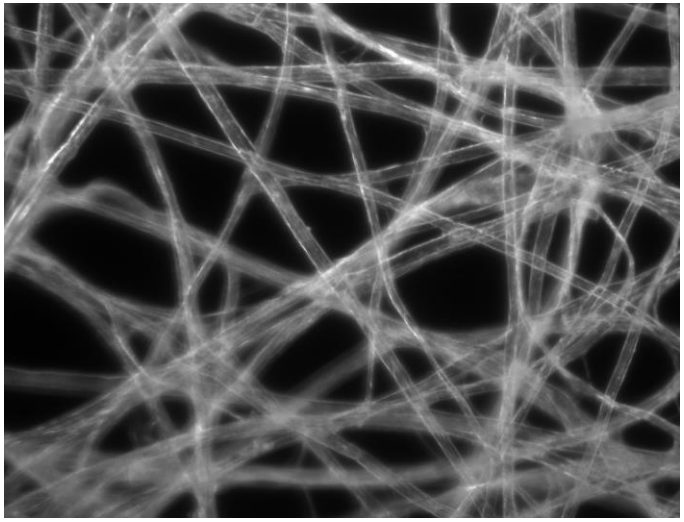

Dark-field illumination, sample contrast comes from scattering

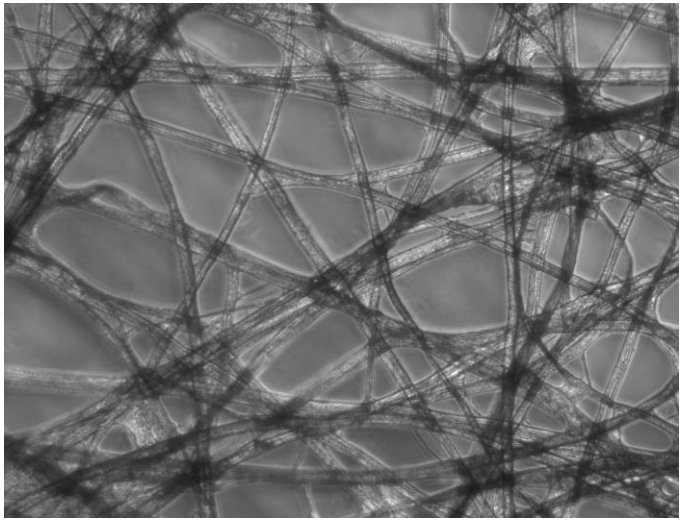

Phase-contrast illumination, sample contrast comes from interference

Fluorescent and confocal microscopy

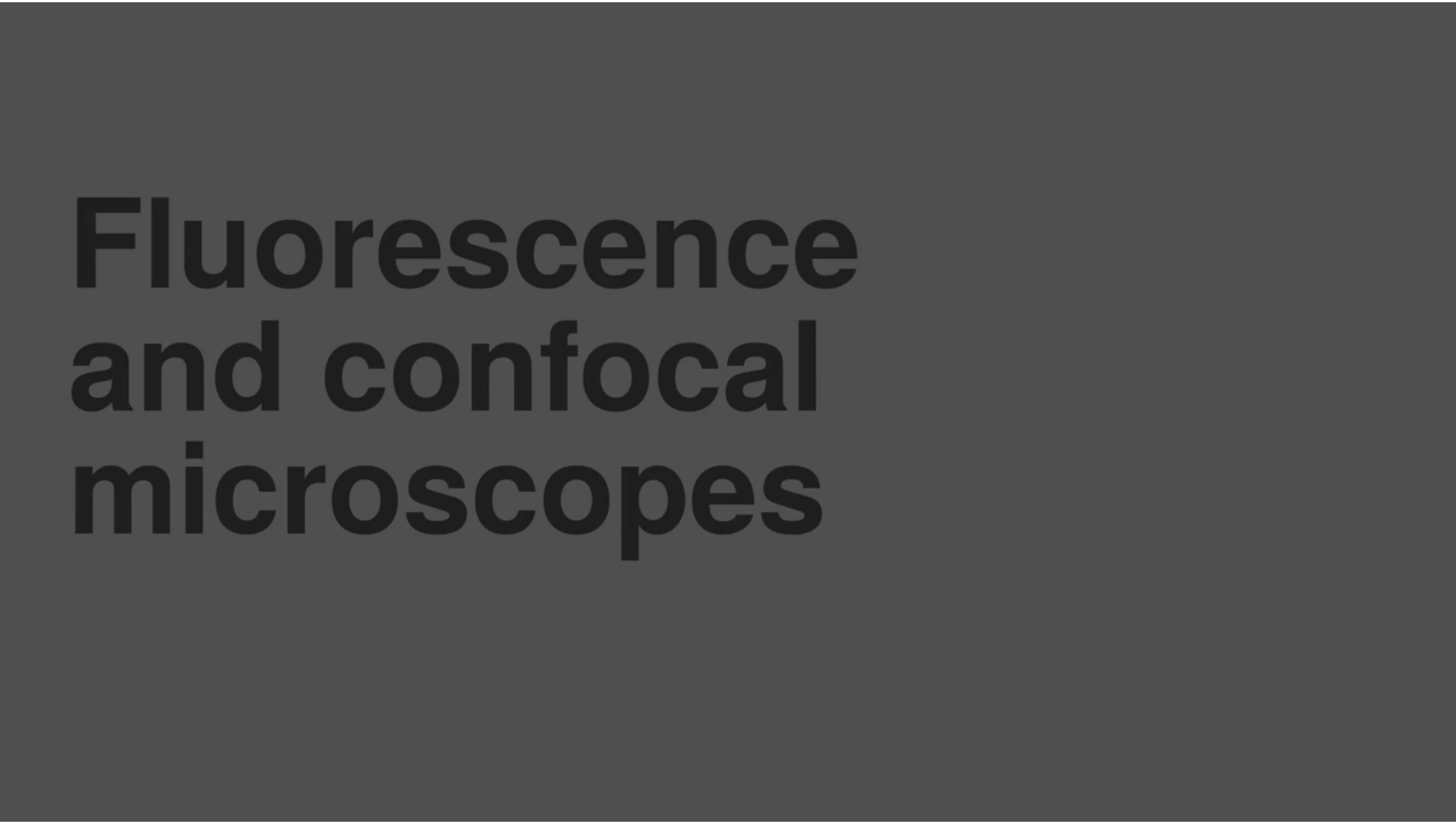

Confocal microscopy

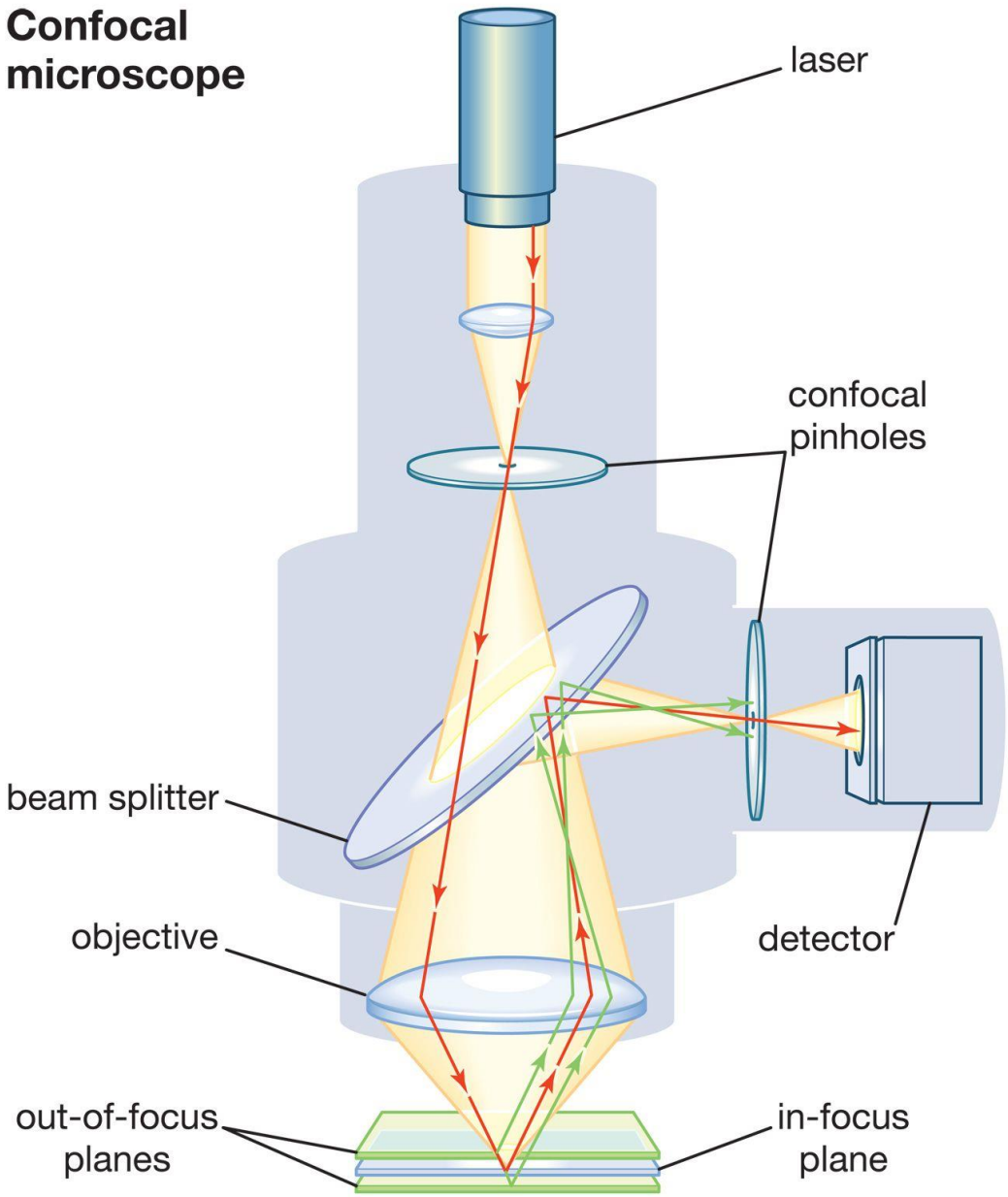

Standard fluorescence microscopy

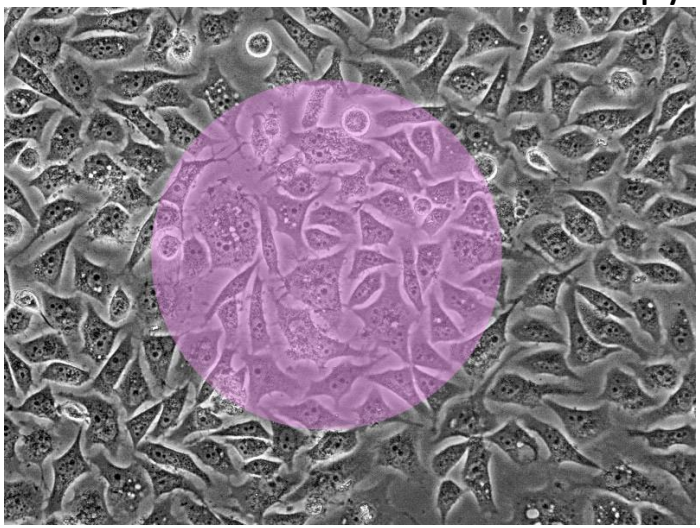

Confocal microscopy

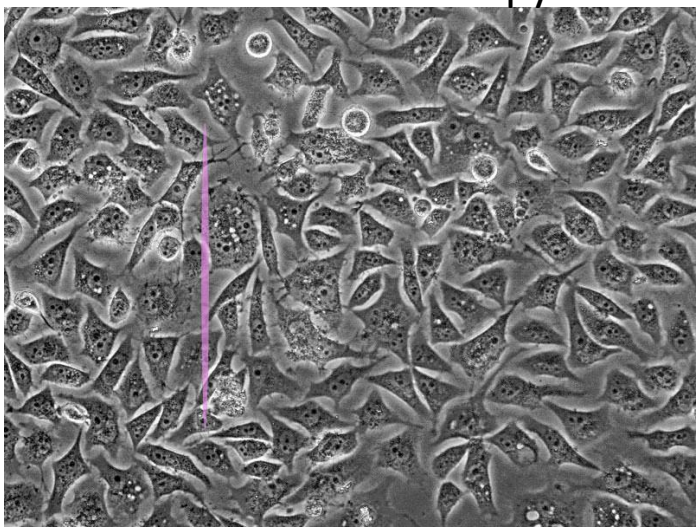

Stimulated emission depletion microscopy

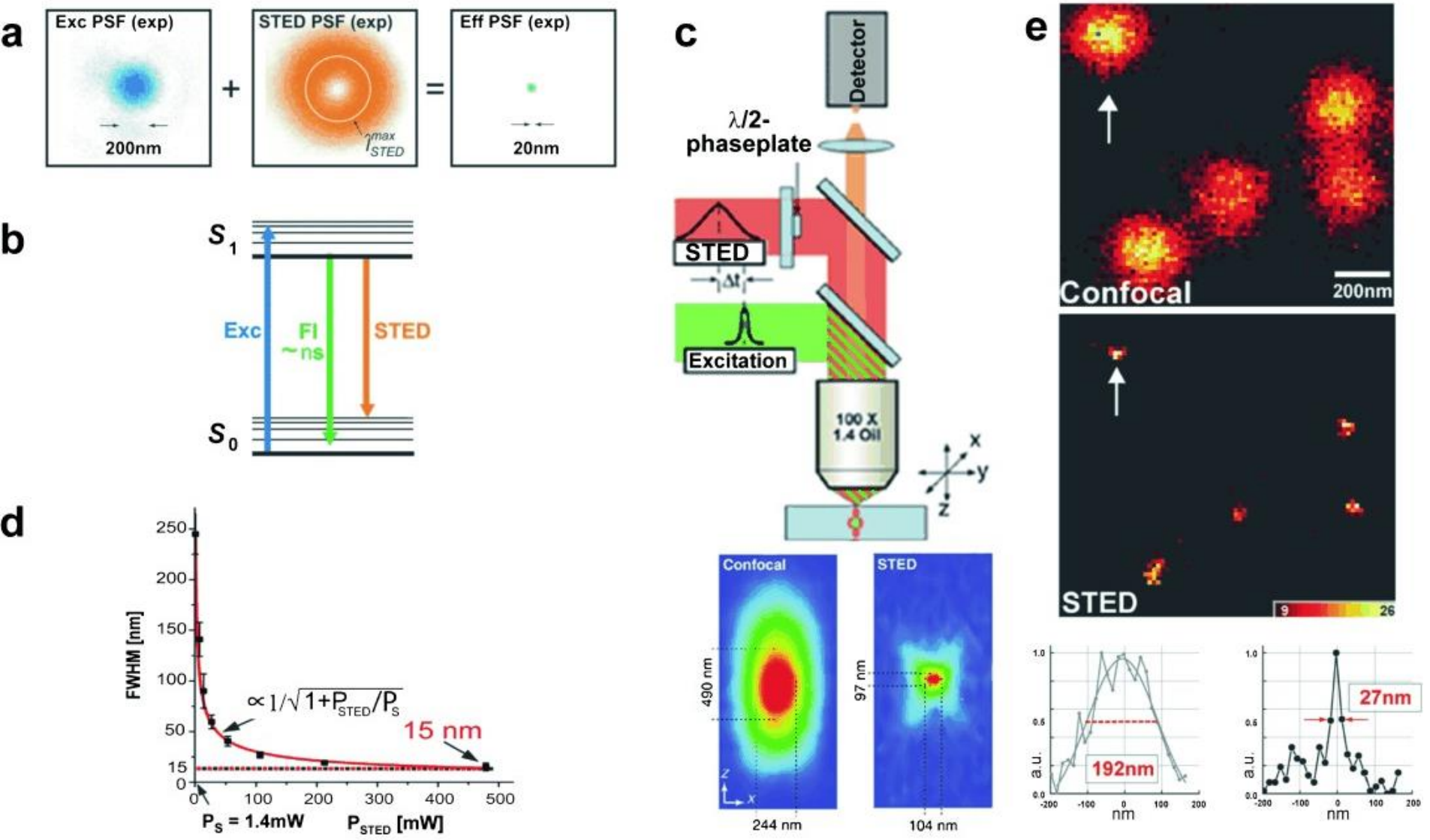

Möckl et al., Angew. Chem. Int. Ed. 53, 13972 (2014)

Confocal and STED microscopy

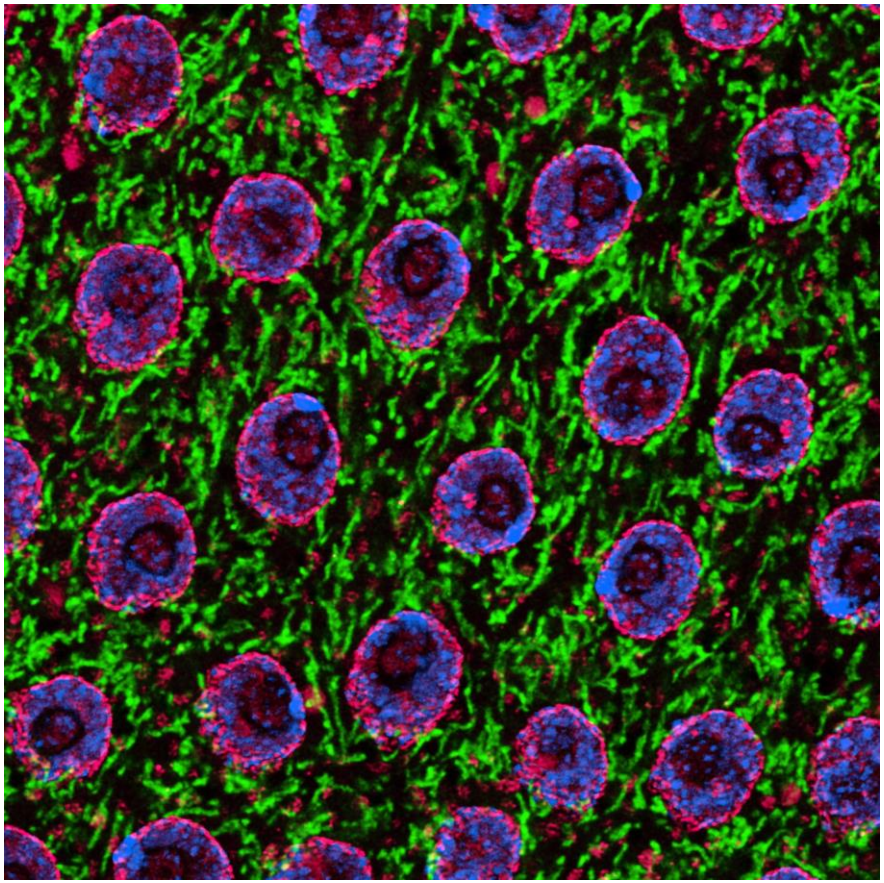

drosophila follicle cells imaged with a marker for mitochondria

about.illinoisstate.edu/confocal/gallery/

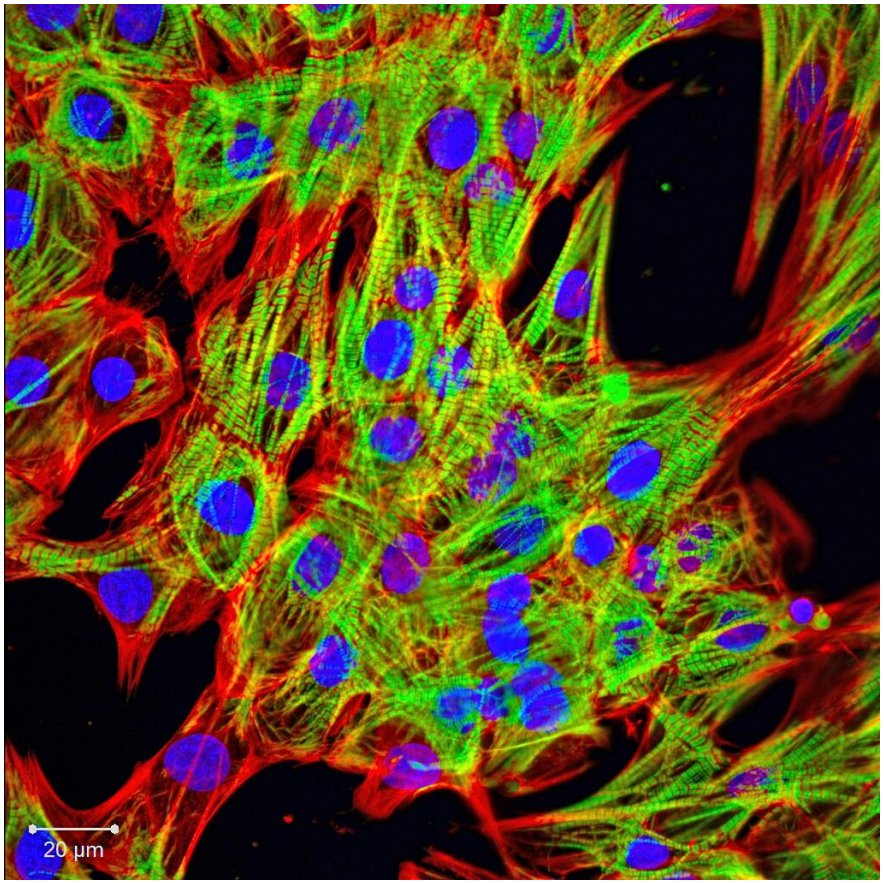

cultured heart muscle cells

christianz.artstation.com/projects

Confocal and STED microscopy

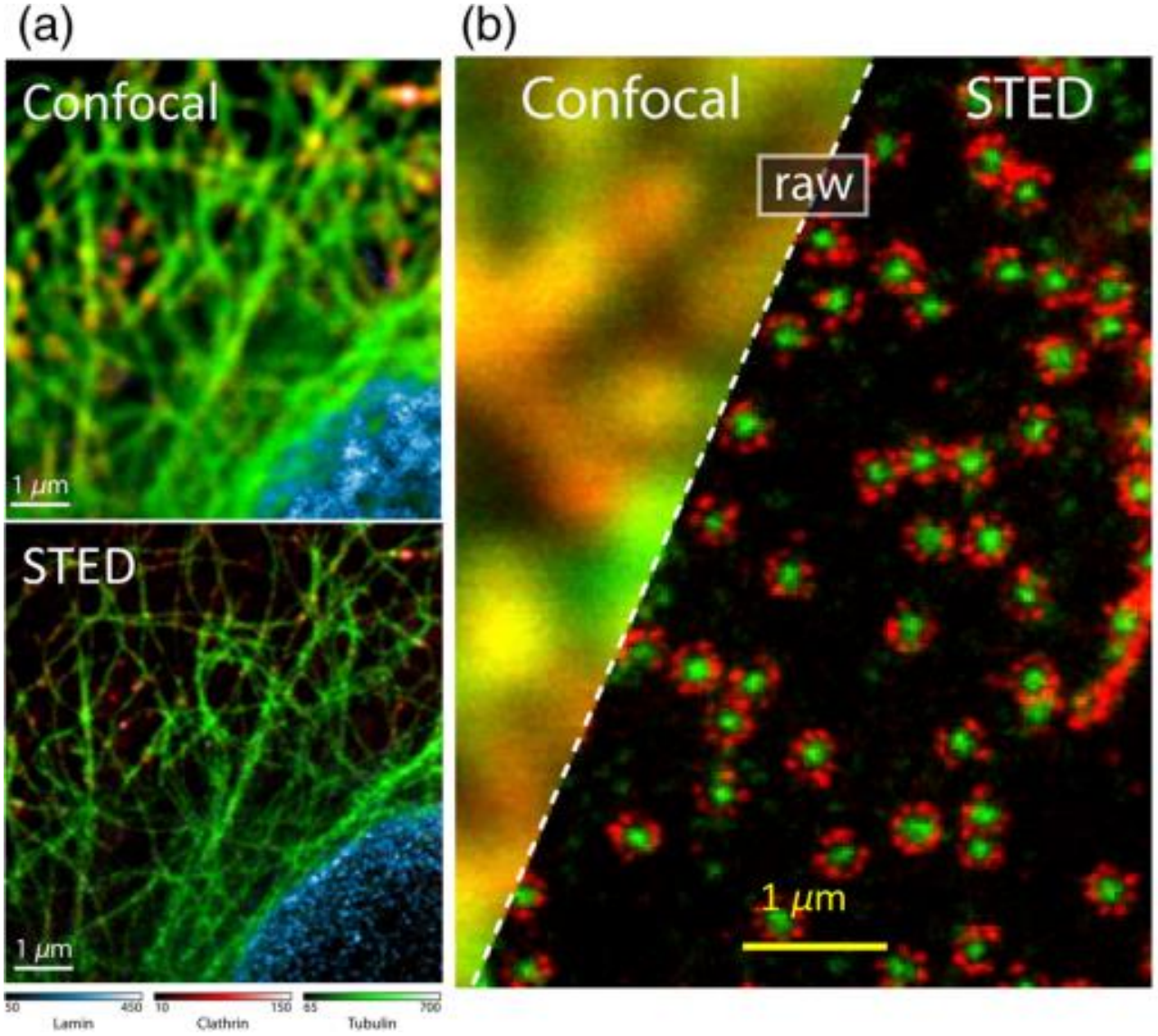

(a) STED microscopy to localize the distribution of lamin, tubulin, and clathrin in fixed PtK2 cells.

(b) Dual channel STED microscopy reveals octametic arrangement of peripheral transmembrane GP210 protein around core protein in a nuclear pore complex in immunolabeled Xenopus cells.

Neupane et al., J. Biomed. Opt., **19** 080901 (2014)

Light aberration

spherical aberration

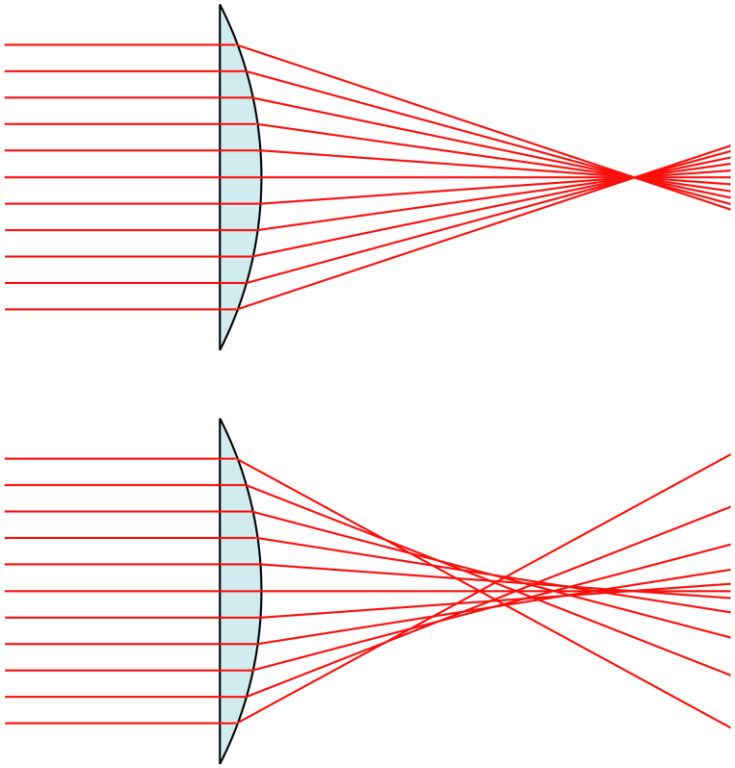

chromatic aberration

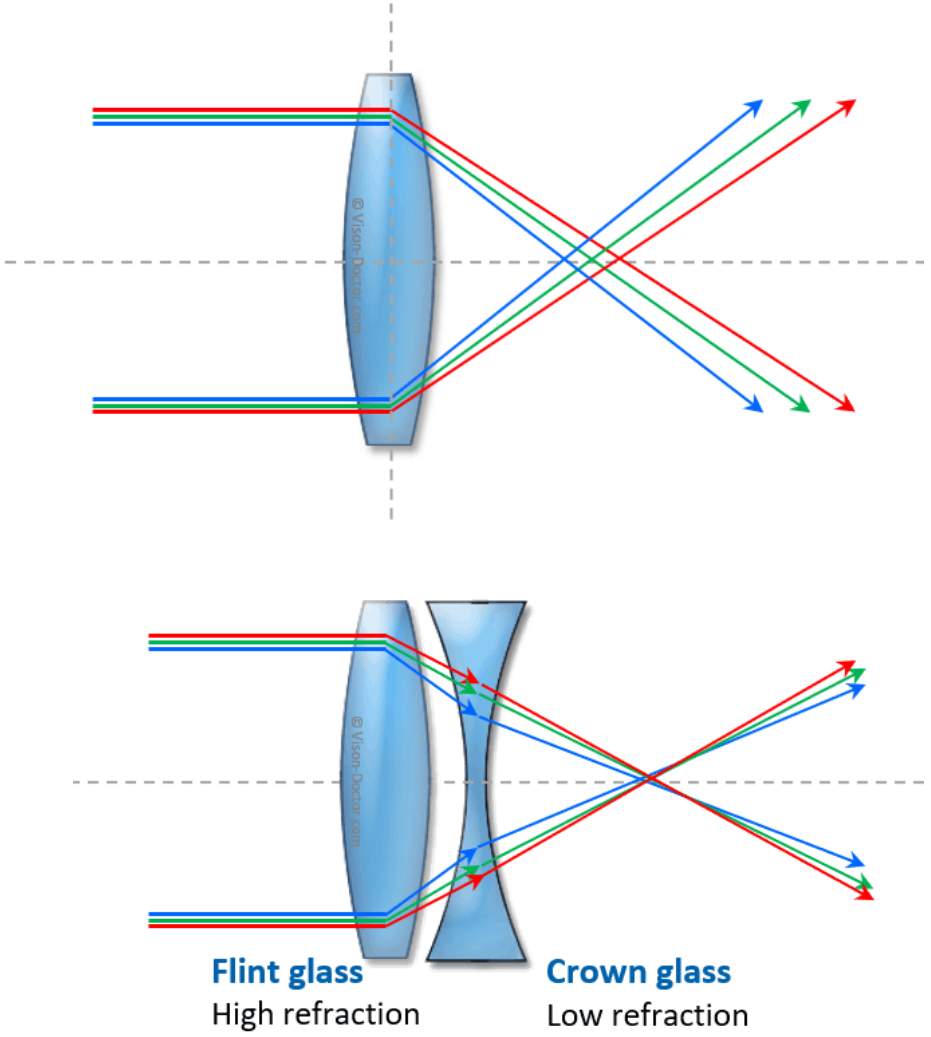

Magnetic lenses for electrons

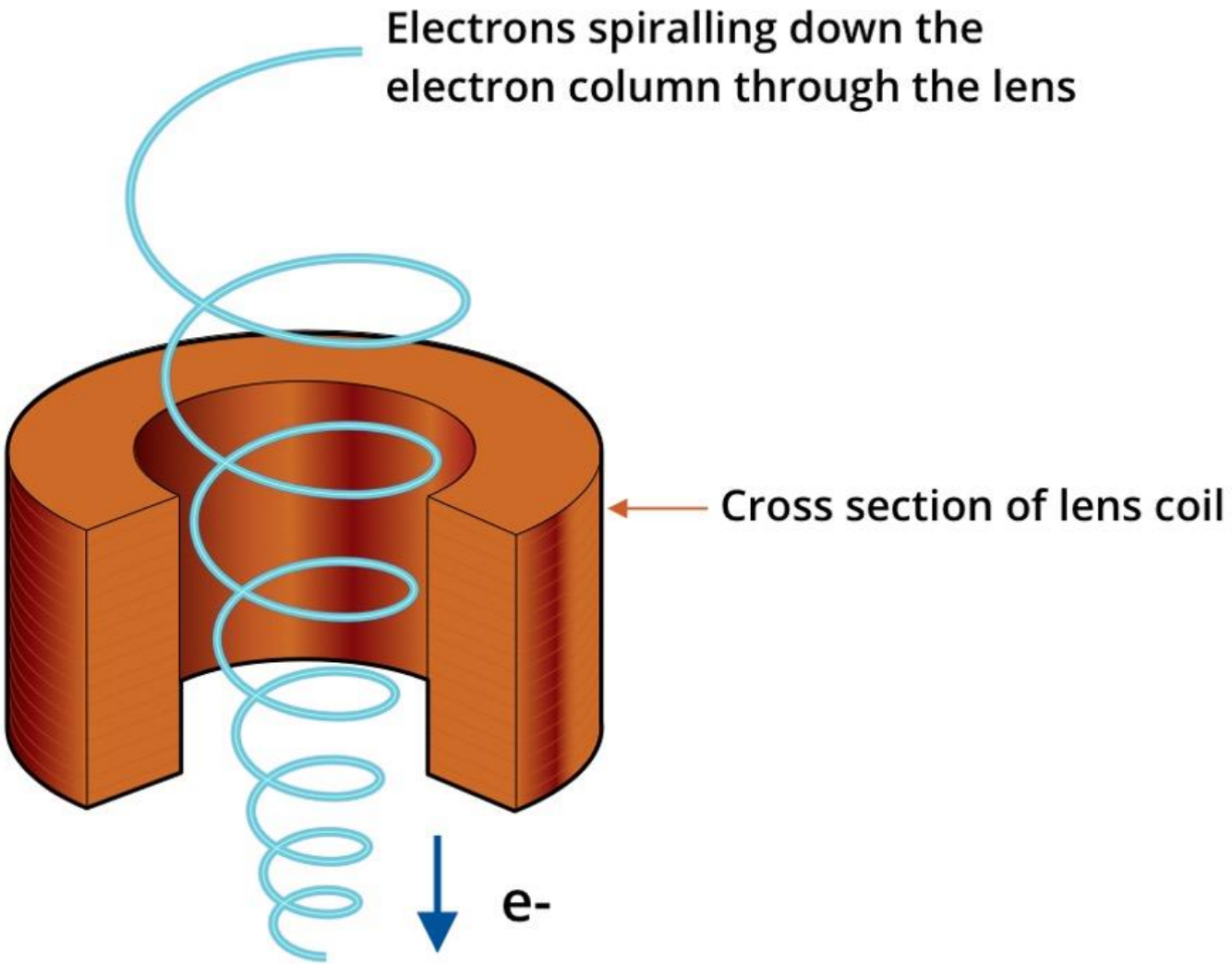

Magnetic lenses for electrons

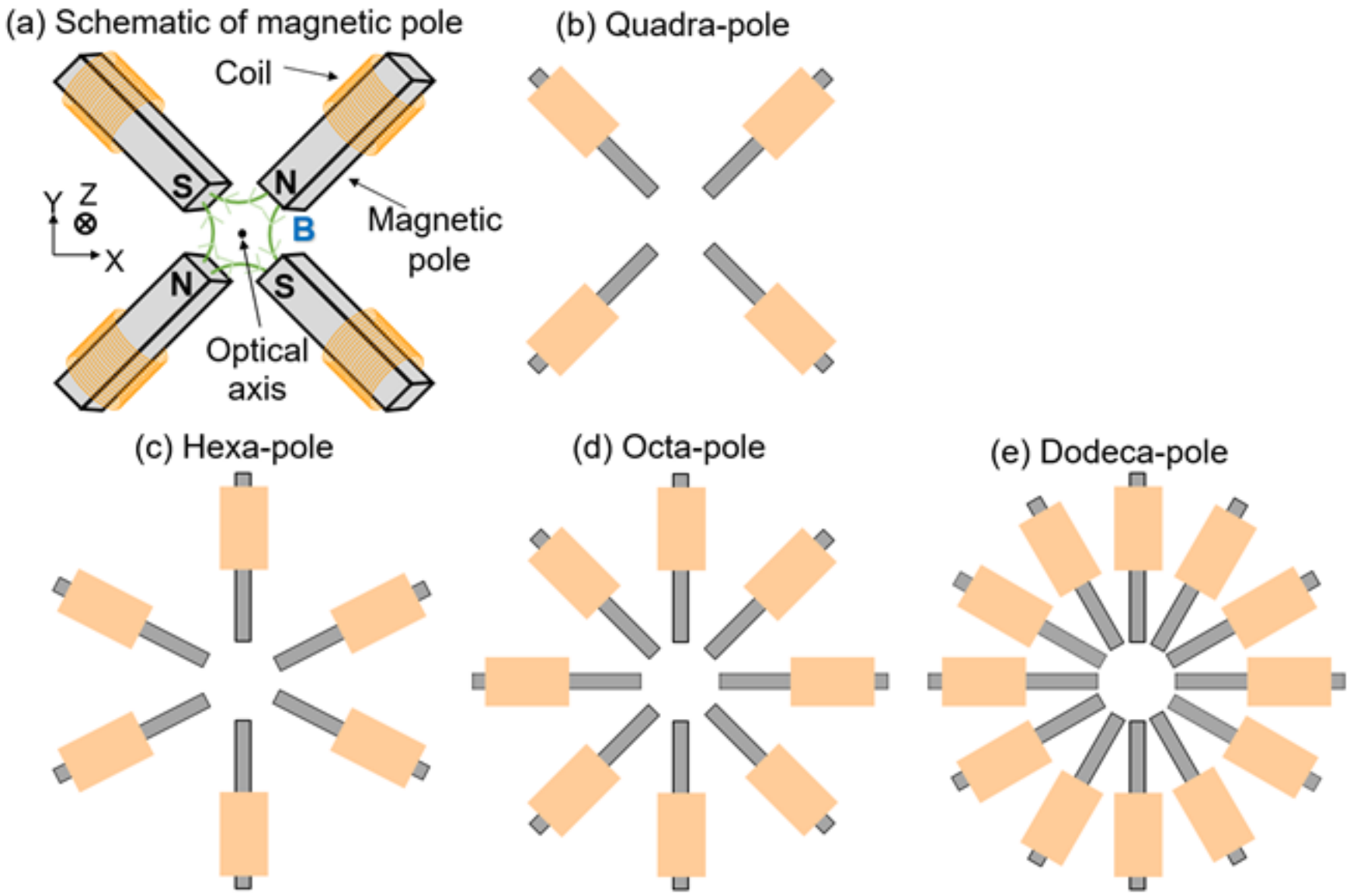

Electron microscope

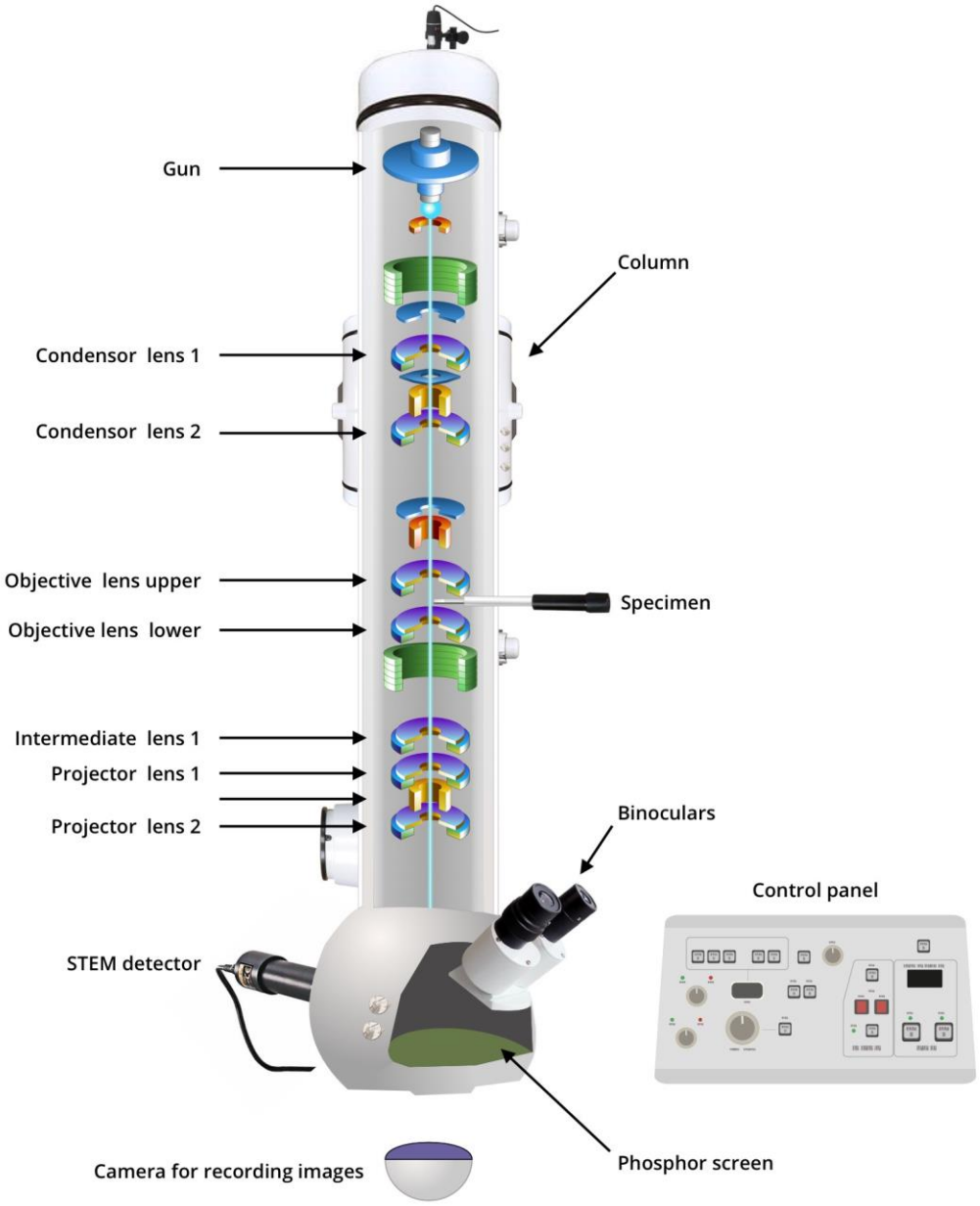

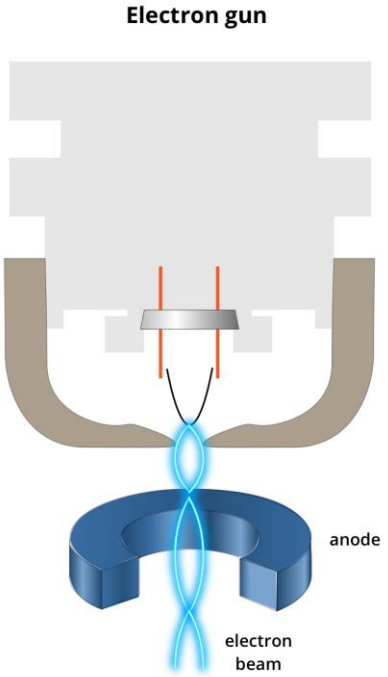

Electron microscope

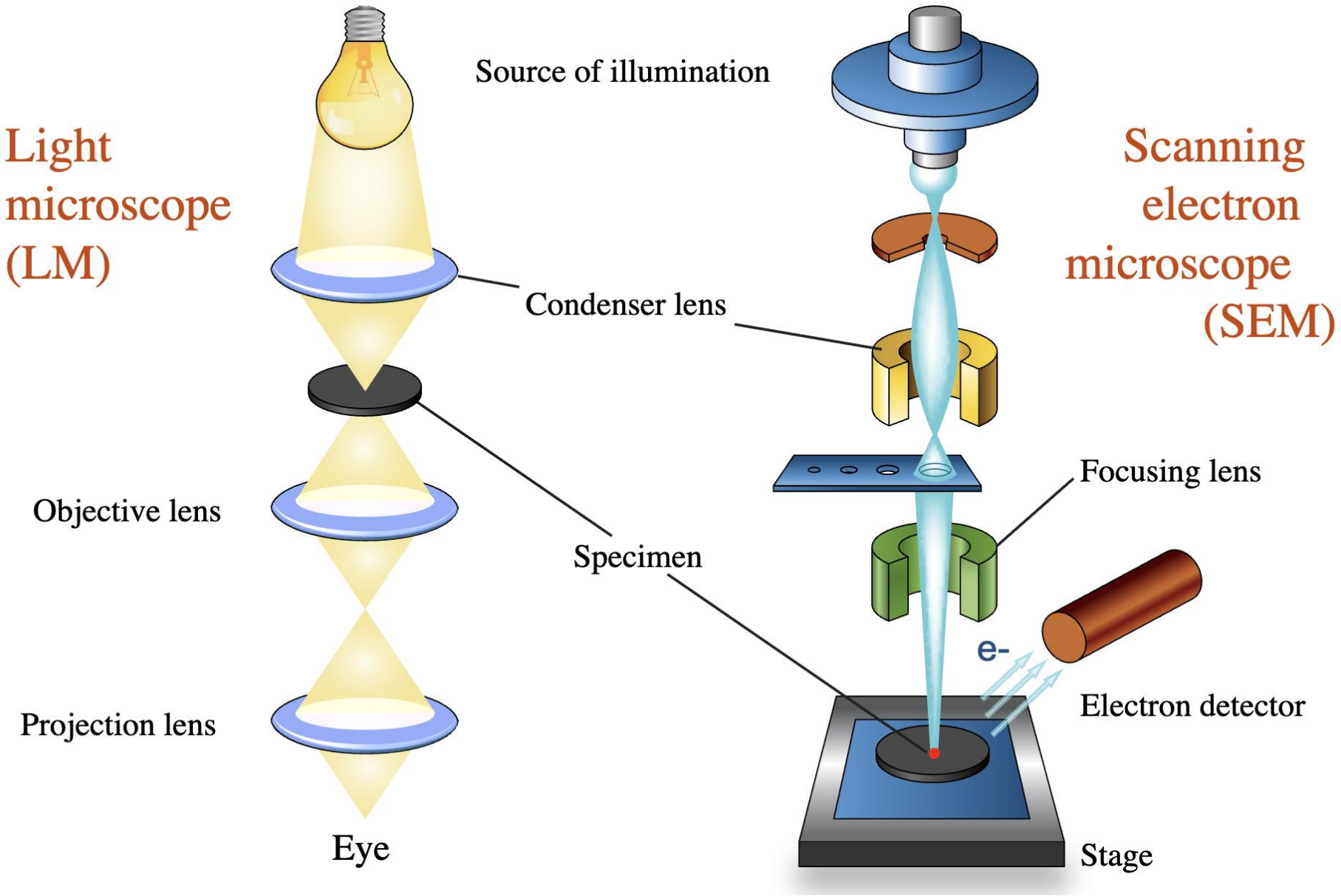

Electron interactions with the specimen

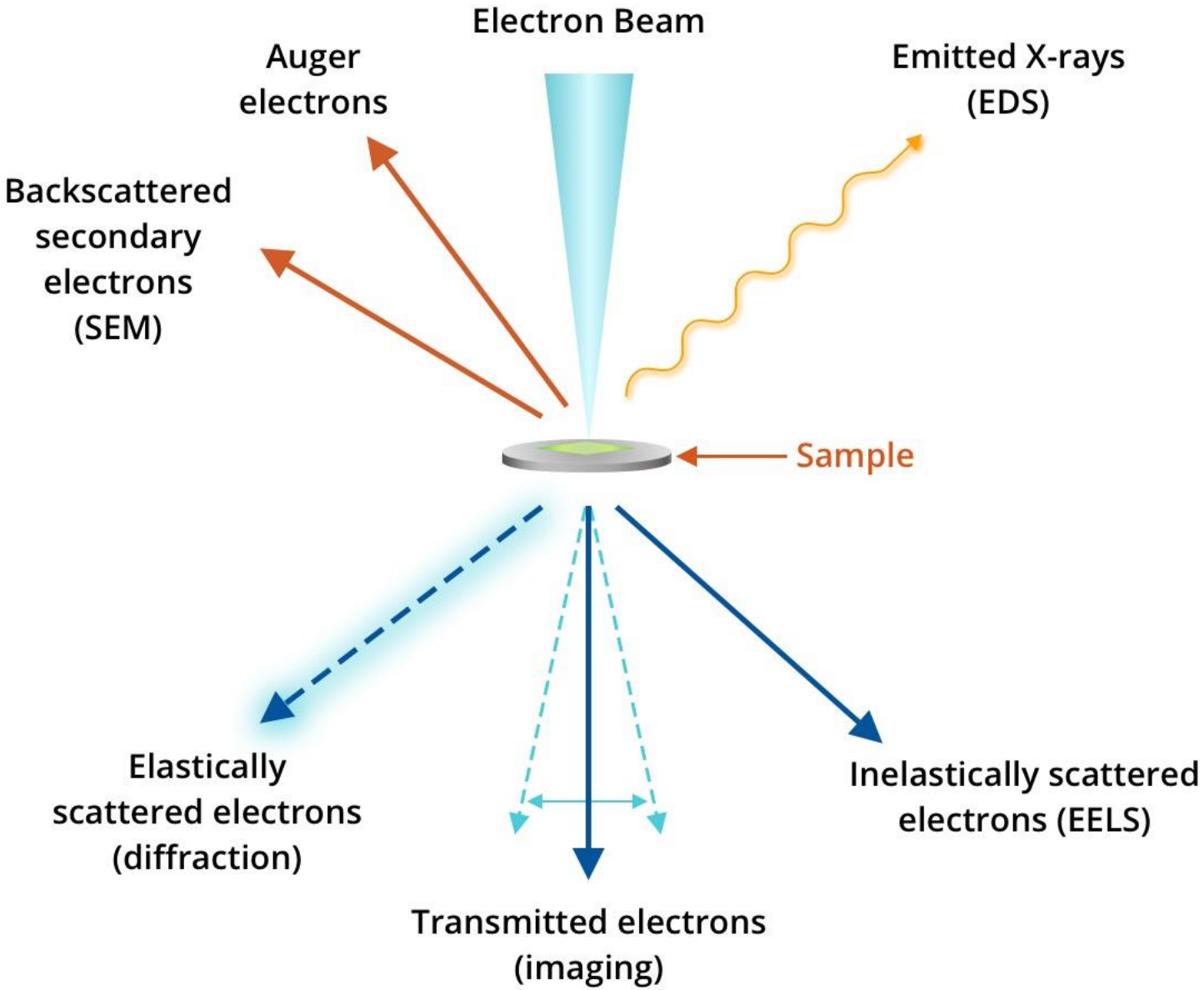

Scanning electron microscopy (SEM)

Electrons (E=5-15 keV) are focused to a spot of 1-2 nm. The beam scans the sample's surface and the scattered electrons are recorded by a detector.

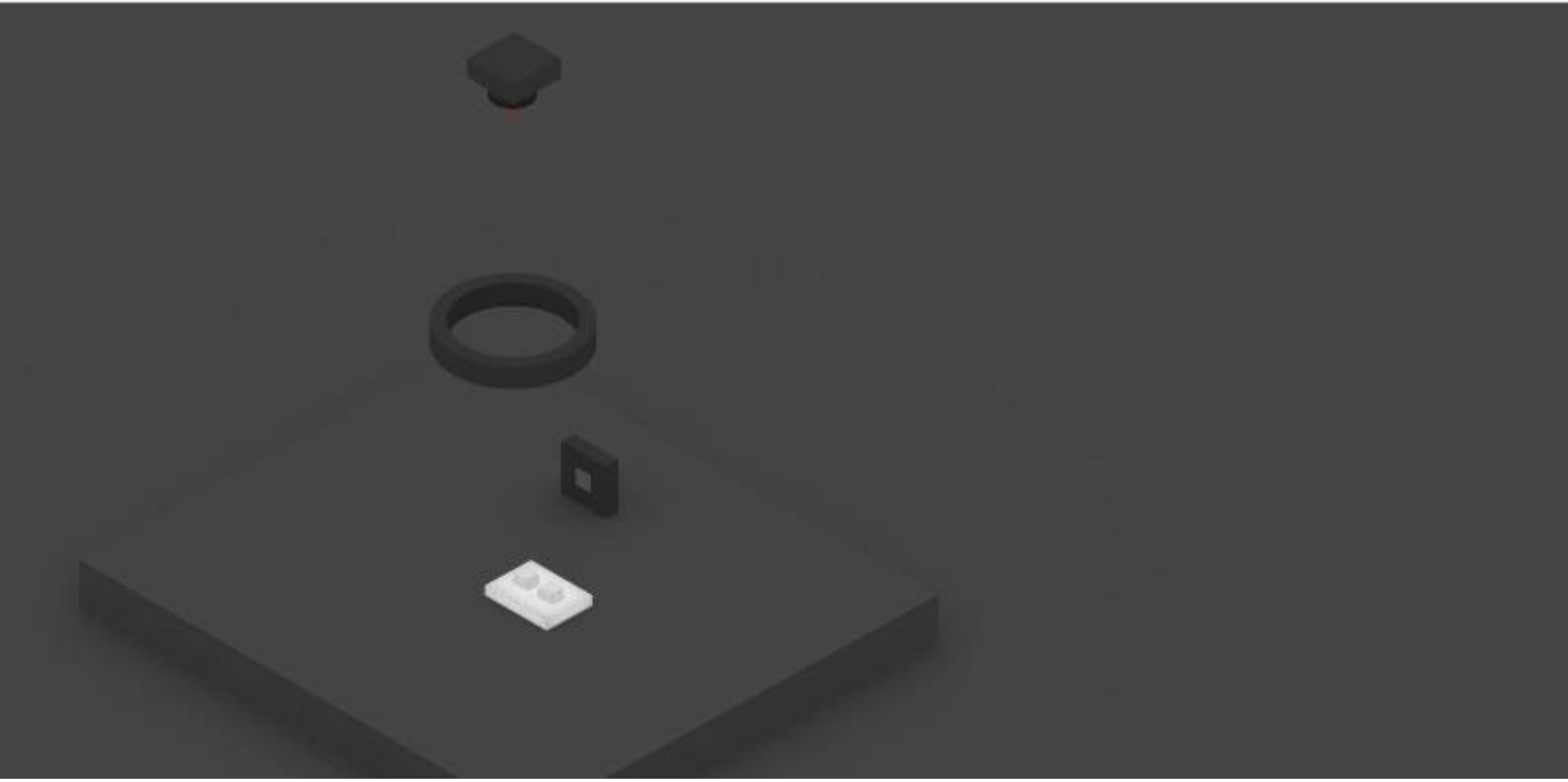

Transmission electron microscopy (TEM)

Diffraction mode

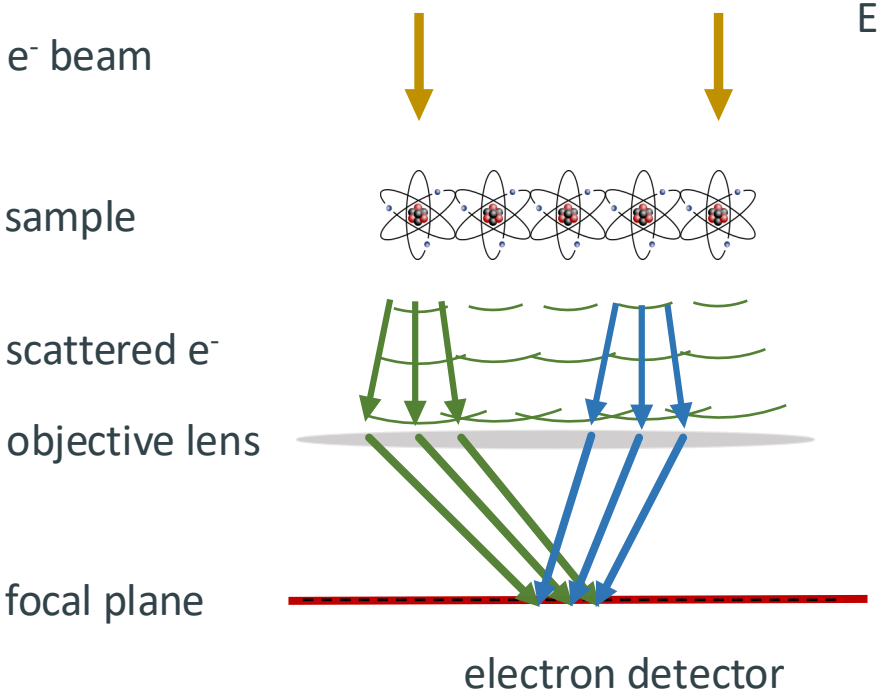

Electron diffraction from K_2PtCl_4 nanoparticle

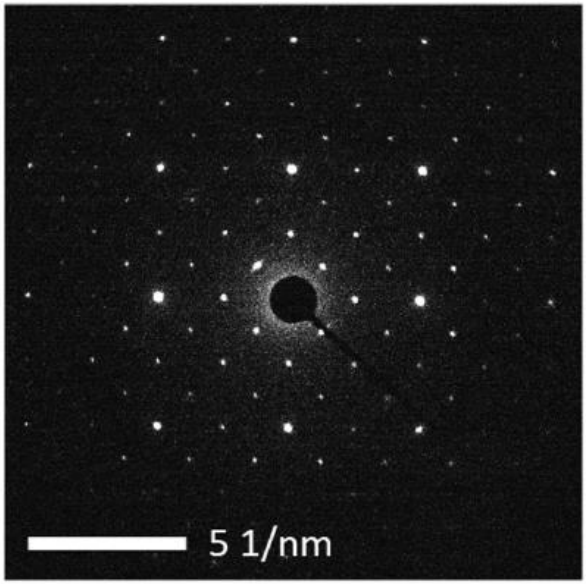

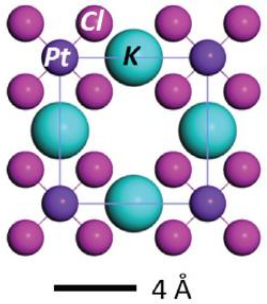

Gao et al., Sci. Adv. 2019; **5** : eaau9590

Transmission electron microscopy (TEM)

Imaging mode

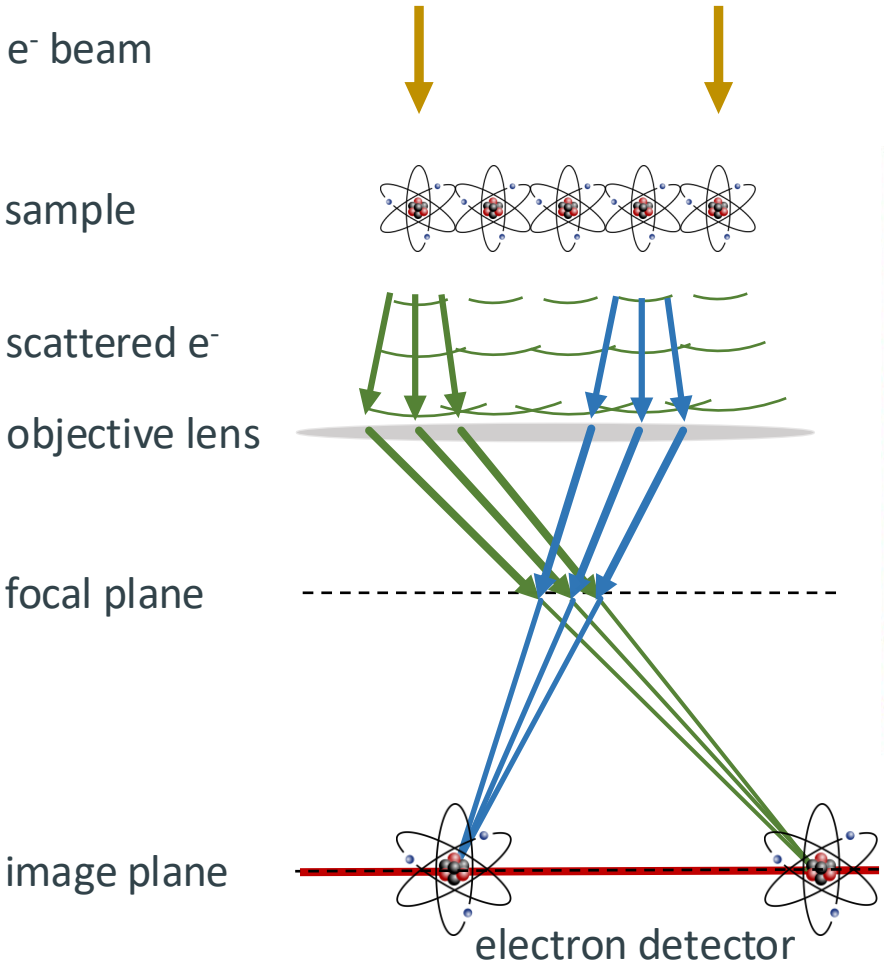

Real-space image of K_2PtCl_4 crystal lattice with an overlaid atomic model

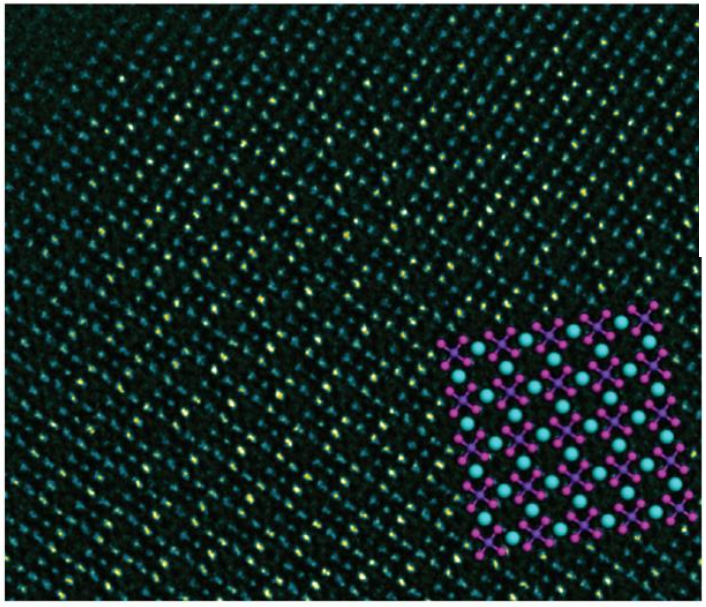

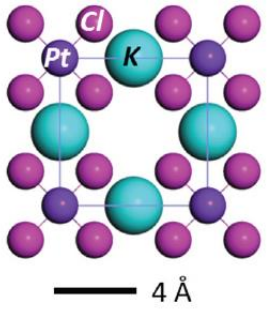

Gao et al., Sci. Adv. 2019; **5** : eaau9590

Electron inelastic mean free path (IMFP)

$$I(d) = I_0 \exp\left(-\frac{d}{\lambda(E)}\right)$$

Decay of the electron intensity in the media due to inelastic scattering

$$\lambda[monolayers] = \frac{538}{E^2[eV^2]} + 0.41\sqrt{a[nm]E[eV]}$$

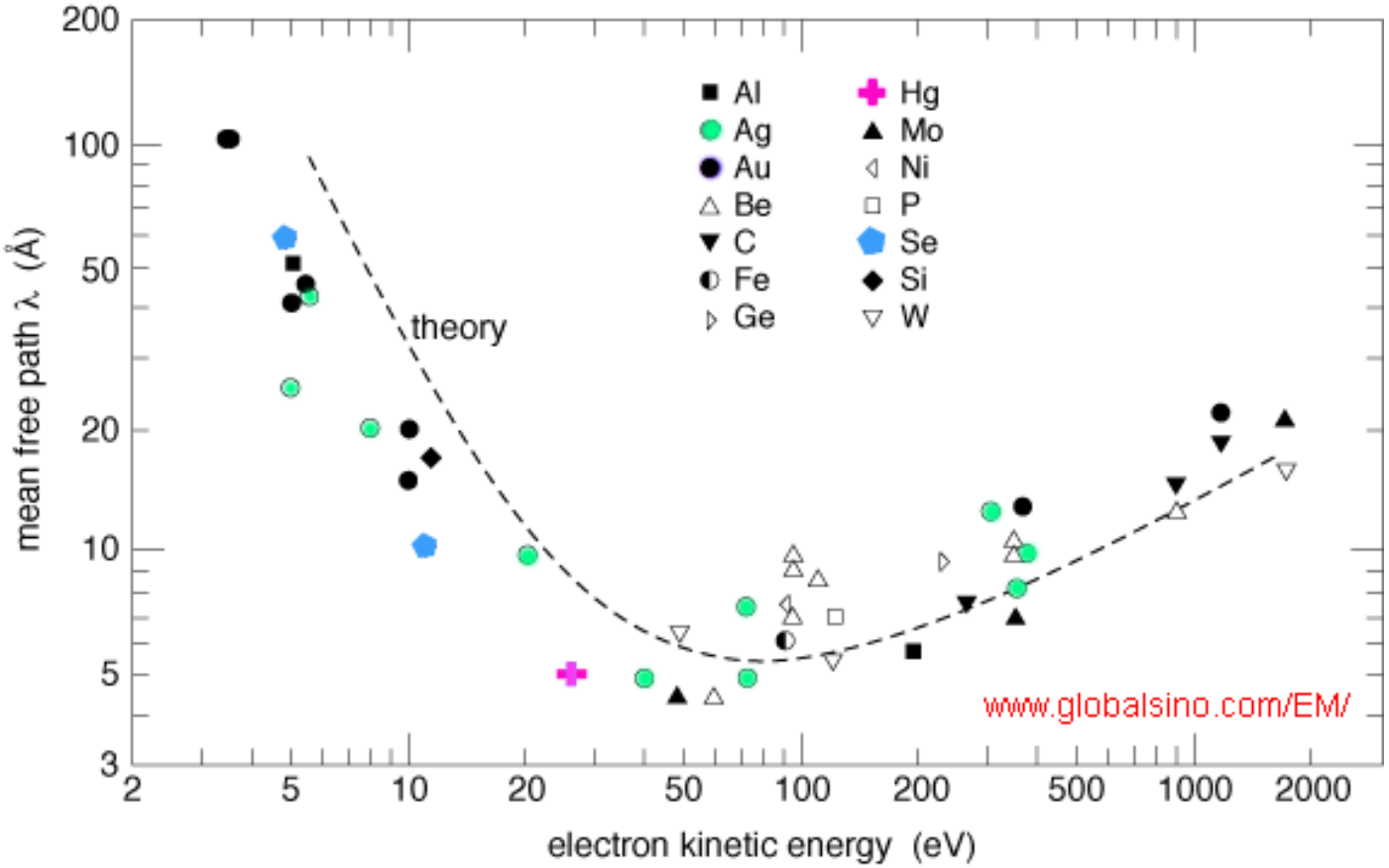

M. Seah and W. Dench, Surf. Interface Anal., **1** 2-11 (1979)

Scanning tunneling microscopy (STM)

Measures quantum tunneling current between the atom and the tip.

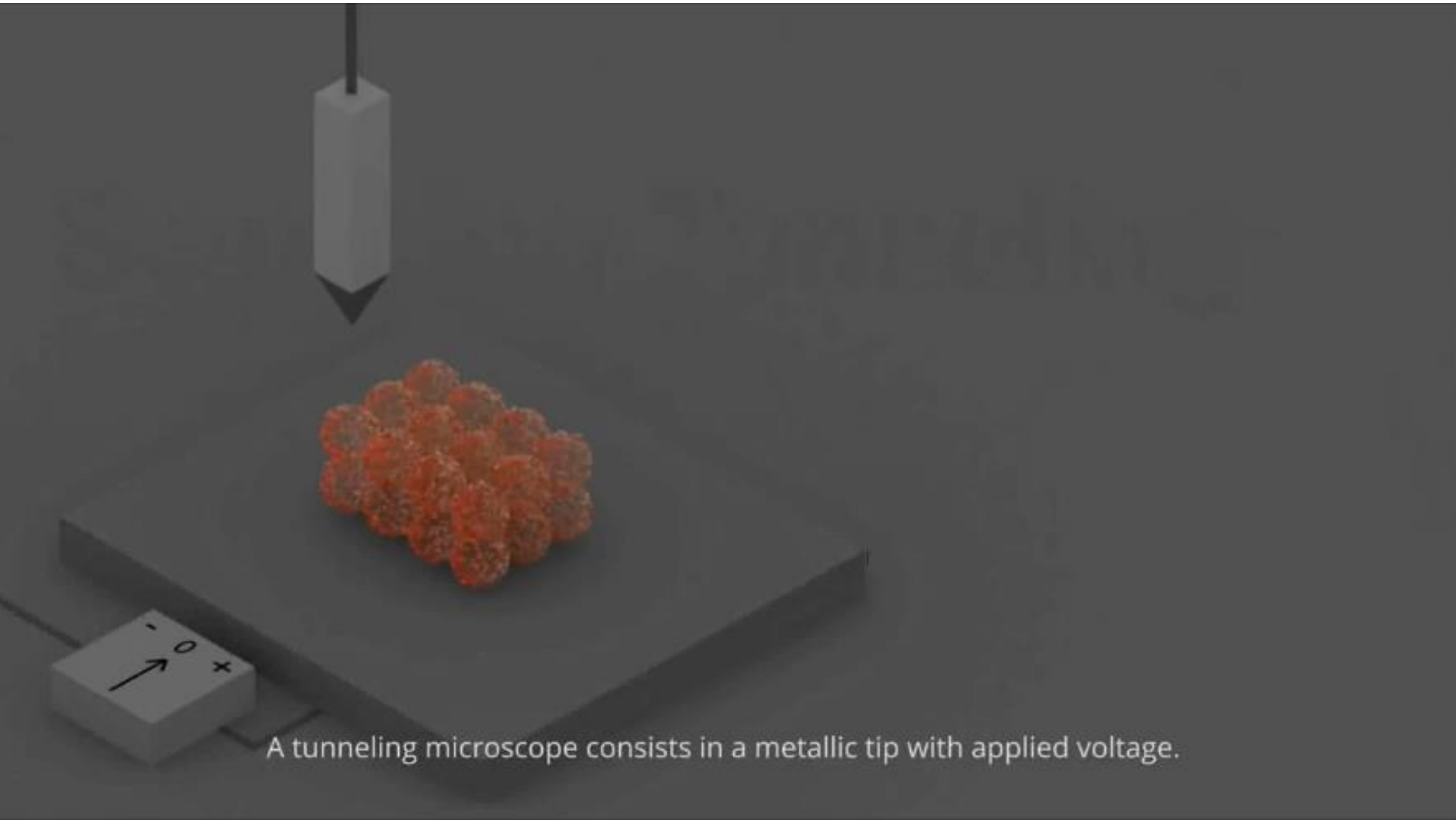

quantummadesimple.com

Atomic Force Microscopy (AFM)

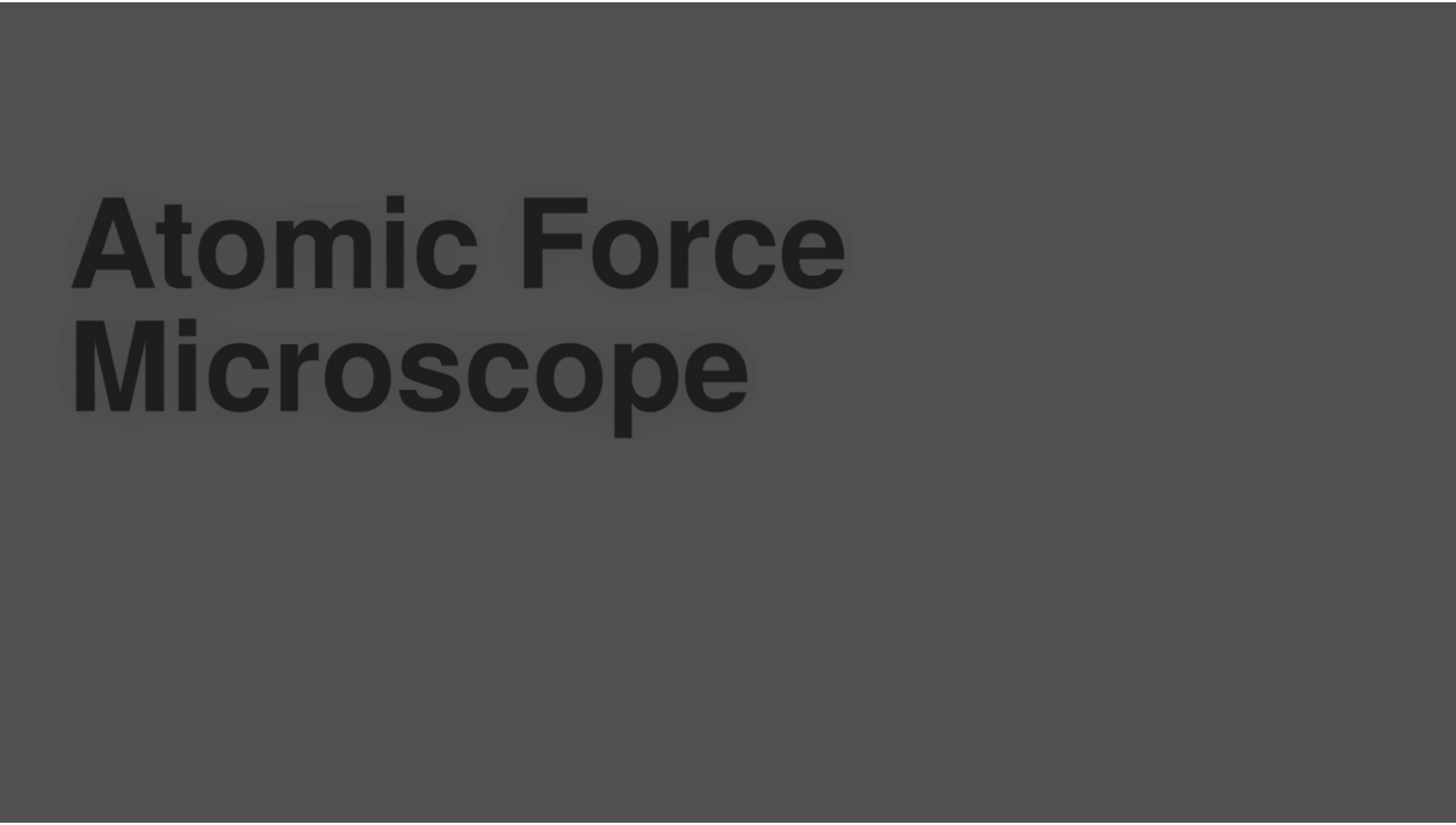

Incomplete list of microscopy techniques

Large field of view

Visible light microscopy
Transmission electron microscopy (TEM) in imaging mode

Small field of view

Confocal microscopy
Stimulated emission depletion (STED) microscopy
Scanning electron microscopy (SEM)
Scanning tunneling microscopy (STM)
Atomic force microscopy (AFM)
Magnetic force microscopy (MFM)
Electrostatic force microscopy (EFM)
Scanning near-field optical microscopy (SNOM)

Scanning probe microscopy (SPM)

Diffraction + microscopy
(imaging in reciprocal space + scanning)

Scanning Transmission Electron Microscopy (STEM)
Scanning Transmission X-ray Microscopy (STXM)

How to see nanoobjects

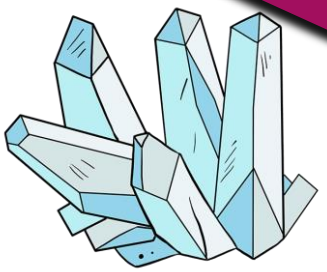

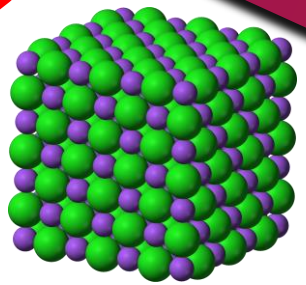

meters (m)

millimeters (10^{-3} m)

micrometers (10^{-6} m)

nanometers (10^{-9} m)

angstroms (10^{-10} m)

Optical resolution limit at

$$\sim\frac{\lambda}{2}\approx 0.2\ \mu\text{m}$$

Visible light:

wavelength: $\lambda = 380 - 850$ nm

energy: $E = 1.65 - 3.25$ eV

Concept of scattering techniques

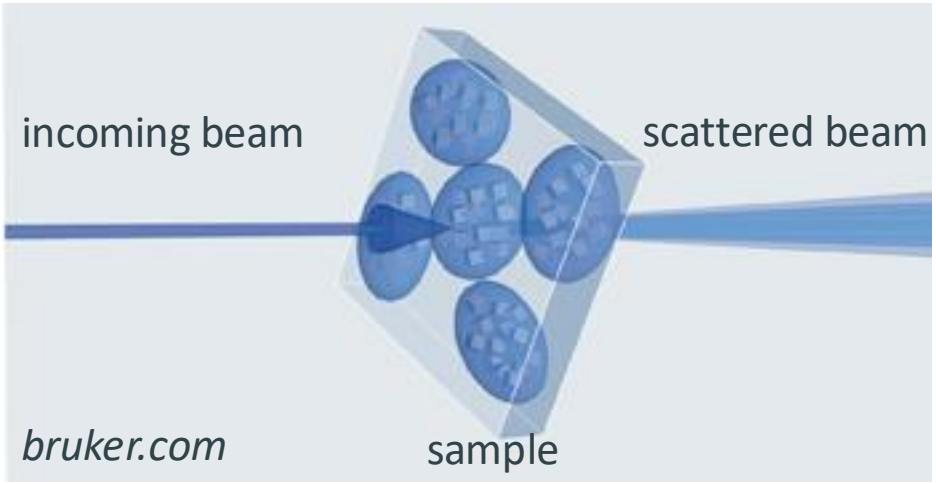

Advantages:

- non-invasive
- statistically significant
- detailed structural information on nanoscale
- applicable *in situ* and in real time
- direct analysis possible (predominantly for single-scattering scenarios)

Examples of structural “inhomogeneities” that can be studied by scattering:

- atomic lattices
- structural domains, nanoparticles, agglomerates, superlattices, etc.
- interfaces and surfaces

Scattering of X-rays, Electrons and Neutrons

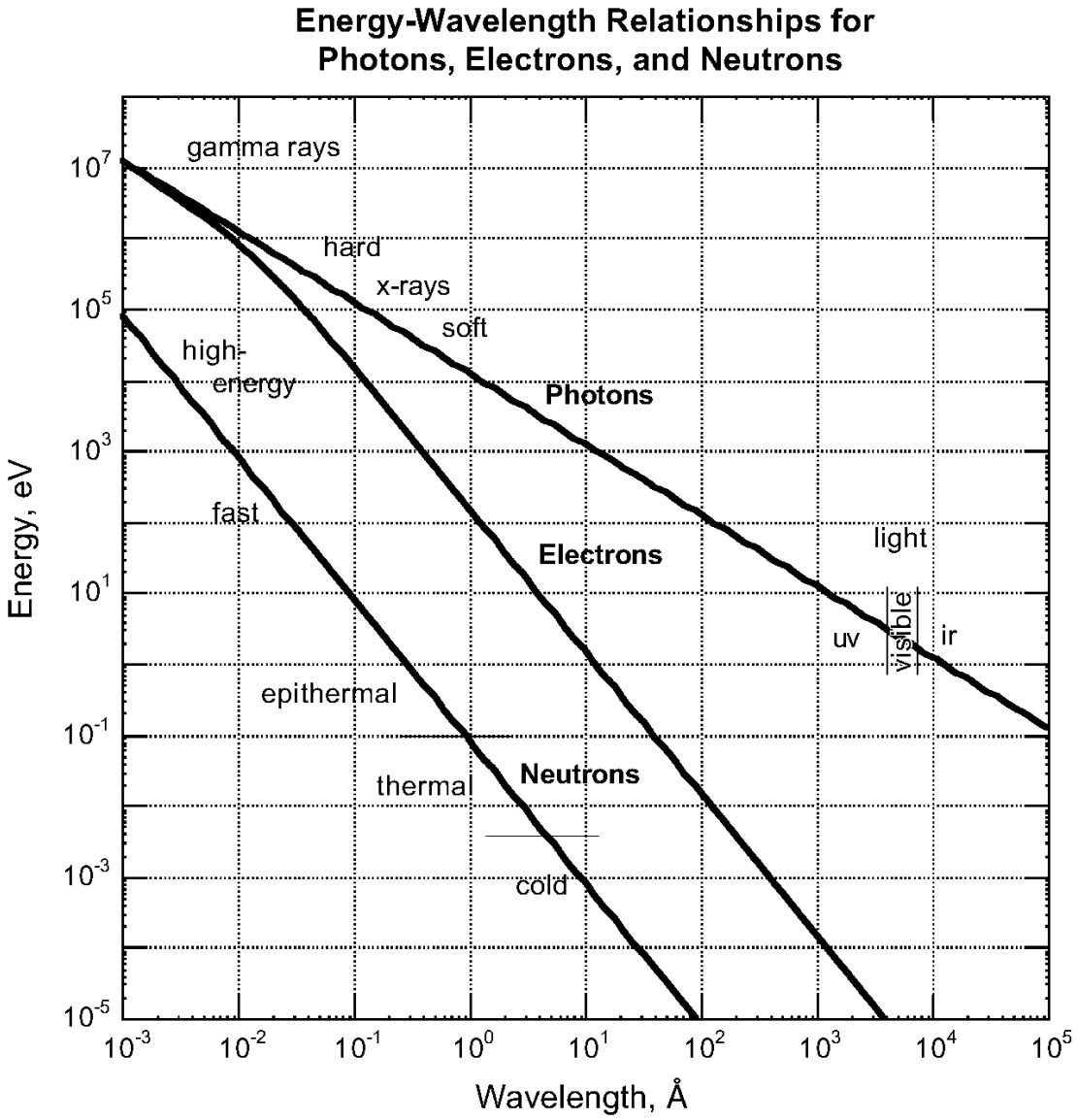

Photons (X-rays):

$$E = \frac{2\pi\hbar c}{\lambda} \qquad E[eV] = \frac{12398}{\lambda[\text{Å}]}$$

Neutrons:

$$E = \frac{2\pi^2\hbar^2}{m_n\lambda^2} \qquad E[meV] = \frac{81.8204}{\lambda^2[\text{Å}^2]}$$

Electrons (non-relativistic):

$$E = \frac{2\pi^2\hbar^2}{m_e\lambda^2} \qquad E[eV] = \frac{150.442}{\lambda^2[\text{Å}^2]}$$

Carpenter & Loong, Elements of slow-neutron scattering (2015)

Scattering of X-rays and Neutrons

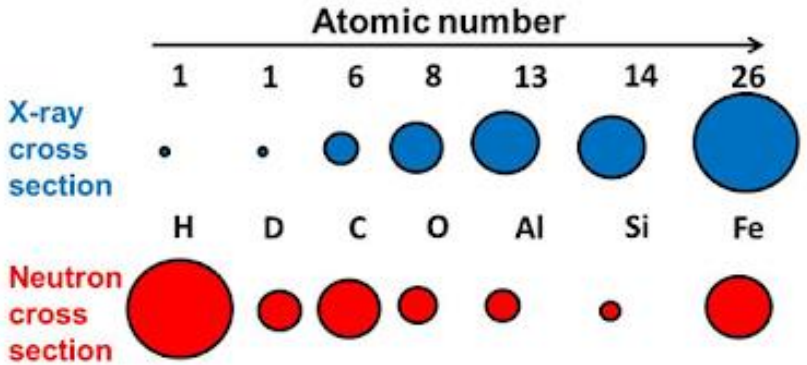

http://worldsciencereport.blogspot.com/

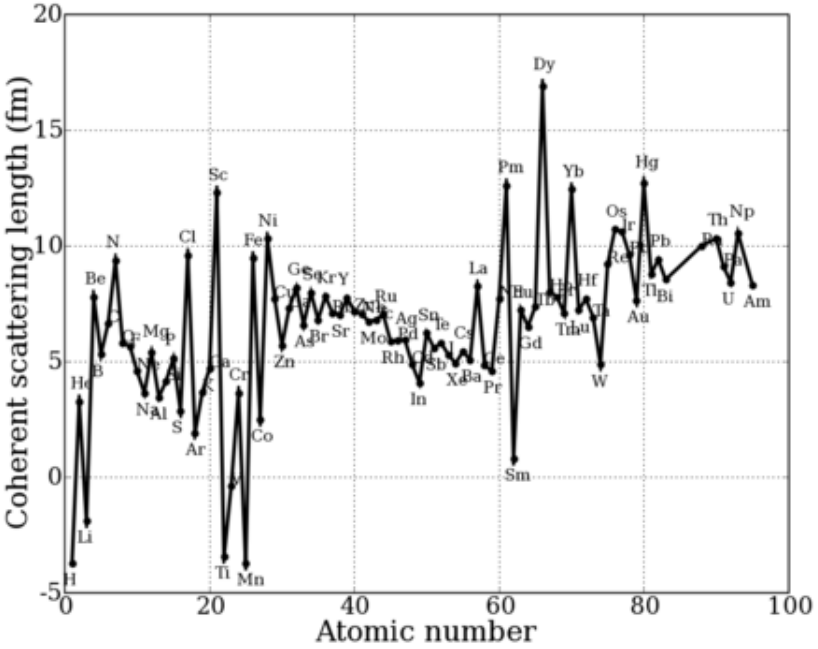

https://www.ncnr.nist.gov/resources/n-lengths/

Scattering Length for Neutrons

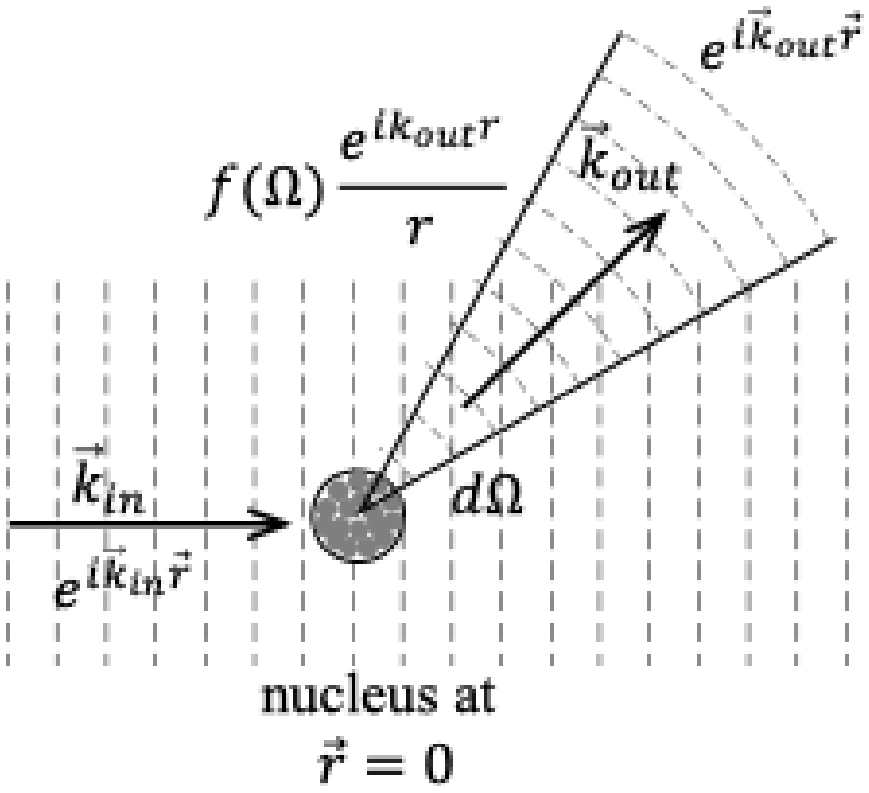

Schrödinger's equation:

$$-\frac{\hbar^2}{2m_n}\nabla^2\psi(\mathbf{r})+\hat{V}_N(\mathbf{r})\psi(\mathbf{r})=\frac{\hbar^2k^2}{2m_n}\psi(\mathbf{r})$$

Solution = incident (plane) wave
+ scattered (spherical) wave

$$\psi(\mathbf{r})\approx \underbrace{e^{i\mathbf{k}_{in}\mathbf{r}}}_{\text{incident wave}} + \underbrace{f_n(\Omega)\frac{e^{ikr}}{r}}_{\text{scattered wave}}$$

Born approximation (weak interaction potential V):

$$f_n(\Omega)=-\frac{m_n}{2\pi\hbar^2}\cdot\langle e^{i\mathbf{k}_{out}\mathbf{r}}|\hat{V}_N^{ps}(\mathbf{r})|e^{i\mathbf{k}_{in}\mathbf{r}}\rangle=-\frac{m_n}{2\pi\hbar^2}\int\hat{V}_N^{ps}(\mathbf{r})e^{-i\mathbf{q}\mathbf{r}}d\mathbf{r}$$

Scattering Length for Neutrons

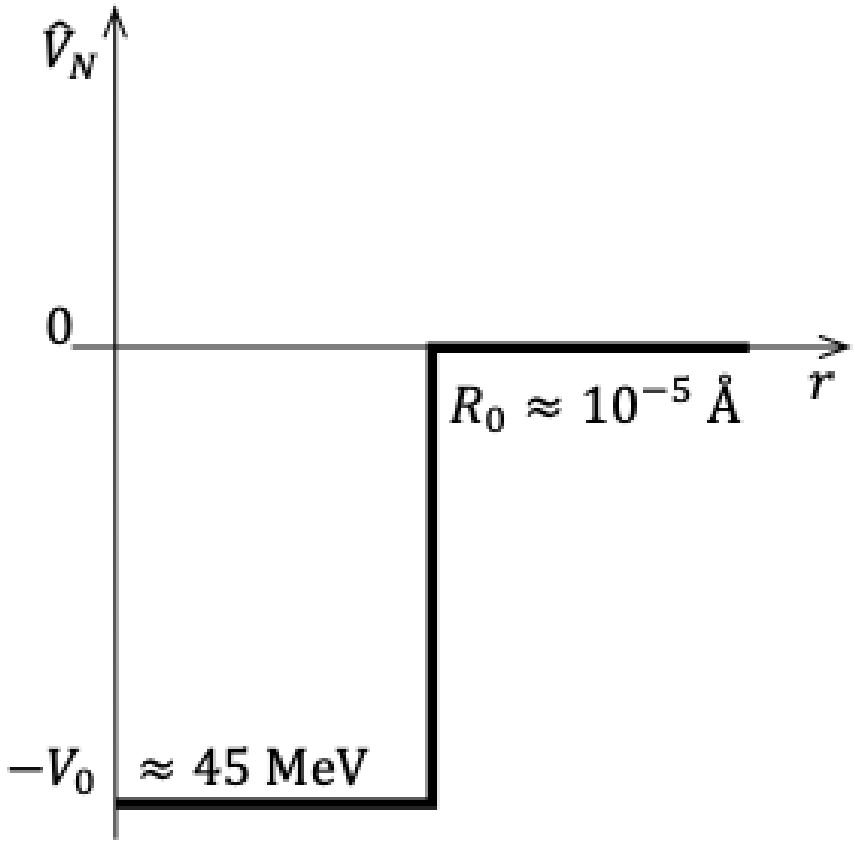

Schrödinger's equation:

$$-\frac{\hbar^2}{2m_n}\nabla^2\psi(\mathbf{r}) + \hat{V}_N(\mathbf{r})\psi(\mathbf{r}) = \frac{\hbar^2 k^2}{2m_n}\psi(\mathbf{r})$$

Solution = incident (plane) wave
+ scattered (spherical) wave

$$\psi(\mathbf{r}) \approx \underbrace{e^{i\mathbf{k}_{in}\mathbf{r}}}_{\text{incident wave}} + \underbrace{f_n(\Omega)\frac{e^{ikr}}{r}}_{\text{scattered wave}}$$

Born approximation (weak interaction potential V):

$$f_n(\Omega) = -\frac{m_n}{2\pi\hbar^2}\cdot\langle e^{i\mathbf{k}_{out}\mathbf{r}}|\hat{V}_N^{ps}(\mathbf{r})|e^{i\mathbf{k}_{in}\mathbf{r}}\rangle = -\frac{m_n}{2\pi\hbar^2}\int \hat{V}_N^{ps}(\mathbf{r})e^{-i\mathbf{q}\mathbf{r}}d\mathbf{r}$$

$$= -\frac{m_n}{2\pi\hbar^2}\int \alpha\delta(\mathbf{r})e^{-i\mathbf{q}\mathbf{r}}d\mathbf{r} = -\frac{m_n}{2\pi\hbar^2}\alpha = -b$$

Partial wave analysis

For slow neutrons ($kR_0 \ll 1$) and no angular dependence (s-wave scattering)

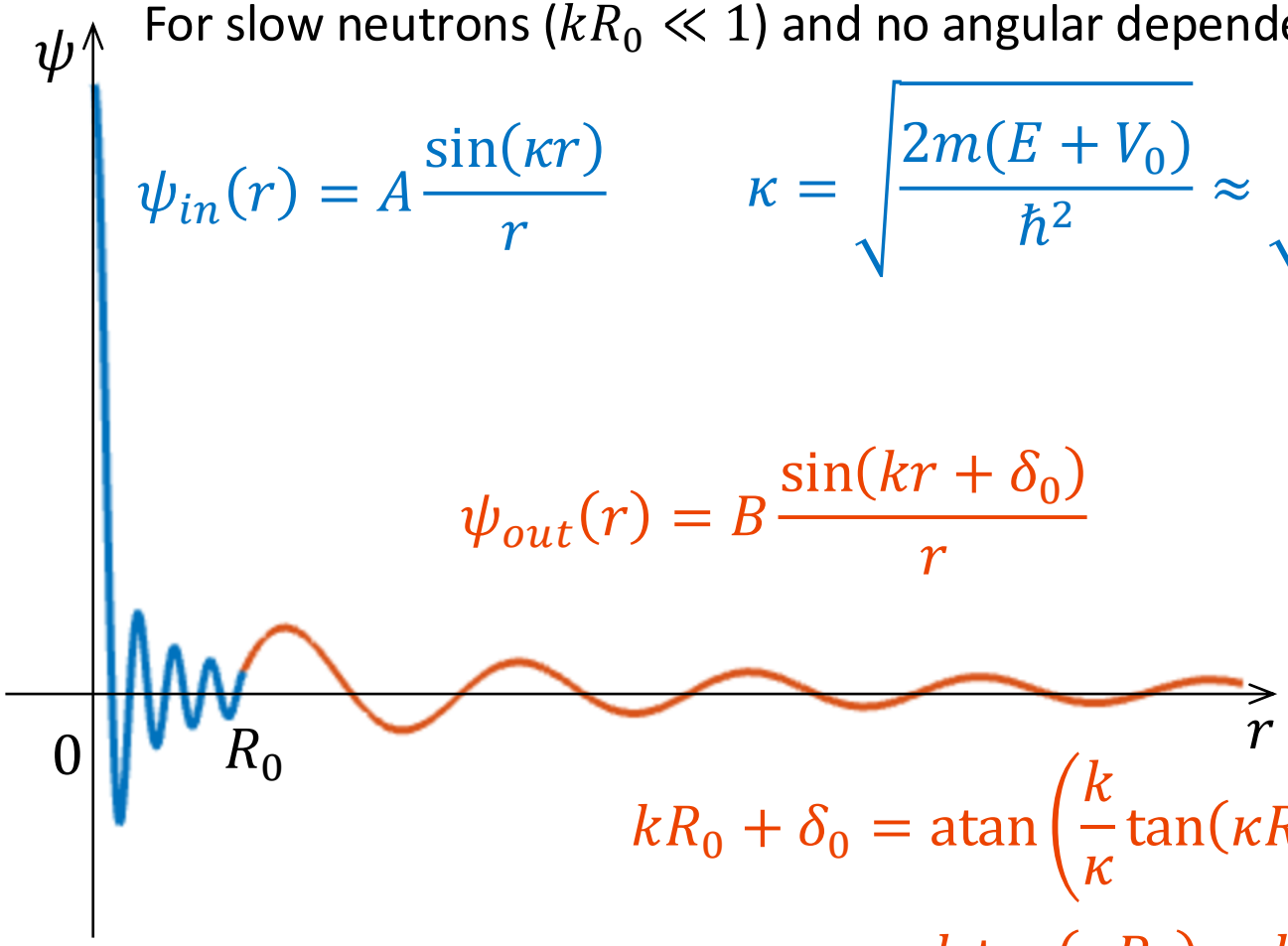

$$\psi_{in}(r) = A\frac{\sin(\kappa r)}{r} \qquad \kappa = \sqrt{\frac{2m(E+V_0)}{\hbar^2}} \approx \sqrt{\frac{2mV_0}{\hbar^2}}$$

$$\psi_{out}(r) = B\frac{\sin(kr+\delta_0)}{r}$$

$$kR_0 + \delta_0 = \operatorname{atan}\left(\frac{k}{\kappa}\tan(\kappa R_0)\right) \approx \frac{k}{\kappa}\tan(\kappa R_0)$$

$$\delta_0 = \frac{k\tan(\kappa R_0) - k\kappa R_0}{\kappa}$$

$$f = \frac{1}{2ik}\left(e^{2i\delta_0} - 1\right) \approx \frac{\delta_0}{k} = \frac{\tan(\kappa R_0) - \kappa R_0}{\kappa} = -b$$

Meaning of the scattering length

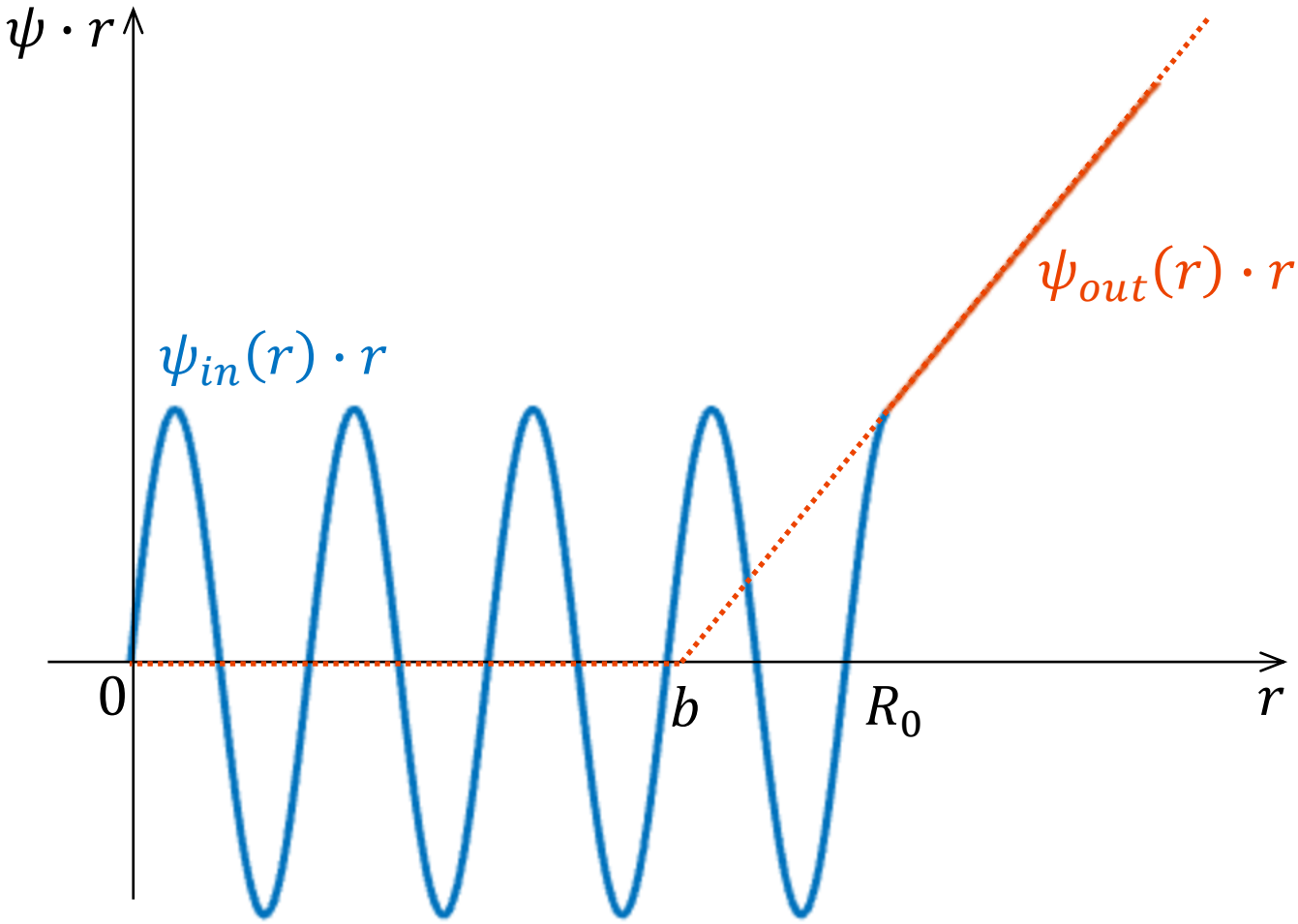

The wave function outside of nucleus $\psi_{out}(r)$ is the same as it would be with an infinite potential

$$V = \begin{cases} 0, & r > b \\ +\infty, & r \leq b \end{cases}$$

$$\psi_{out} = \begin{cases} \neq 0, & r > b \\ 0, & r \leq b \end{cases}$$

Sign of the scattering length

$$b = \frac{\kappa R_0 - \tan(\kappa R_0)}{\kappa} < 0$$

$$\tan(\kappa R_0) > \kappa R_0$$

$$\kappa \approx \sqrt{\frac{2mV_0}{\hbar^2}} \approx 1.5 \cdot 10^5 \text{ Å}^{-1}$$

$$R_0 \approx 1.45 \sqrt[3]{A} \cdot 10^{-5} \text{Å}$$

$$= (2.3 \ - 9.3) \cdot 10^{-5} \text{Å}$$

$$\kappa R_0 = 3.45 \ - 14$$

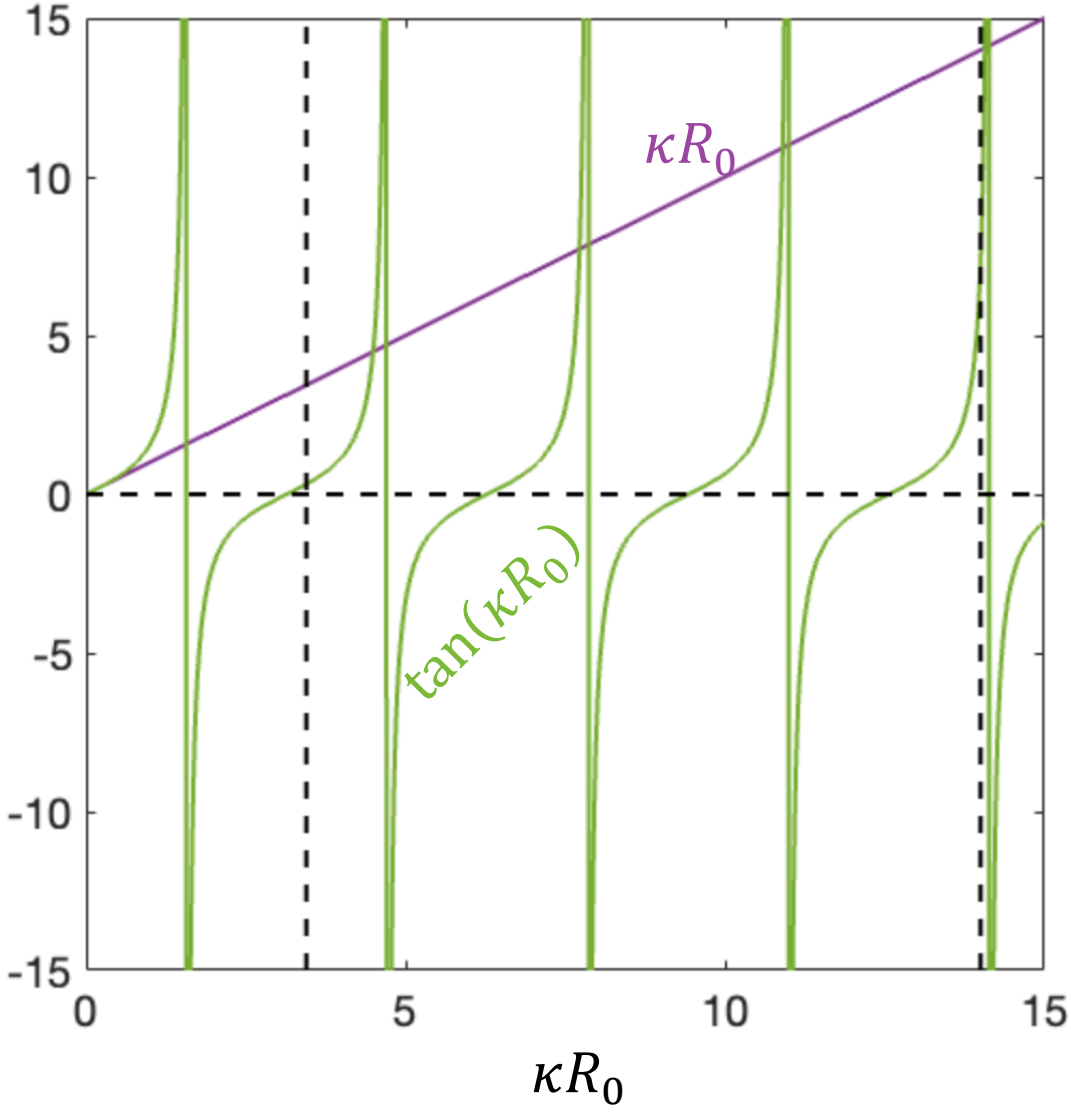

Probability of $b < 0$ is about

$w \sim \frac{1}{\pi \kappa \langle R_0 \rangle} \sim 3\%$ (for ^{1}H, ^{48}Ti, ^{55}Mn, ^{62}Ni)

More in V.F. Turchin “Slow neutrons” (1965)

Scattering by a single atom

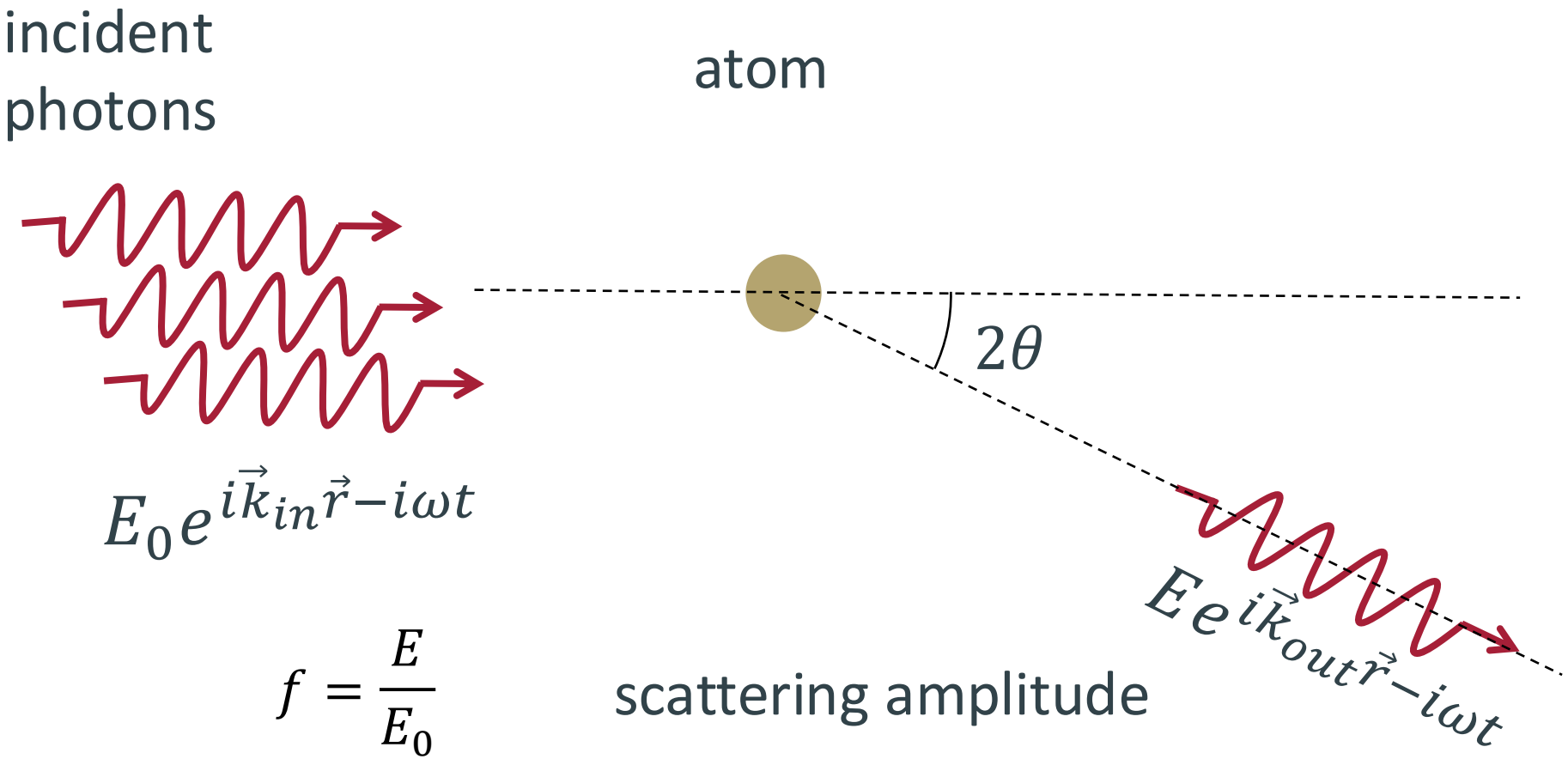

$$f = \frac{E}{E_0}$$ scattering amplitude

$$\frac{\partial\sigma}{\partial\Omega} = |f(\Omega)|^2$$ differential cross section

Scattering by two atoms

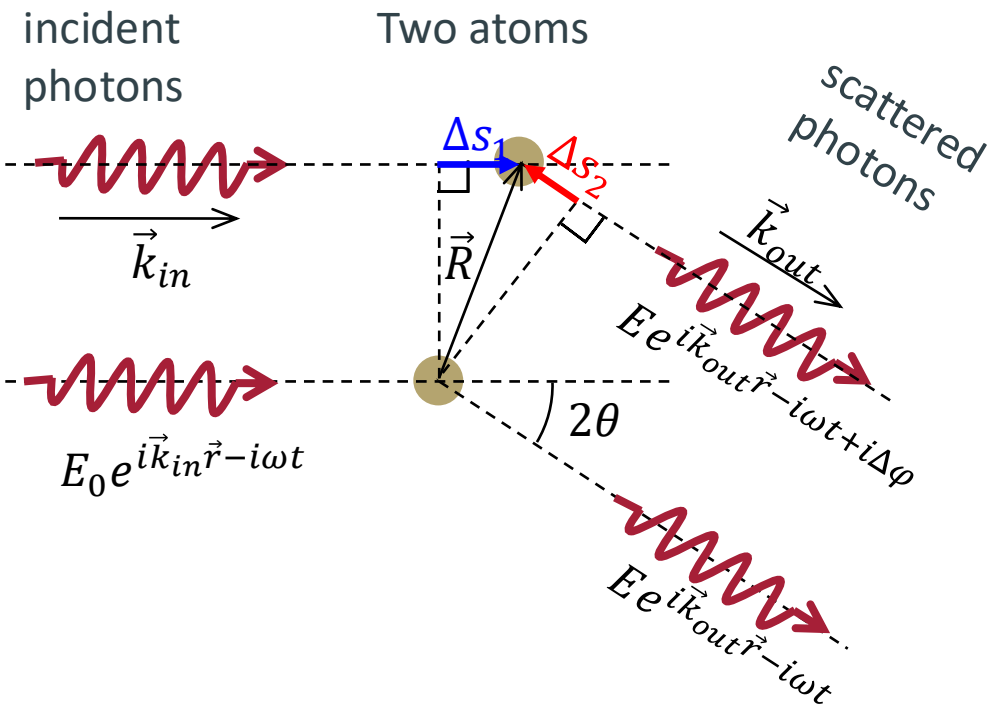

Phase difference between the waves scattered by two electrons

$$\Delta\varphi = k\Delta s = \frac{2\pi}{\lambda}(\Delta s_1 + \Delta s_2)$$

$$= k_{in}\Delta s_1 + k_{out}\Delta s_2$$

$$= \vec{k}_{in}\vec{R} - \vec{k}_{out}\vec{R} = -(\vec{k}_{out} - \vec{k}_{in})\vec{R}$$

$$= -\vec{q}\vec{R}$$

Resulting scattered field at point $\vec{r}$

$$E \propto E_0\, e^{i\vec{k}_{out}\vec{r}-i\omega t} + E_0\, e^{i\vec{k}_{out}\vec{r}-i\omega t-i\vec{q}\vec{R}}$$

$$\propto E_0\left(1 + e^{-i\vec{q}\vec{R}}\right)$$

Scattering by many atoms

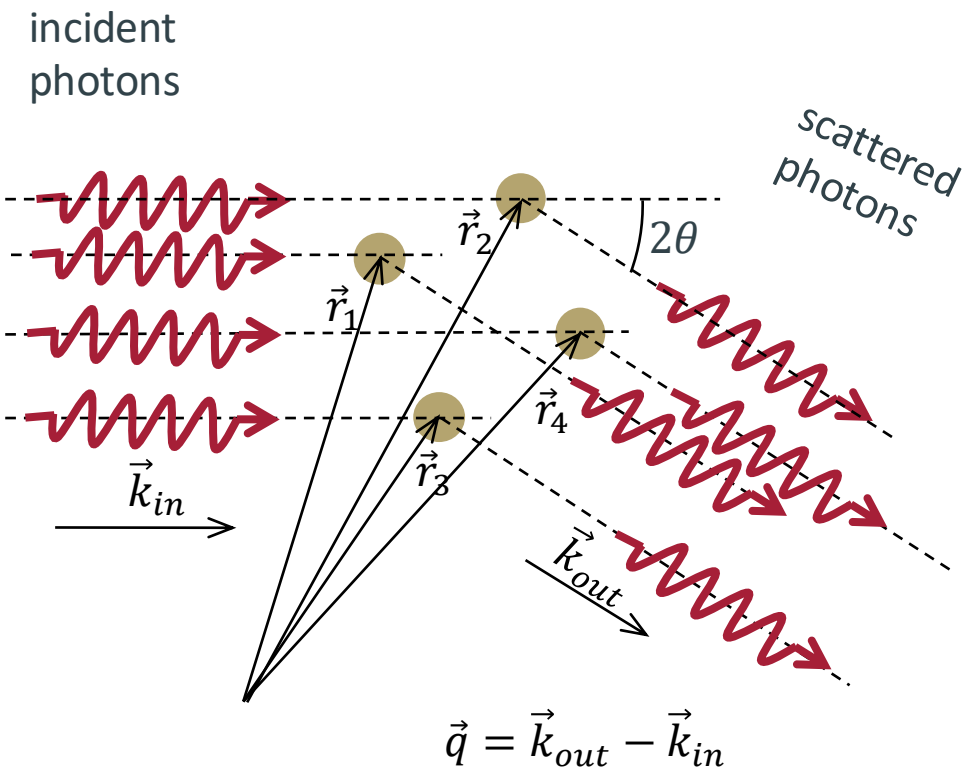

$$\vec{q} = \vec{k}_{out} - \vec{k}_{in}$$

Resulting scattered field:

$$E \propto \sum_{n=1}^{N} E_0 f_n(q) e^{i\vec{k}_{out}\vec{r} - i\omega t - i\vec{q}\vec{r}_n} \propto E_0 \underbrace{\sum_{n=1}^{N} f_n(q) e^{-i\vec{q}\vec{r}_n}}$$

Interference between photons scattered from different atoms

Scattering by nanoparticles

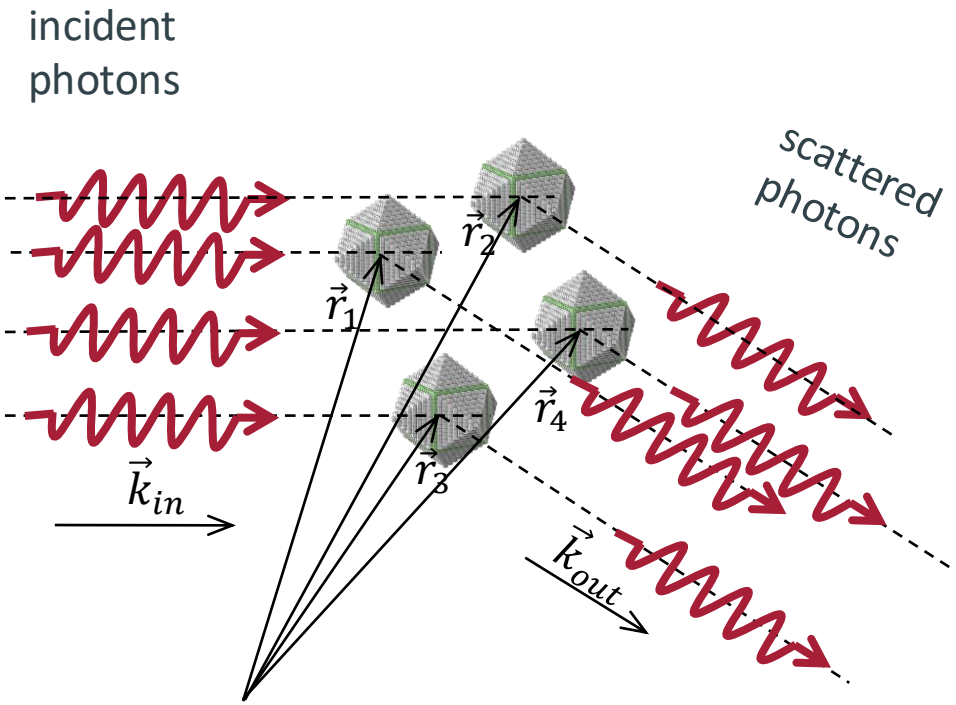

$$\vec{q} = \vec{k}_{out} - \vec{k}_{in}$$

Resulting scattered field:

Interference between photons scattered from different atoms

- Many nanoparticles

$$E \propto E_0 \sum_{n=1}^{N} f_n(q) e^{-i\vec{q}\vec{r}_n}$$

scattering form factor of a nanoparticle

$$f(q) = \int \rho_{el}(\vec{r}) e^{-i\vec{q}\vec{r}} d\vec{r}$$

scattering form factor of a nanoparticle

Scattering by a 1D periodic array of atoms

Scattering in phase:

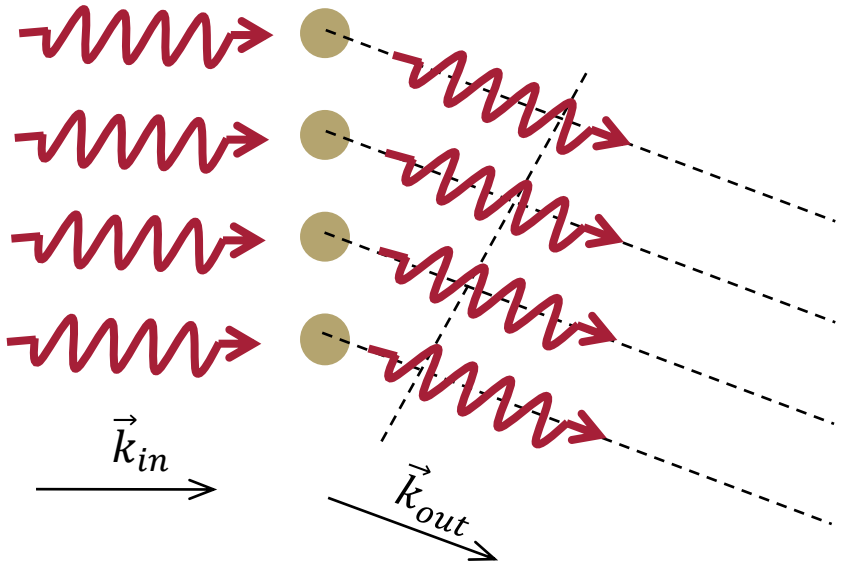

$$E \propto f(q) \sum_{n=1}^{N} e^{-i\vec{q}\vec{r}_n} = f(q) \sum_{n=1}^{N} 1 \propto N \cdot f(q)$$

If for all atoms, $\vec{q}\vec{r}_n = 2\pi \cdot m$

sharp and intense diffraction peak (Bragg peak)

Scattering out of phase:

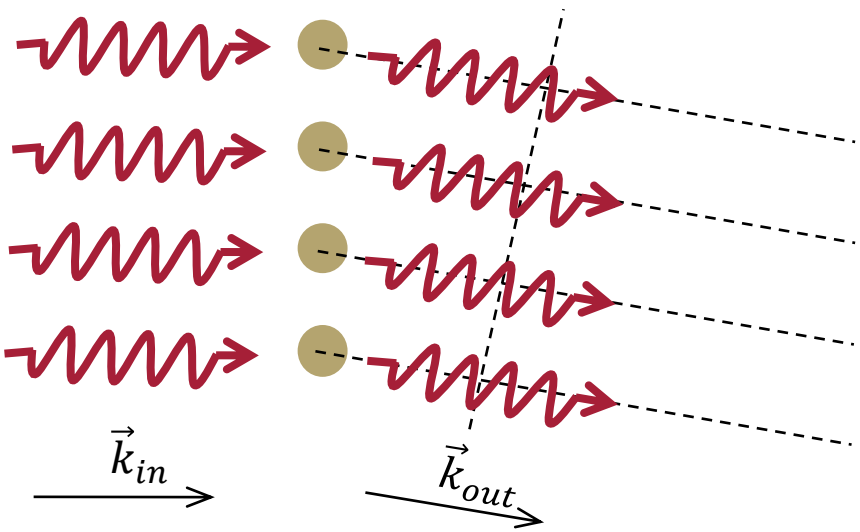

$$E \propto f(q) \sum_{n=1}^{N} e^{-i\vec{q}\vec{r}_n} = f(q) \sum_{n=1}^{N} (\pm 1) \approx 0$$

If for all atoms, $\vec{q}\vec{r}_n = \pi \cdot m$

very weak scattering signal between the diffraction peaks

Scattering by a 1D periodic array of atoms

Scattering in phase:

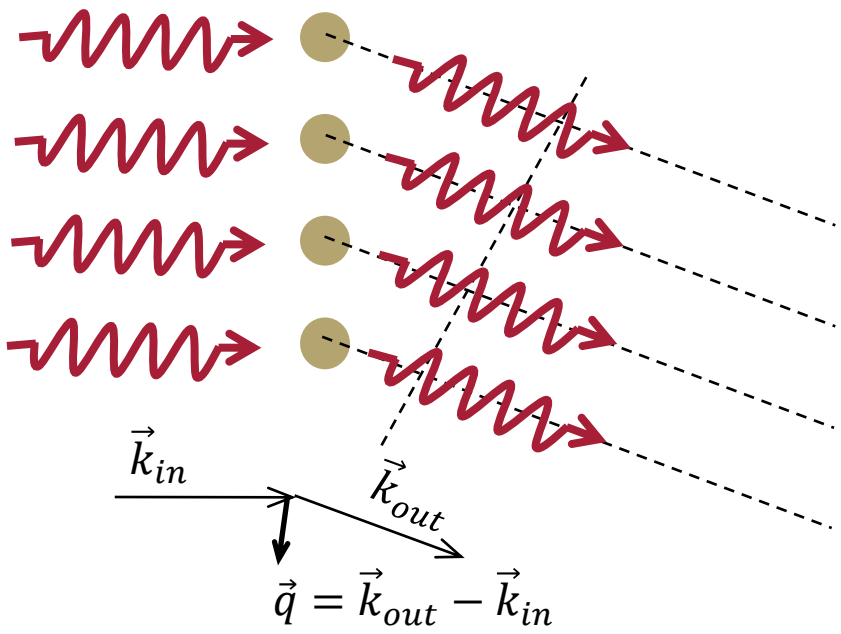

For a periodic array of atoms: $x_n = n \cdot a$

$$E \propto f(q) \sum_{n=1}^{N} e^{-iq_x x_n} = f(q) \sum_{n=1}^{N} e^{-iq_x a \cdot n}$$

$$= f(q) e^{-iq_x a} \frac{1 - e^{-iq_x a \cdot N}}{1 - e^{-iq_x a}}$$

$$I \propto |E|^2 \propto |f(q)|^2 \cdot \left| \frac{\sin\left(\frac{q_x a}{2} \cdot N\right)}{\sin\left(\frac{q_x a}{2}\right)} \right|^2$$

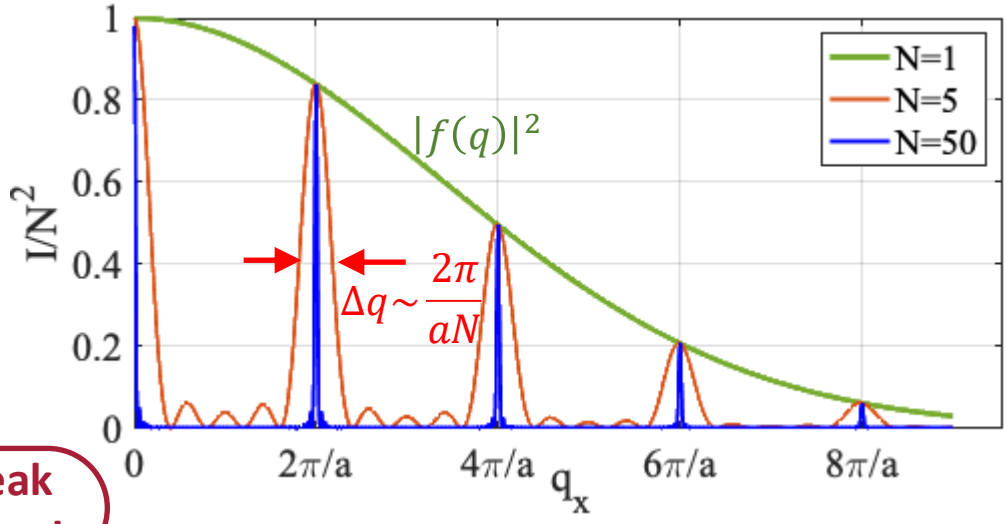

Size of a crystal → Width of the Bragg peak
Shape of a crystal → Shape of the Bragg peak

Strain of the atomic lattice

- Perfect crystal lattice

$$I \propto \left| \sum_{n=1}^{N} e^{-iq \cdot a \cdot n} \right|^2$$

Diffraction peaks at $q = \frac{2\pi}{a} m = q_m$

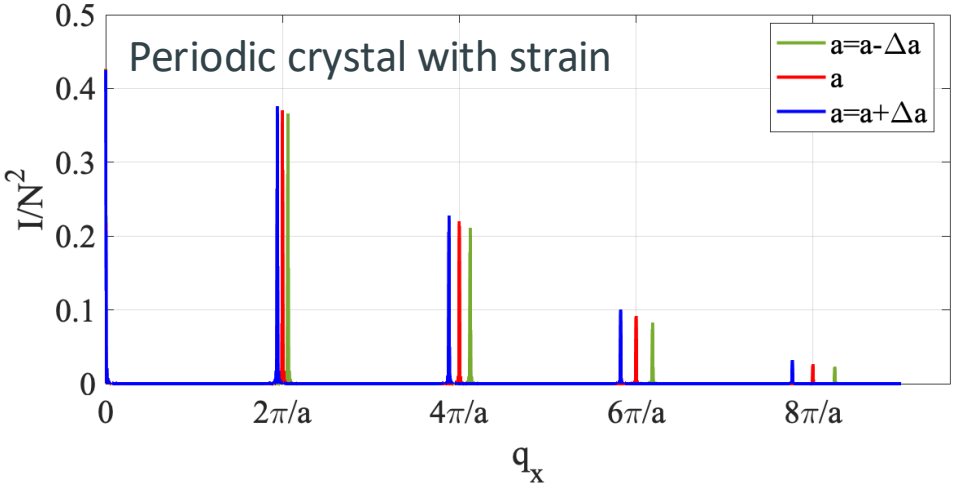

- Compressive strain $\varepsilon < 0$

Diffraction peaks at $q = \frac{2\pi}{a-\Delta a} m$

$$\approx q_m \left(1 + \frac{\Delta a}{a}\right)$$

- Tensile strain $\varepsilon > 0$

Diffraction peaks at $q = \frac{2\pi}{a+\Delta a} m$

$$\approx q_m \left(1 - \frac{\Delta a}{a}\right)$$

- Real crystal with defects

Diffraction peaks at $q = \frac{2\pi}{\langle a \rangle} m$

Width of the peaks $\Delta q = q_m \frac{\Delta a}{\langle a \rangle}$

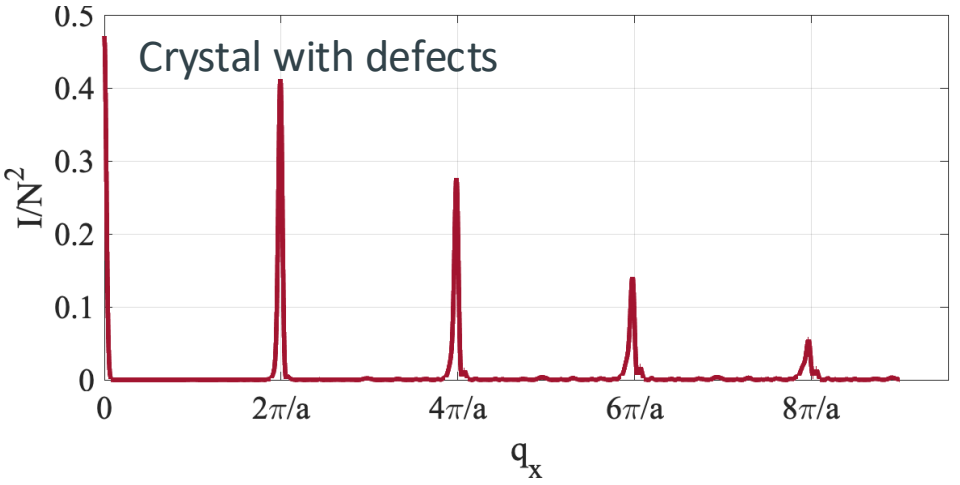

Deposition of C_{60} on mica

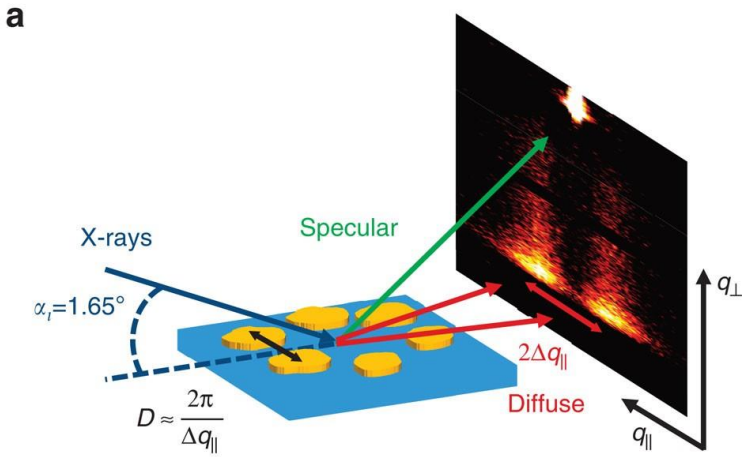

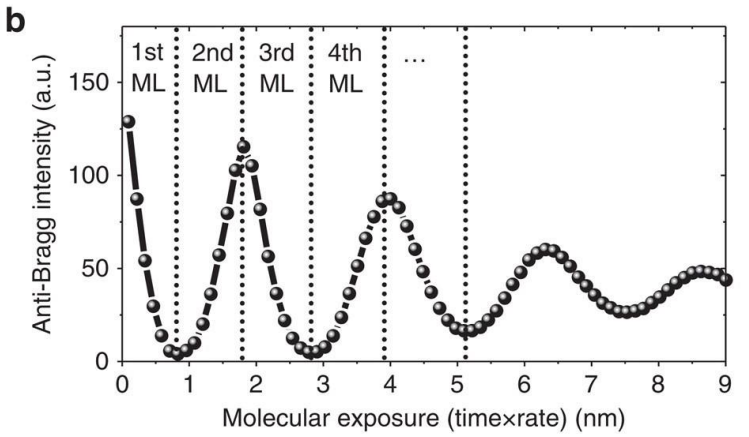

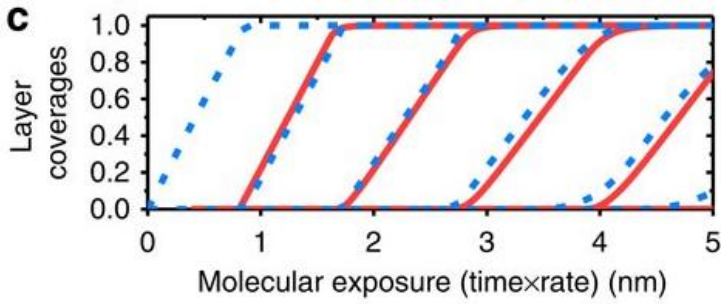

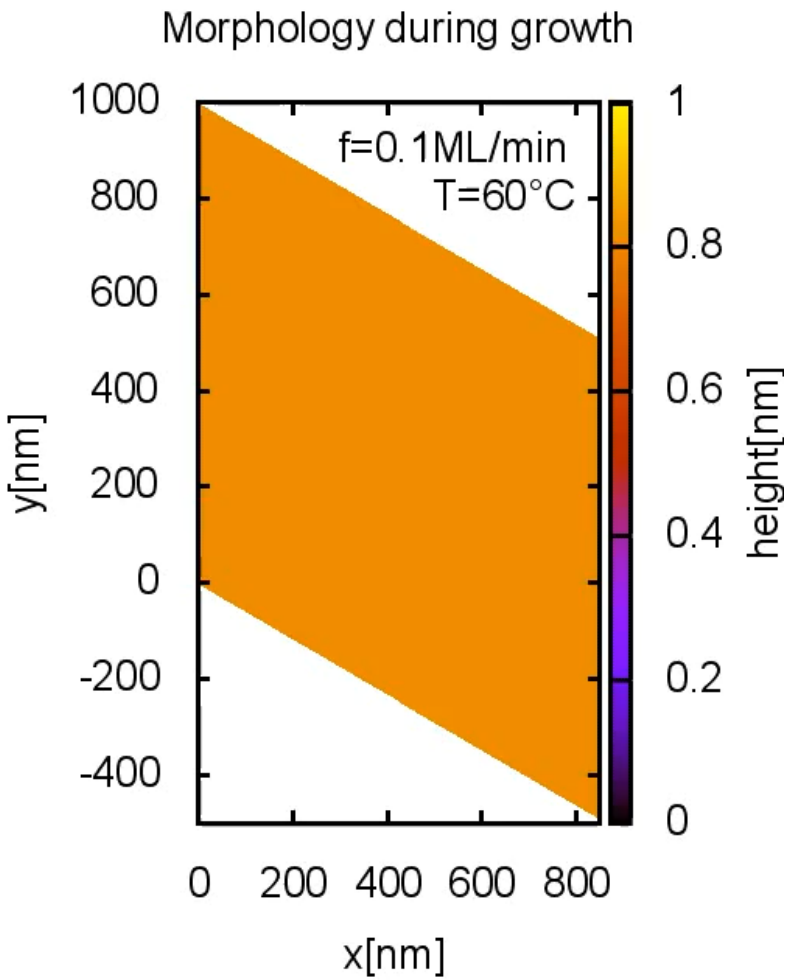

S. Bommel, *et al. Nat. Commun* **5**, 5388 (2014)

Scherrer's broadening

The smaller is the sample, the broader are the Bragg reflections:

$$B(2\theta) = \frac{K\lambda}{L\cos\theta},$$

where $B(2\theta)$ is the width (FWHM) of the diffraction peak in radians and $K \sim 1$ is the shape factor.

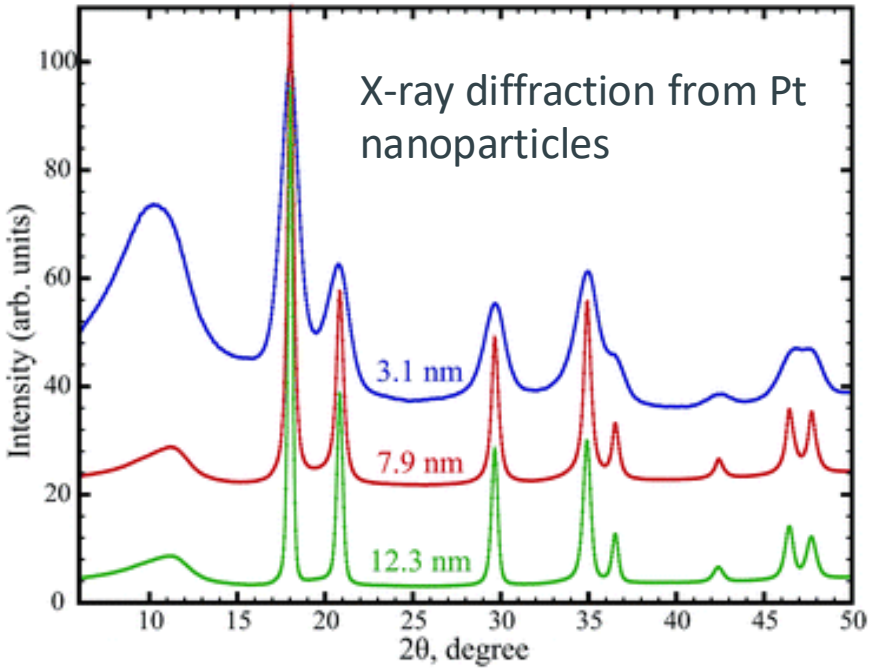

Leontyev et al., RSC Adv., **2014** 35959-35965

$a_{Pt} = 3.9231$ Å (bulk crystal)

Small Angle X-ray Scattering (SAXS)

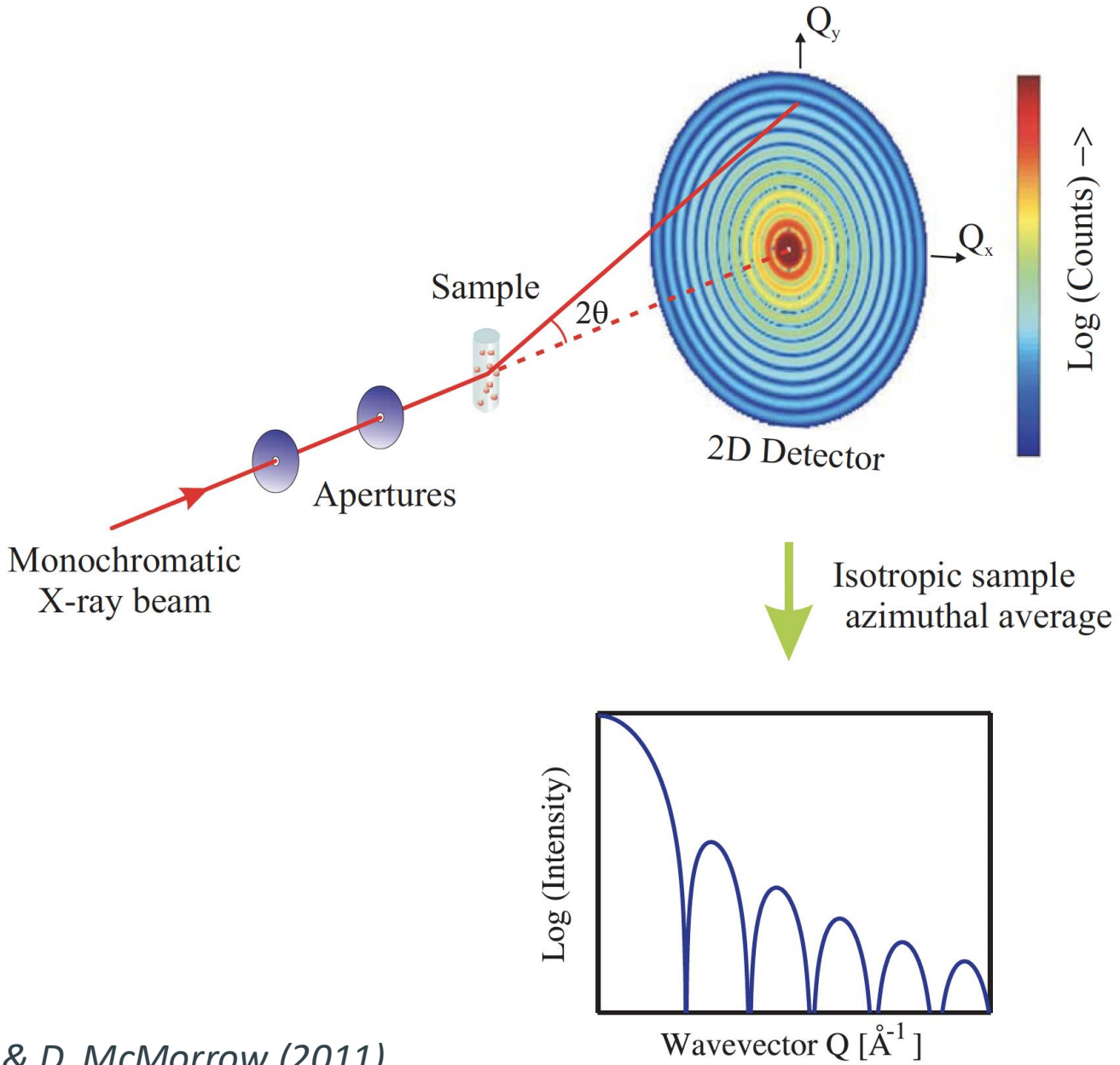

J. Als-Nielsen & D. McMorrow (2011)

SAXS on proteins

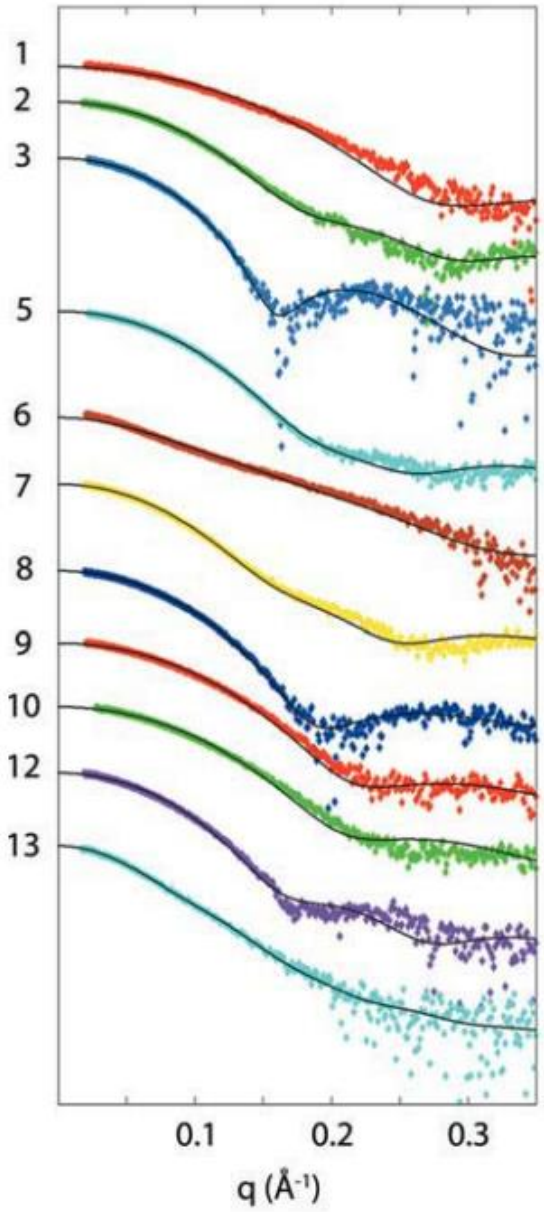

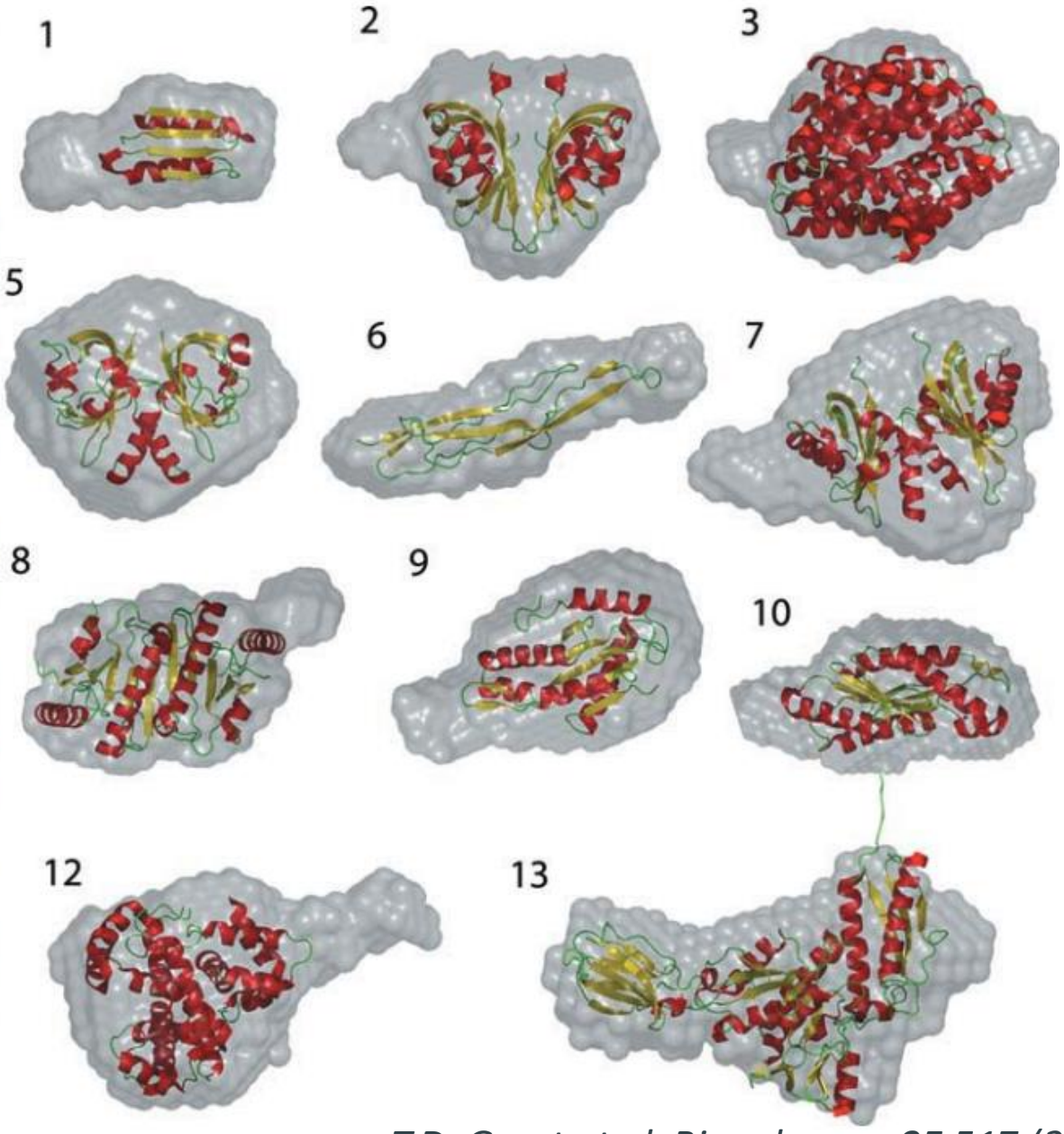

*T.D. Grant et al. Biopolymers **95** 517 (2011)*

Small Angle X-ray Scattering (SAXS)

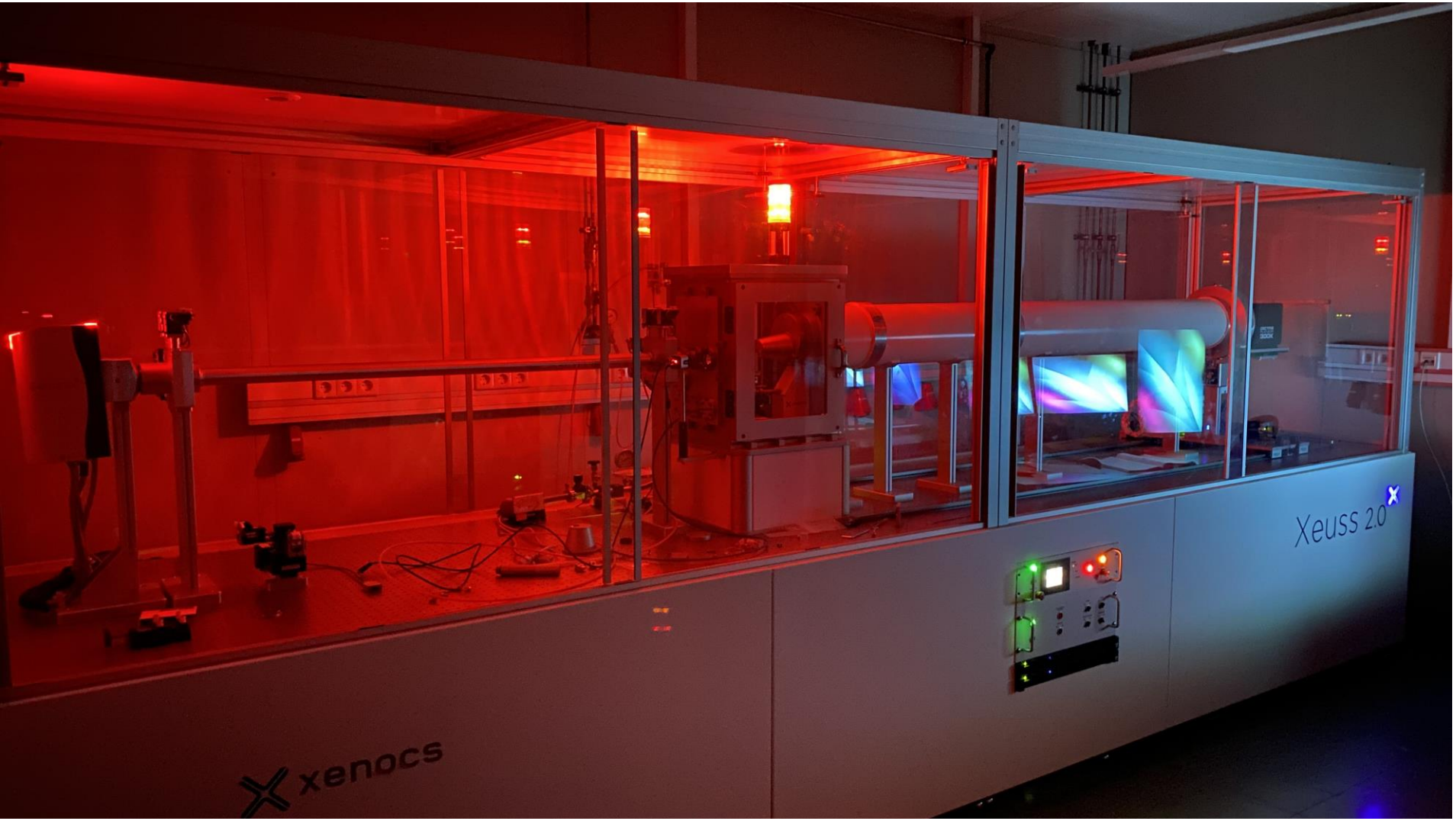

Neutrons / X-rays contrast

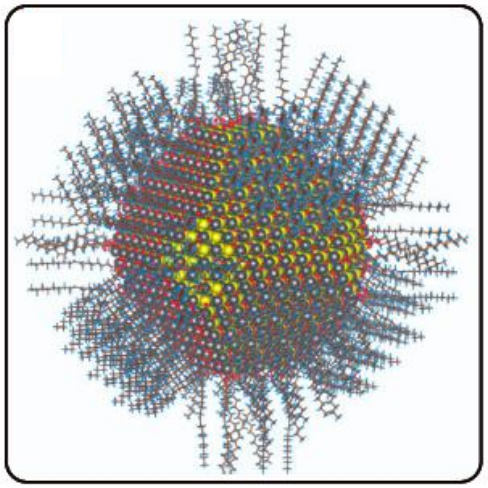

PbS nanoparticle
coated with oleic acid

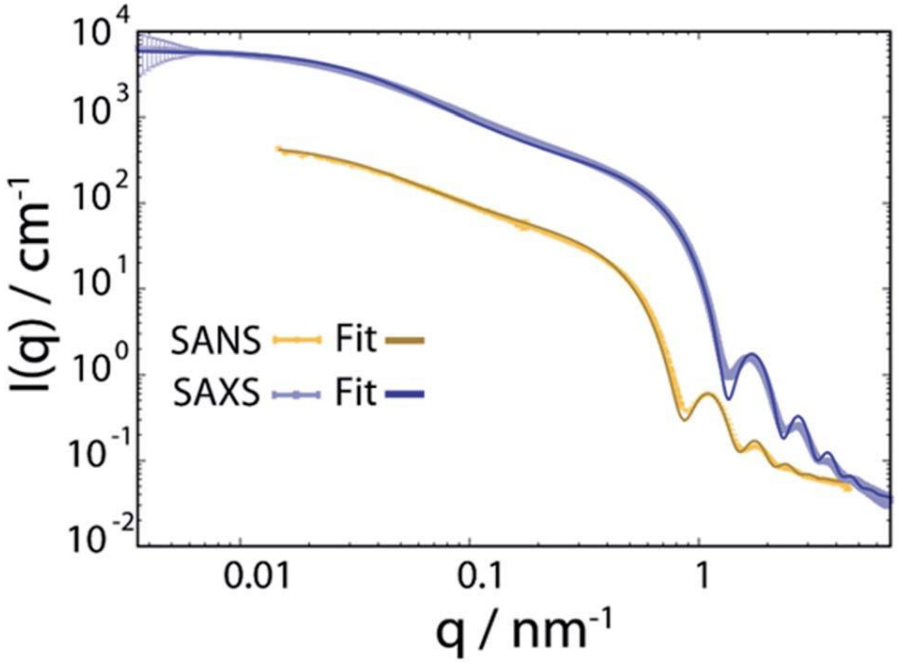

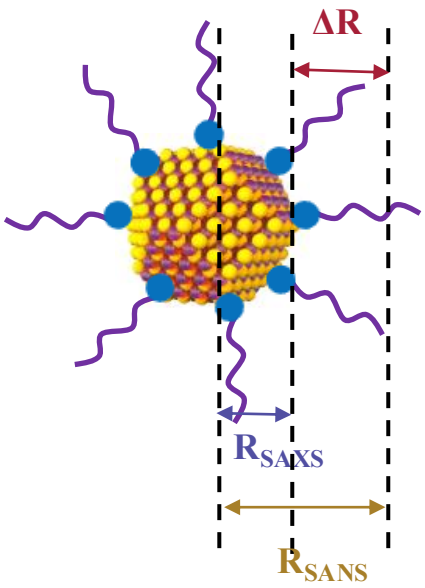

X-rays ”see” almost exclusively the PbS core
Neutrons “see” both the PbS core and OA shell

T. Seydel et al., Chem. Sci. **11**, 8875 (2020)

Possibilities for *in situ* experiments

1. X-ray diffraction in extreme conditions (high pressure, high/low temperatures, etc)

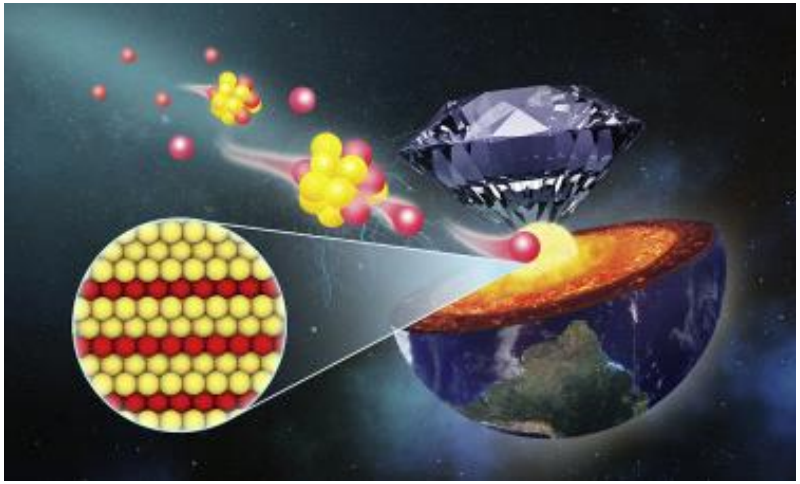

Liu et al., The Innovation 4 100354 (2023)

2. X-ray diffraction with time resolution (tracking chemical reactions)

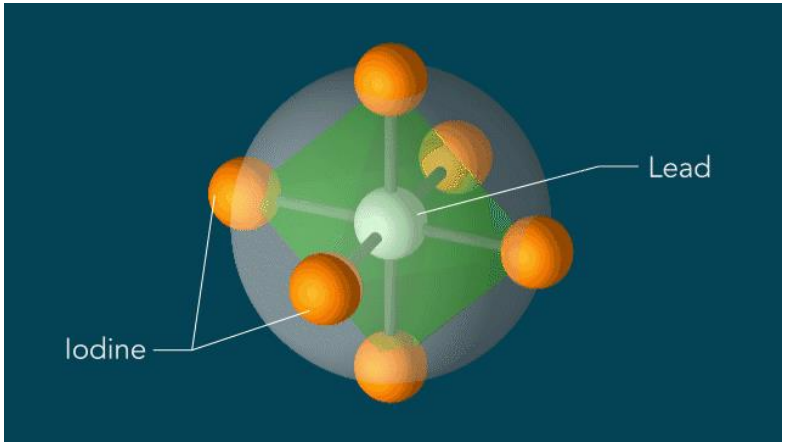

SLAC National Accelerator Laboratory

3. X-ray diffraction *in operando* (catalysis, voltage-induced changes, etc)

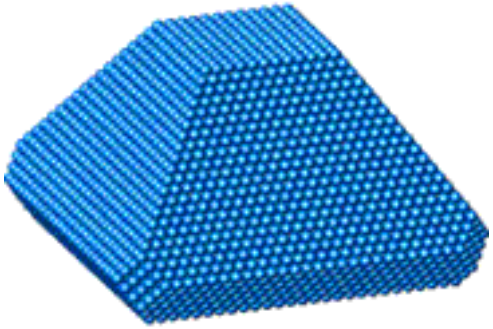

DESY

4. X-ray diffraction of biologically important systems

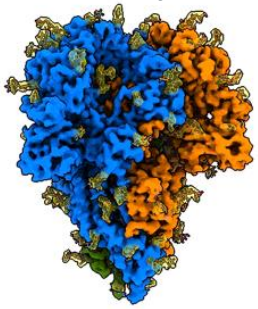

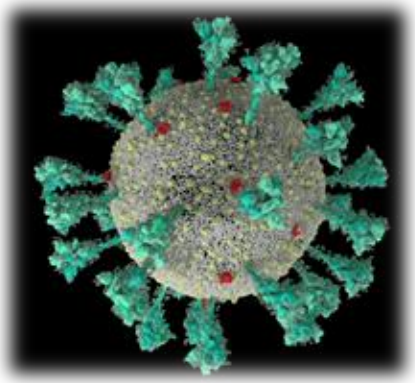

SLAC National Accelerator Laboratory

Scattering by a 3D periodic array of atoms

In a crystal lattice, $\vec{r}_n = n_1\vec{a}_1 + n_2\vec{a}_2 + n_3\vec{a}_3$

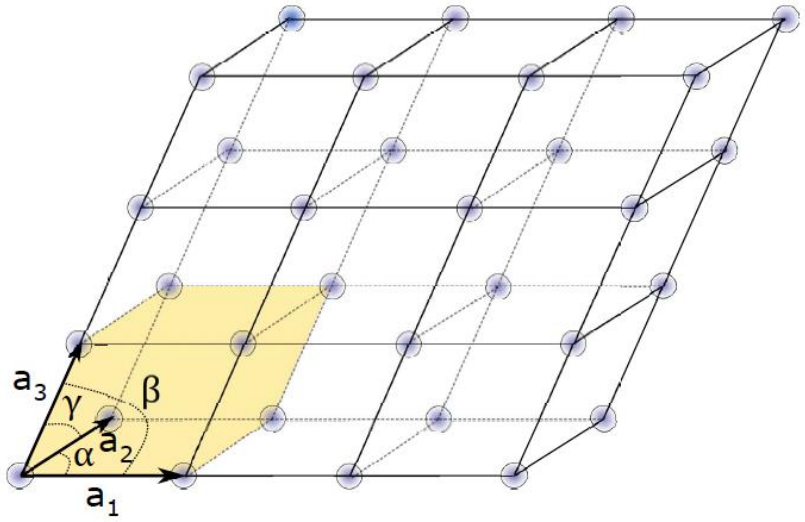

A reciprocal lattice: $\vec{G}_{hkl} = h\vec{a}_1^* + k\vec{a}_2^* + l\vec{a}_3^*$

with the reciprocal unit vectors

$$\vec{a}_1^* = \frac{2\pi[\vec{a}_2 \times \vec{a}_3]}{\vec{a}_1 \cdot [\vec{a}_2 \times \vec{a}_3]}$$

$$\vec{a}_2^* = \frac{2\pi[\vec{a}_3 \times \vec{a}_1]}{\vec{a}_2 \cdot [\vec{a}_3 \times \vec{a}_1]}$$

$$\vec{a}_3^* = \frac{2\pi[\vec{a}_1 \times \vec{a}_2]}{\vec{a}_3 \cdot [\vec{a}_1 \times \vec{a}_2]}$$

Note that

$$\vec{a}_1^* \cdot \vec{a}_1 = 2\pi$$
$$\vec{a}_2^* \cdot \vec{a}_2 = 2\pi$$
$$\vec{a}_3^* \cdot \vec{a}_3 = 2\pi$$

All mixed products are zero

$$\vec{a}_i^* \cdot \vec{a}_j = 0$$

We observe a diffraction peak, if for all atoms, $\vec{q}\vec{r}_n = 2\pi \cdot m$

$$E \propto f(q)\sum_{n=1}^{N} e^{-i\vec{q}\vec{r}_n} = f(q)\sum_{n=1}^{N} 1 \propto N \cdot f(q)$$

For any atom of the real lattice

$$\vec{G}_{hkl}\vec{r}_n = 2\pi \cdot (hn_1 + kn_2 + ln_3) = 2\pi \cdot m$$

The condition to observe a Bragg peak

$$\vec{q} = \vec{k}_{out} - \vec{k}_{in} = \vec{G}_{hkl}$$

Real space and reciprocal space

Scattering in real space

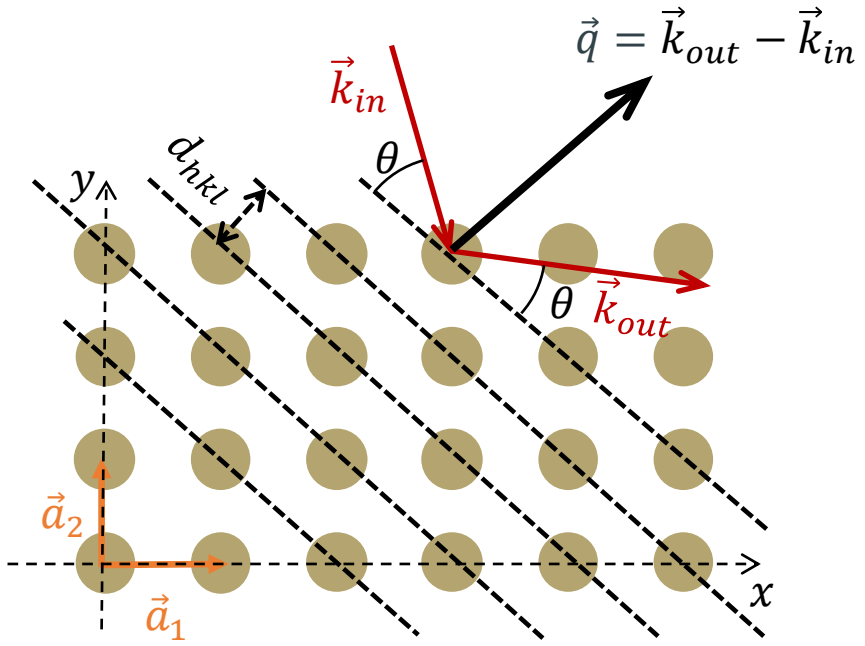

Scattering in reciprocal space

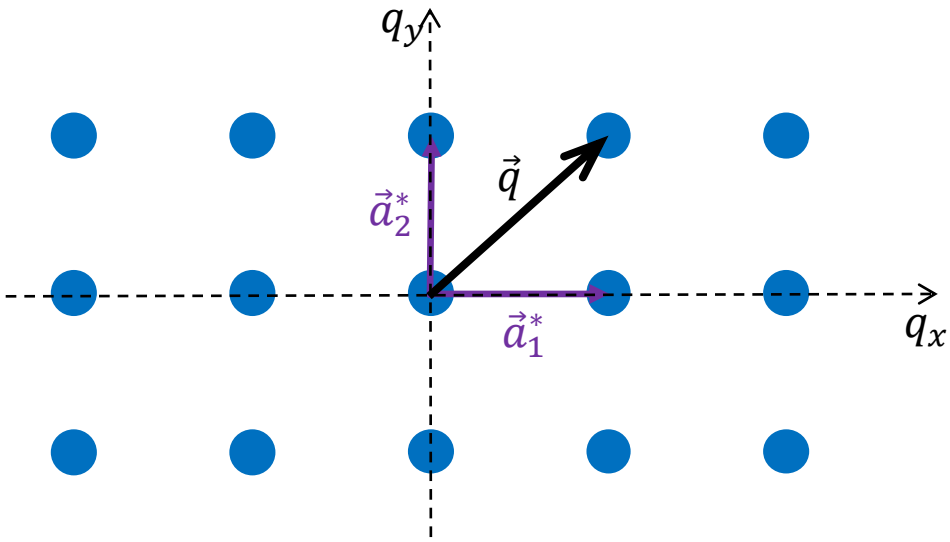

$$\vec{q} = \vec{a}_1^* + \vec{a}_2^* = \vec{G}_{hkl}$$

The scattering can be seen as specular reflection from a set of parallel atomic planes. The interference between the photons scattered from different planes will be constructive if the Bragg condition is satisfied:

$$2d_{hkl}\sin\theta = \lambda$$

Laue condition is satisfied, so we will see a diffraction peak in this experiment.

Real space and reciprocal space

Scattering in real space

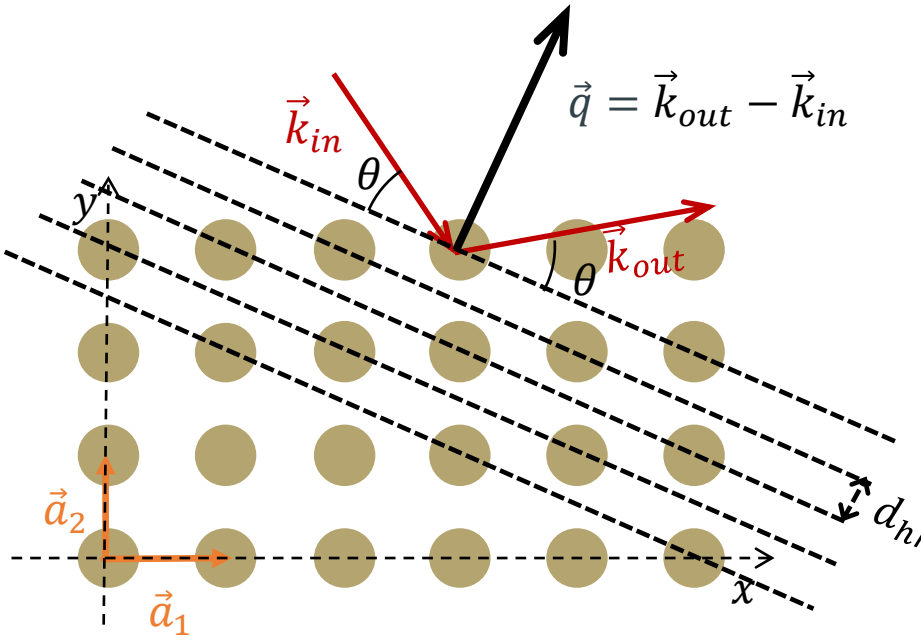

Scattering in reciprocal space

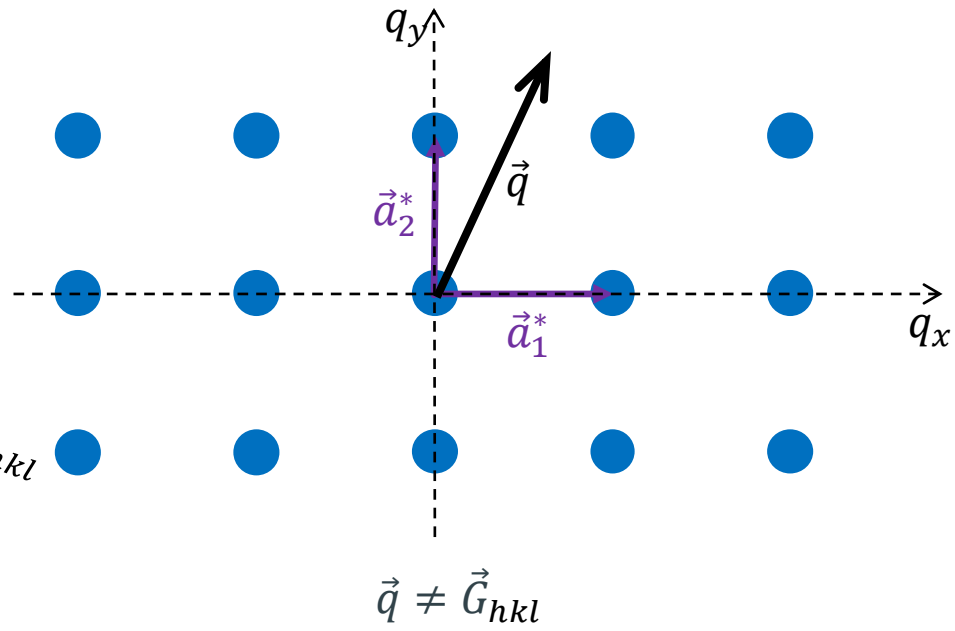

Bragg condition is not satisfied:

$2d_{hkl} \sin\theta \neq \lambda$

Laue condition is not satisfied, so we will not see a diffraction peak in this experiment.

Real space and reciprocal space

Scattering in real space

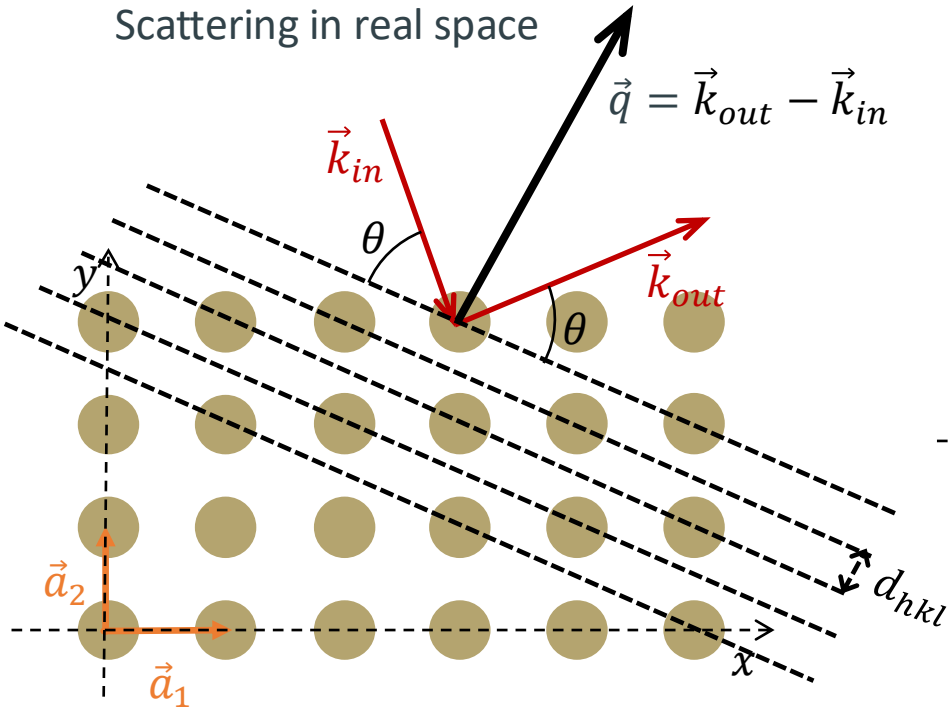

Scattering in reciprocal space

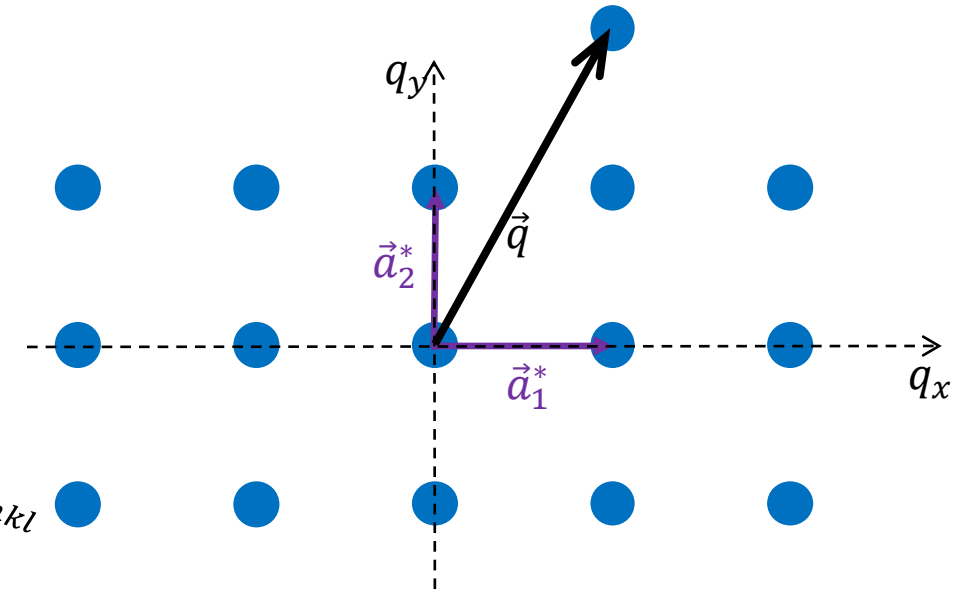

$$\vec{q} = \vec{a}_1^* + 2\vec{a}_2^* = \vec{G}_{hkl}$$

Laue condition is satisfied

By adjusting the incidence angle, Bragg condition is satisfied again, so we can see the diffraction peak

$$2d_{hkl}\sin\theta = \lambda$$

The Ewald sphere

For elastic scattering, $|\vec{k}_{in}| = |\vec{k}_{out}| = \frac{2\pi}{\lambda}$. It means, that all possible scattering vectors $\vec{q} = \vec{k}_{in}$ form a sphere of radius $\frac{2\pi}{\lambda}$ in reciprocal space. A diffraction pattern, measured with a 2D detector, is a cross section of reciprocal space with the Ewald sphere.

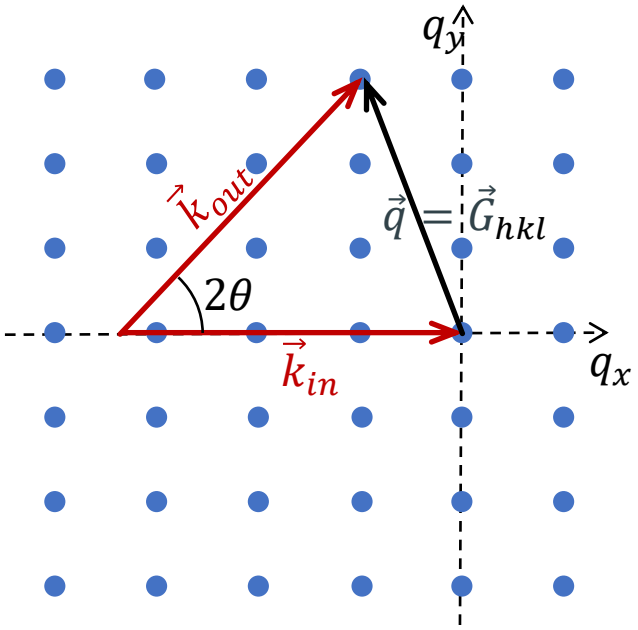

Ewald's sphere in reciprocal space

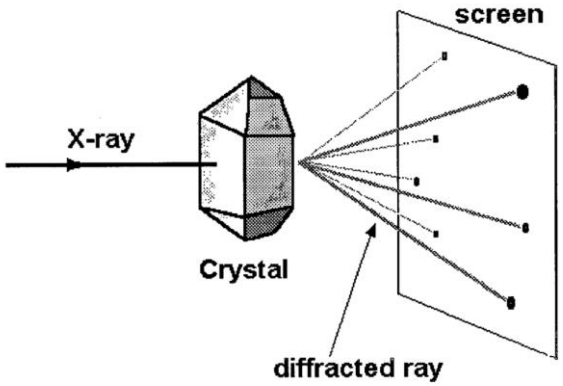

Single crystal diffraction experiment

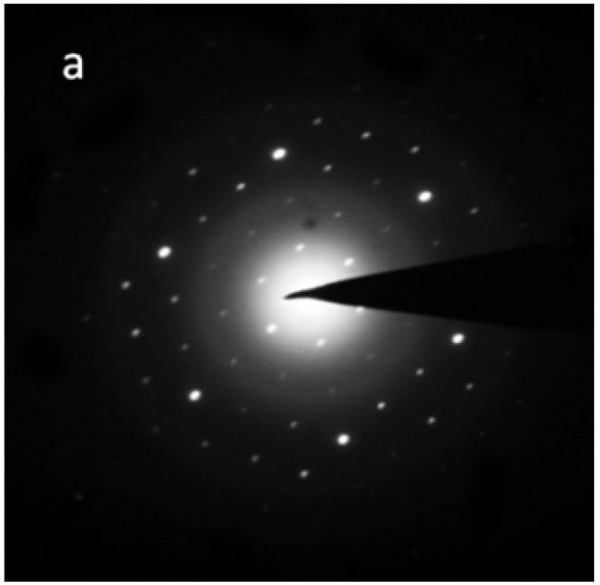

Diffraction pattern

Powder diffraction

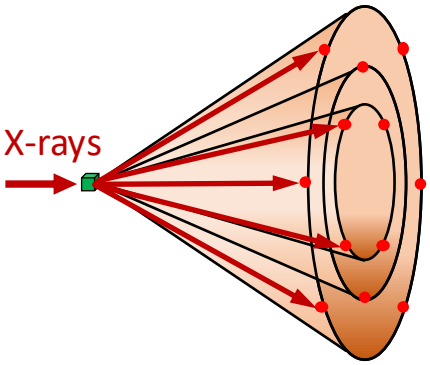

Single crystal diffraction (Bragg reflections)

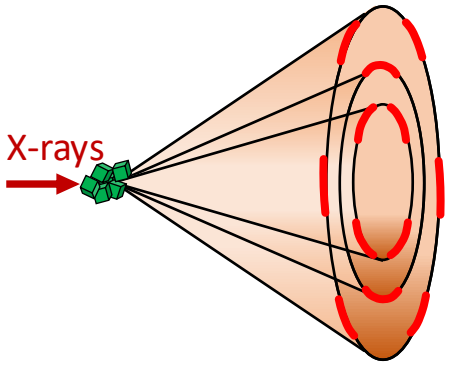

Polycrystalline sample with preferred orientation of crystal grains

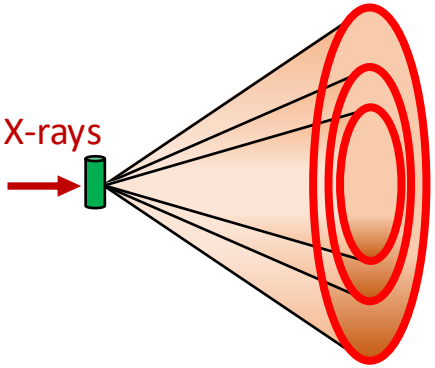

Perfect powder diffraction (Debye-Scherrer rings)

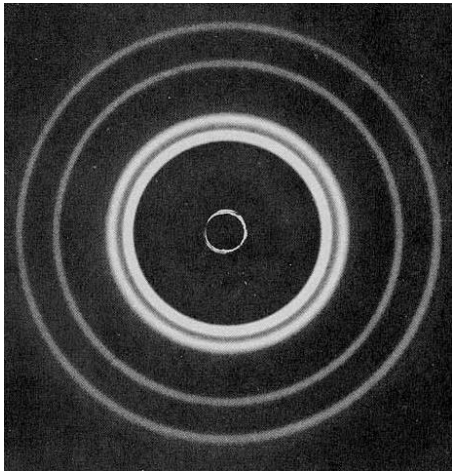

Debye-Scherrer diffraction rings from aluminum foil

Powder diffraction

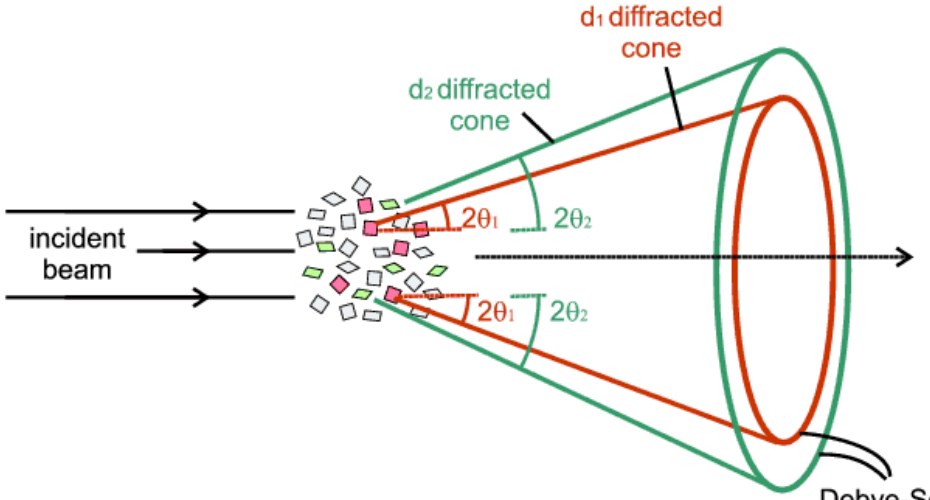

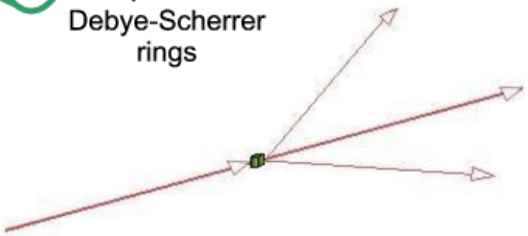

Single Crystal

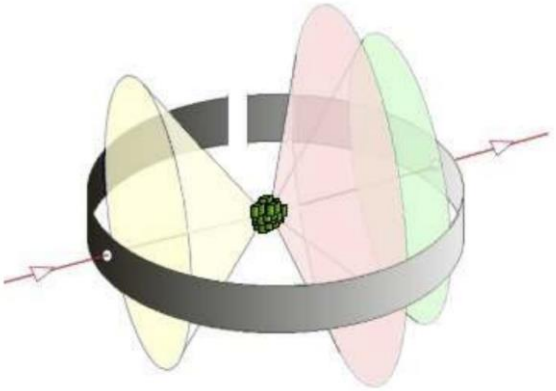

Polycrystalline Powder

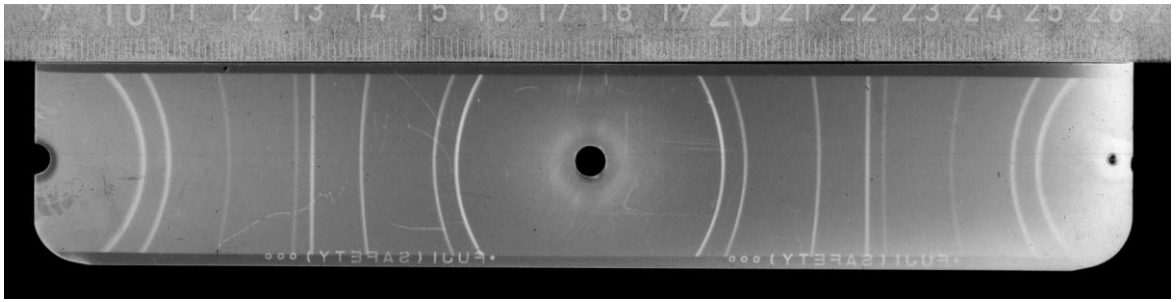

Mosaic spread (azimuthal broadening)

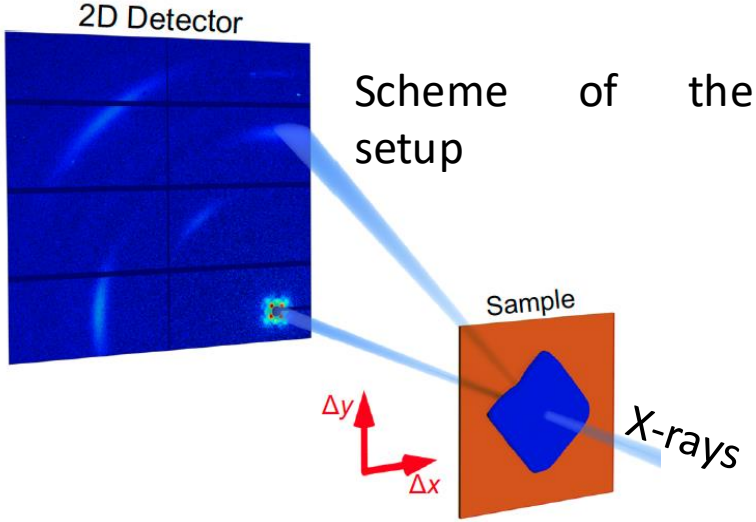

Scheme of the setup

Diffraction pattern

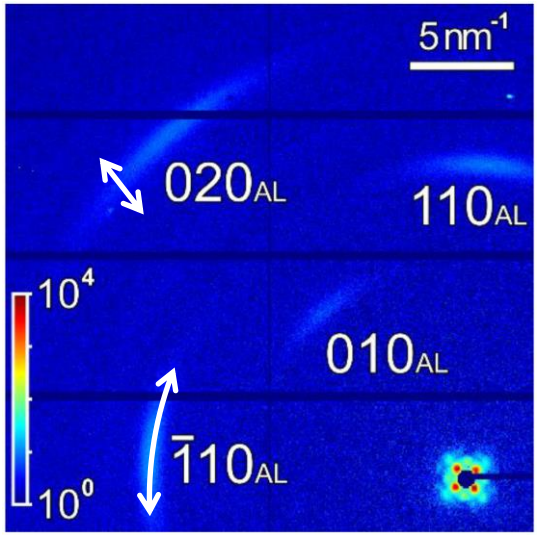

Structure of mesocrystal

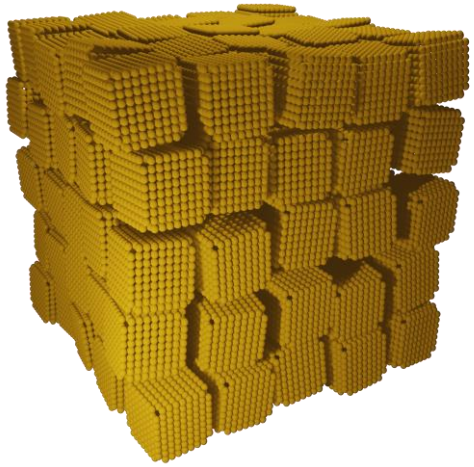

Radial width of the peak (Scherrer's broadening) – size of a nanoparticle

Azimuthal width of the peak – orientational distributions of nanoparticles

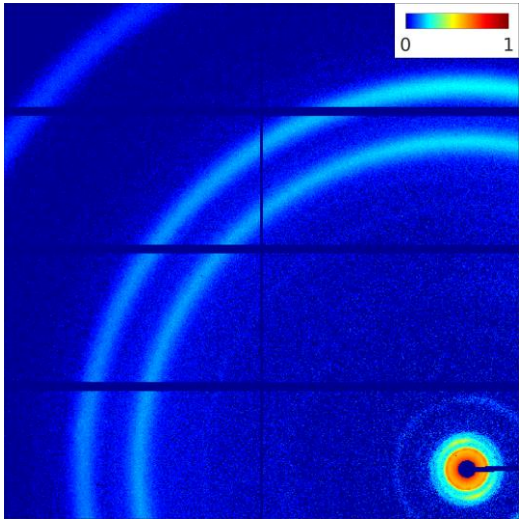

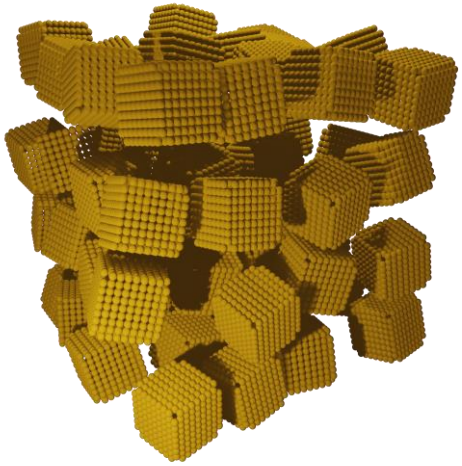

D. Lapkin et al., Nat. Commun. ***13*** *892 (2022)*

Diffraction from quantum dot solids

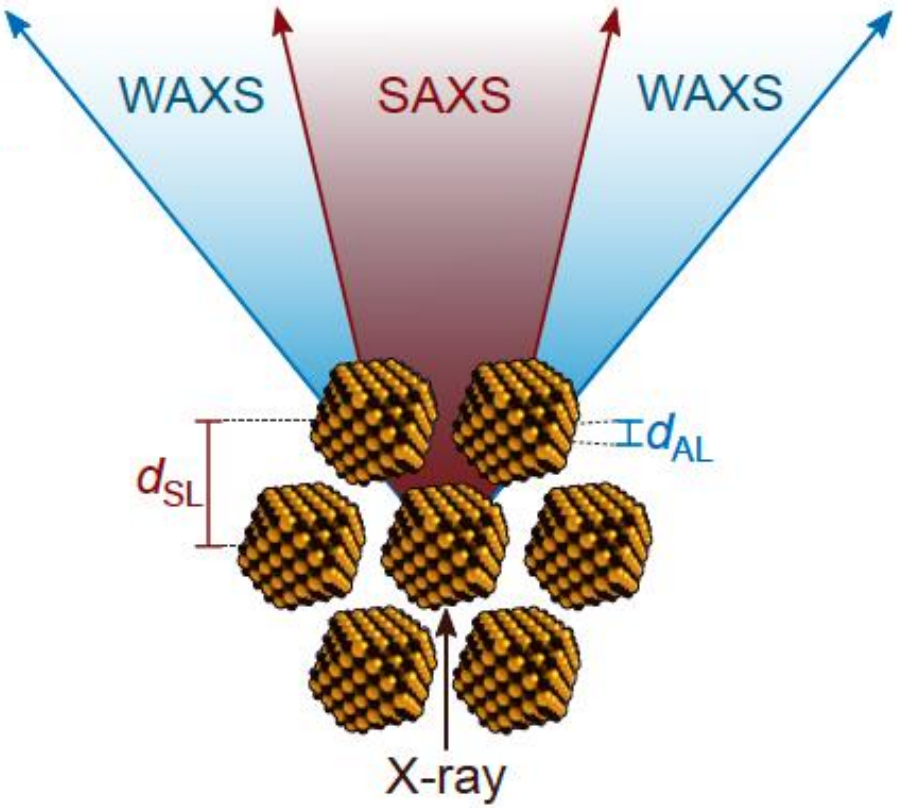

- Small Angle X-ray Scattering (SAXS) is sensitive to the distance between the nanoparticles (superlattice)
- Wide Angle X-ray Scattering (WAXS) is sensitive to the distance between atoms (atomic lattice of nanoparticles)

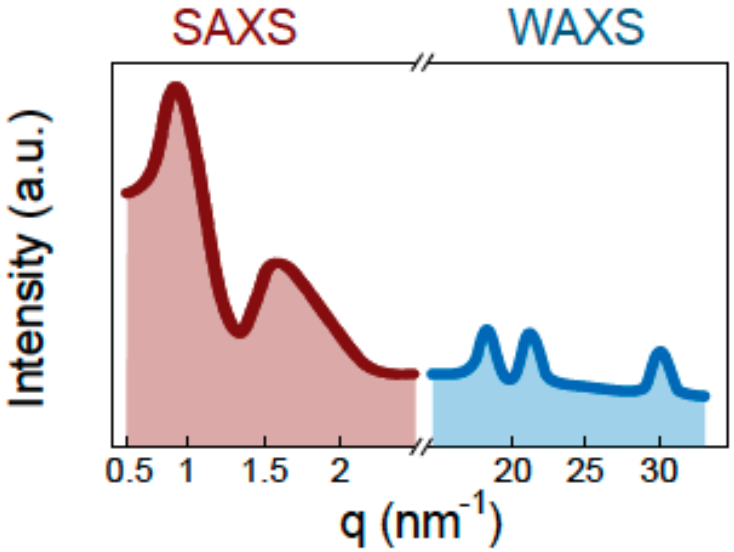

with X-ray diffraction one can simultaneously "see" the structure on two length scales: atomic lattice and superlattice

A. Maier, PhD thesis (2021)

Structure of superlattice

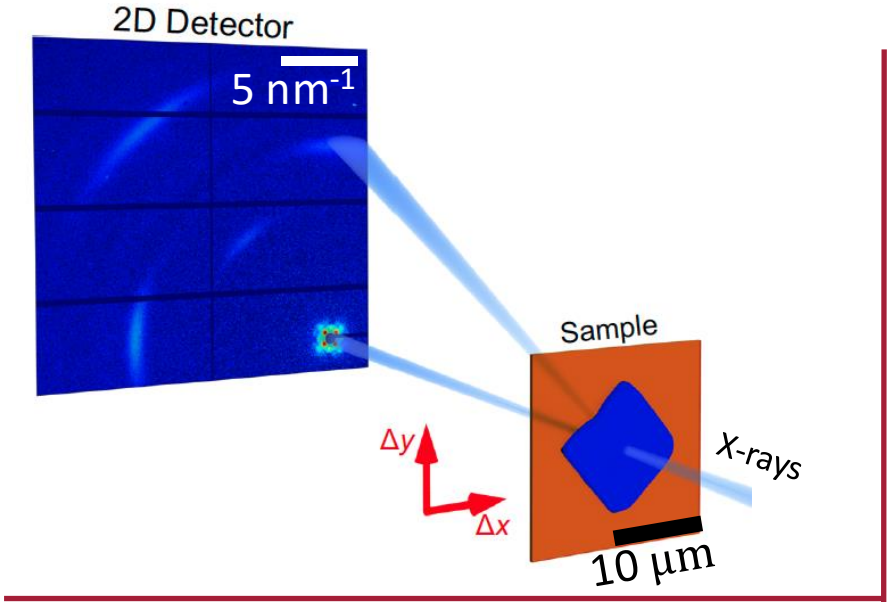

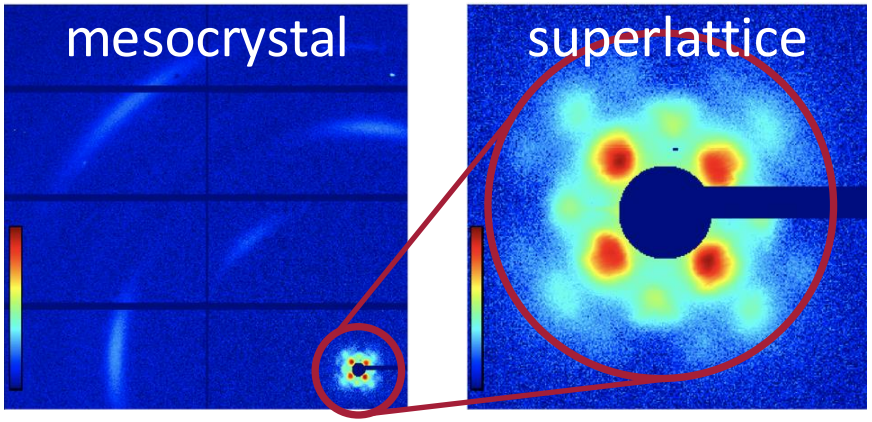

Structure of the superlattice

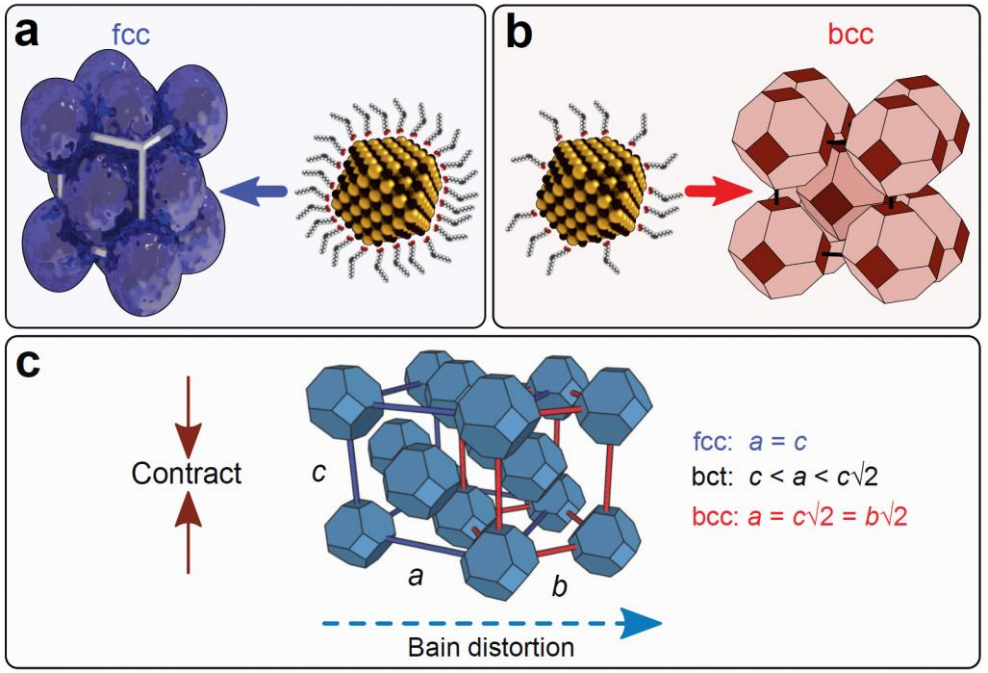

J. Novák et al., ACS Appl. Mater. Interfaces ***8****, 22526 (2016)*

A. Maier, PhD thesis (2021)

D. Lapkin et al., Nat. Commun. ***13*** *892 (2022)*

Diffraction from a single superlattice

Rigaku diffractometer in the institute of inorganic chemistry

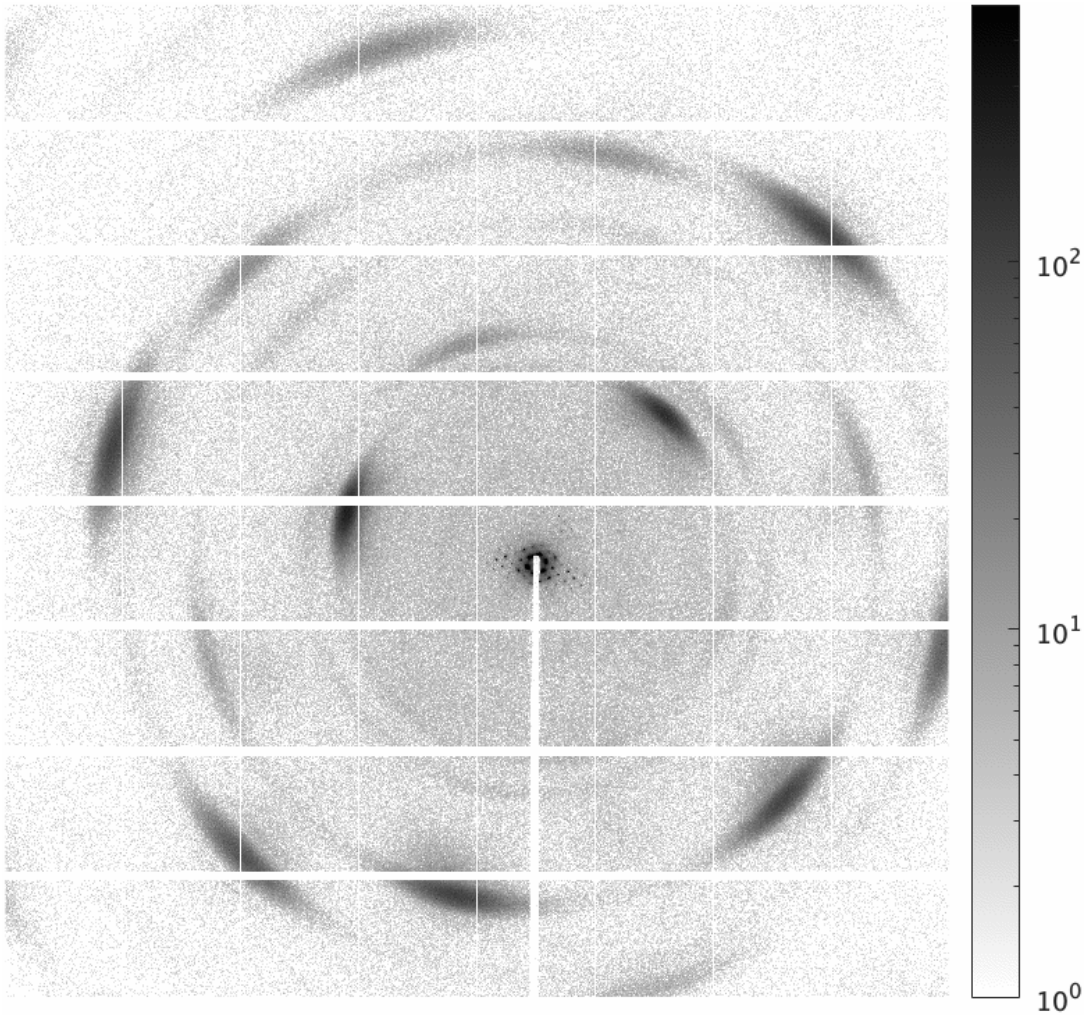

Diffraction patterns from PbS supercrystal measured at P14 (EMBL, Hamburg)

Reflection High-Energy Electron Diffraction (RHEED)

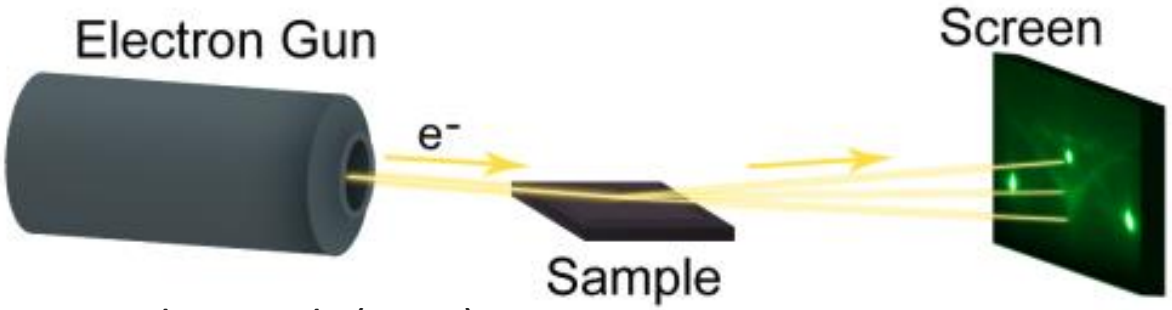

N. Derriche, *et al.* (2019).

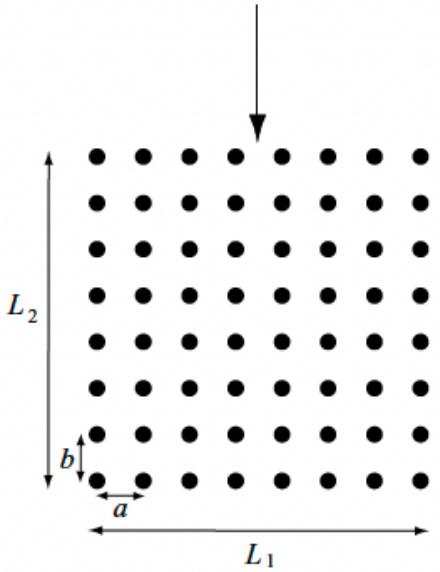

Scattering from atoms on a surface (scattering from a 2D crystal)

$$A \propto \sum_{n=1}^{N} e^{-i\vec{q}\vec{r}_n} = \sum_{n=1}^{N} e^{-i(q_x x_n + q_y y_n + q_z z_n)} = \sum_{n=1}^{N} e^{-i(q_x x_n + q_y y_n)}$$

$$z_n = 0$$

Scattering will occur (constructive interference) for certain values of q_x and q_y and all values of q_z (reciprocal rods). For example, for a simple rectangular lattice:

$$q_x = \frac{2\pi}{a} h, \qquad (h, k \ - integers)$$
$$q_y = \frac{2\pi}{b} k,$$

Reflection High-Energy Electron Diffraction (RHEED)

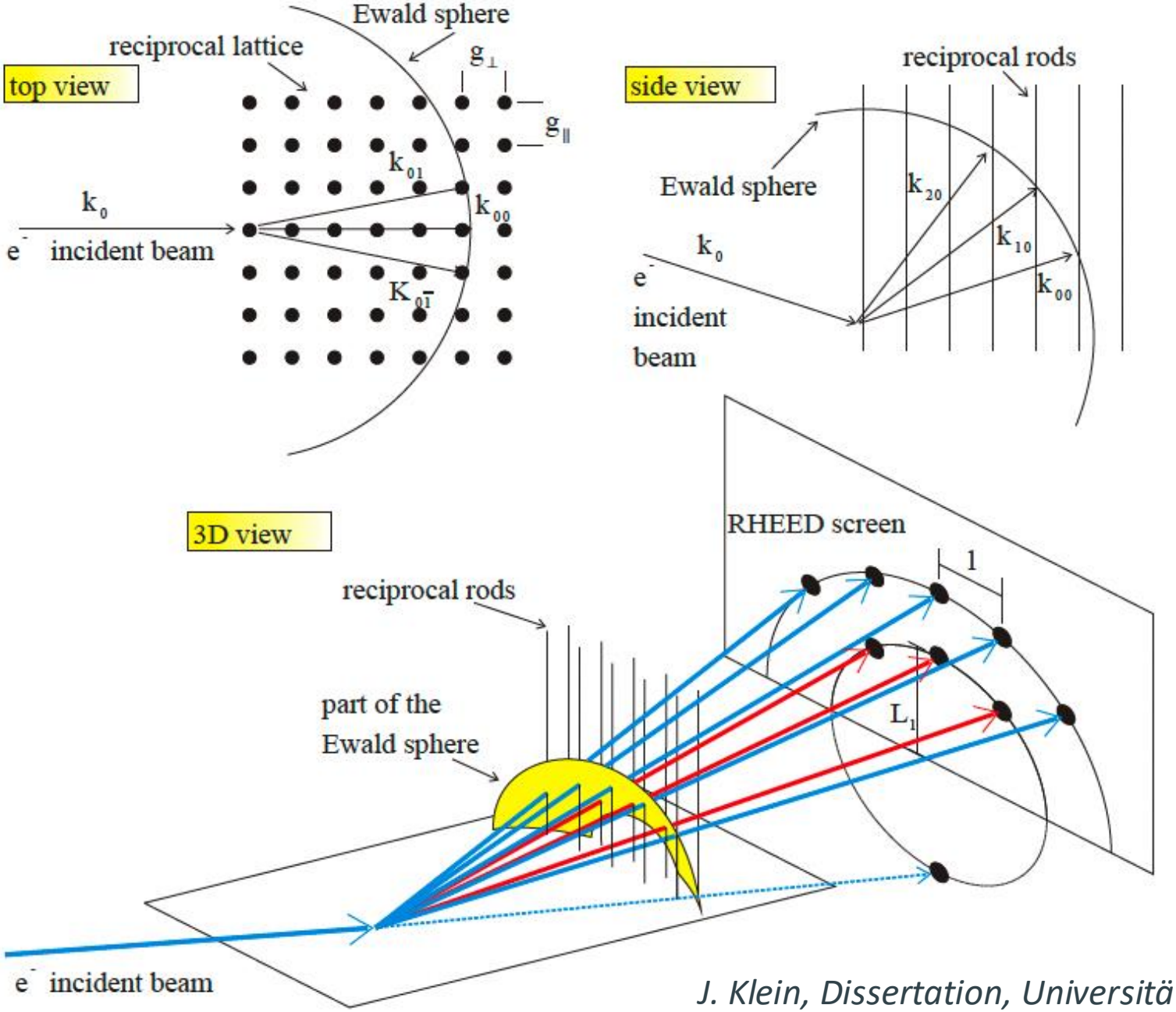

J. Klein, Dissertation, Universität zu Köln (2001)

Reflection High-Energy Electron Diffraction (RHEED)

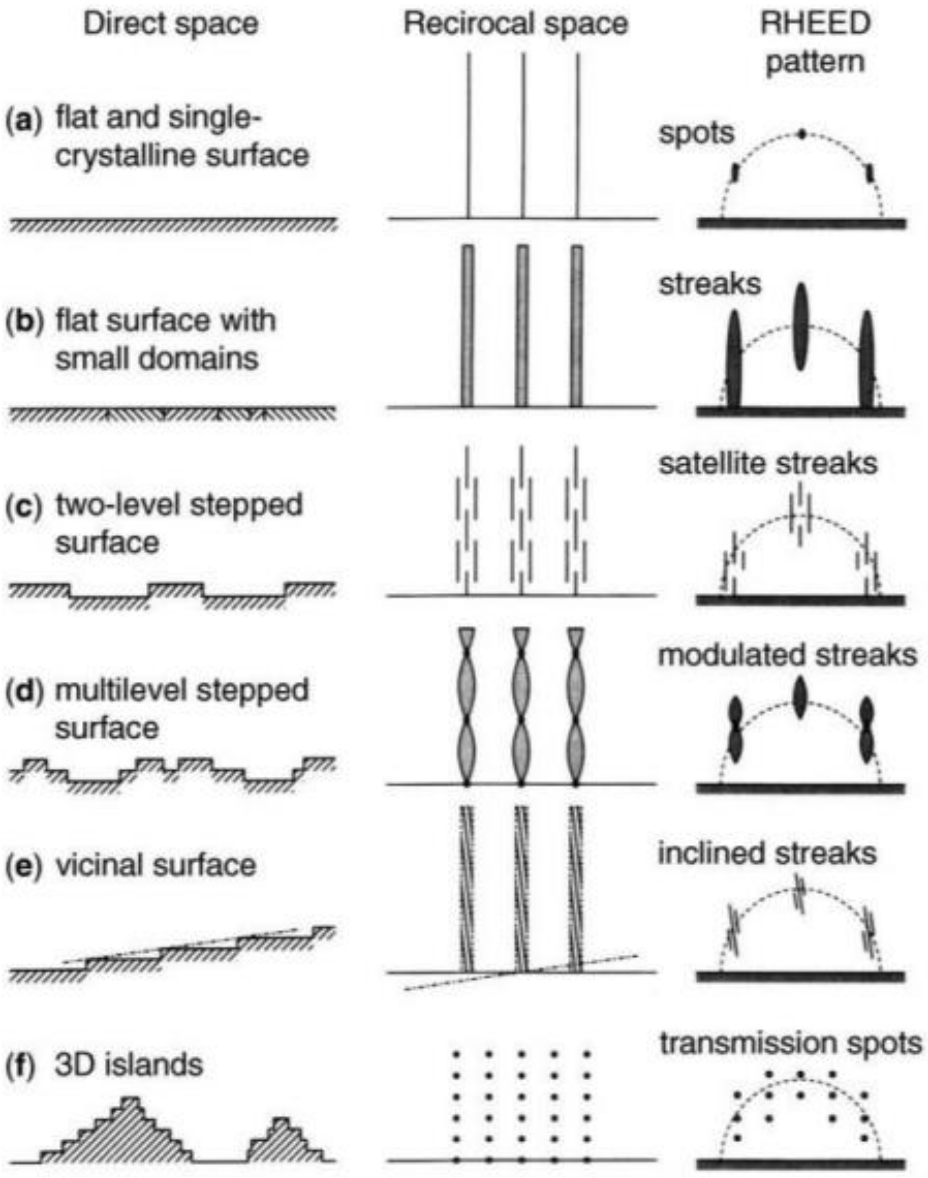

A. Ichimiya, P. Cohen (2004)

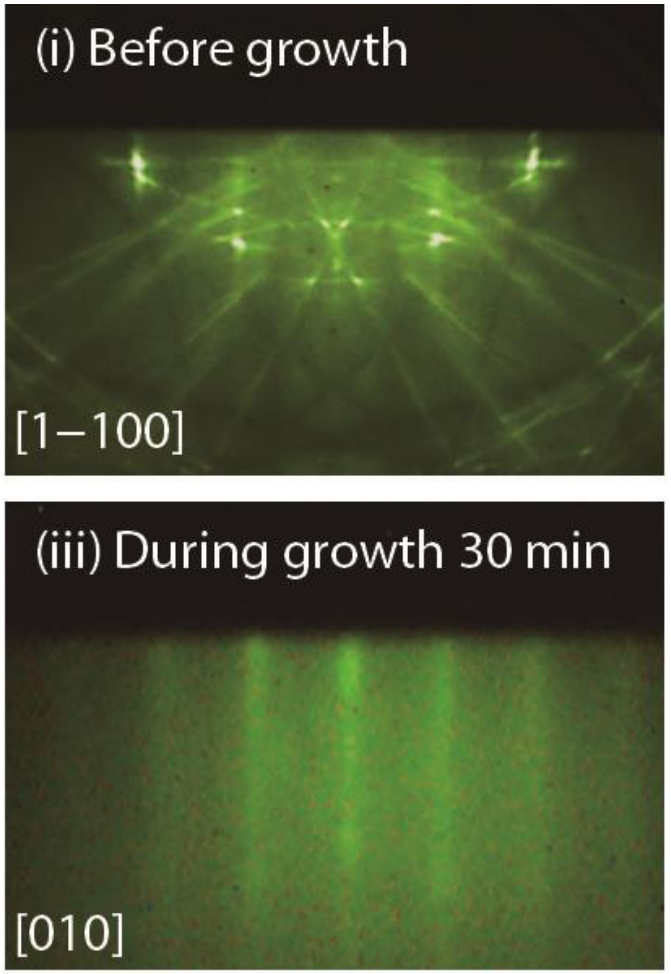

Growth of β-Ga_2O_3 on sapphire (0001-Al_2O_3)

J. Wei et al., J. Semicond. ***40*** *012802 (2019)*

Surface sensitivity

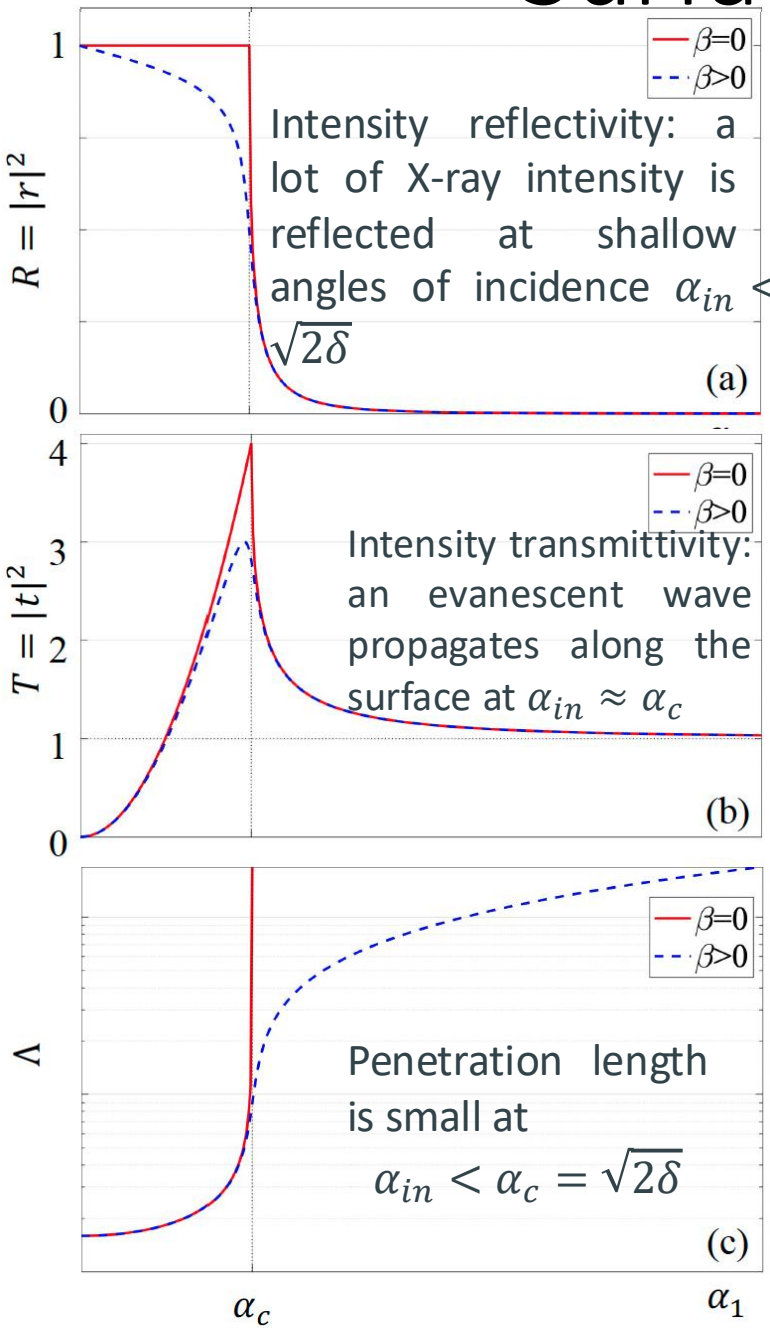

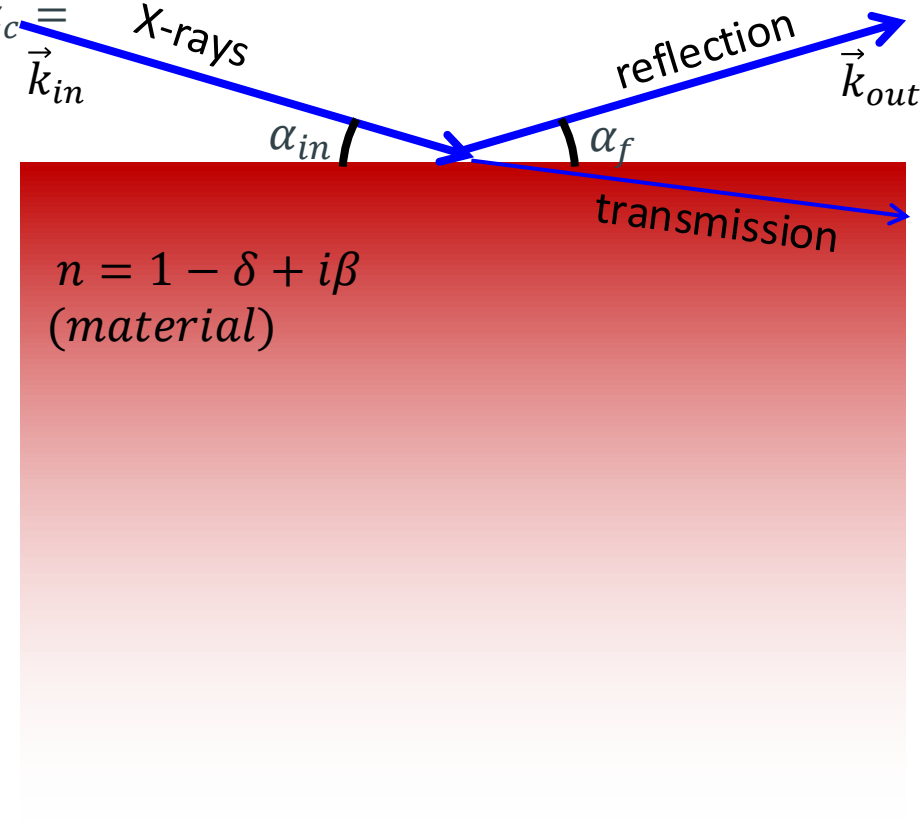

Scattering from rough surfaces

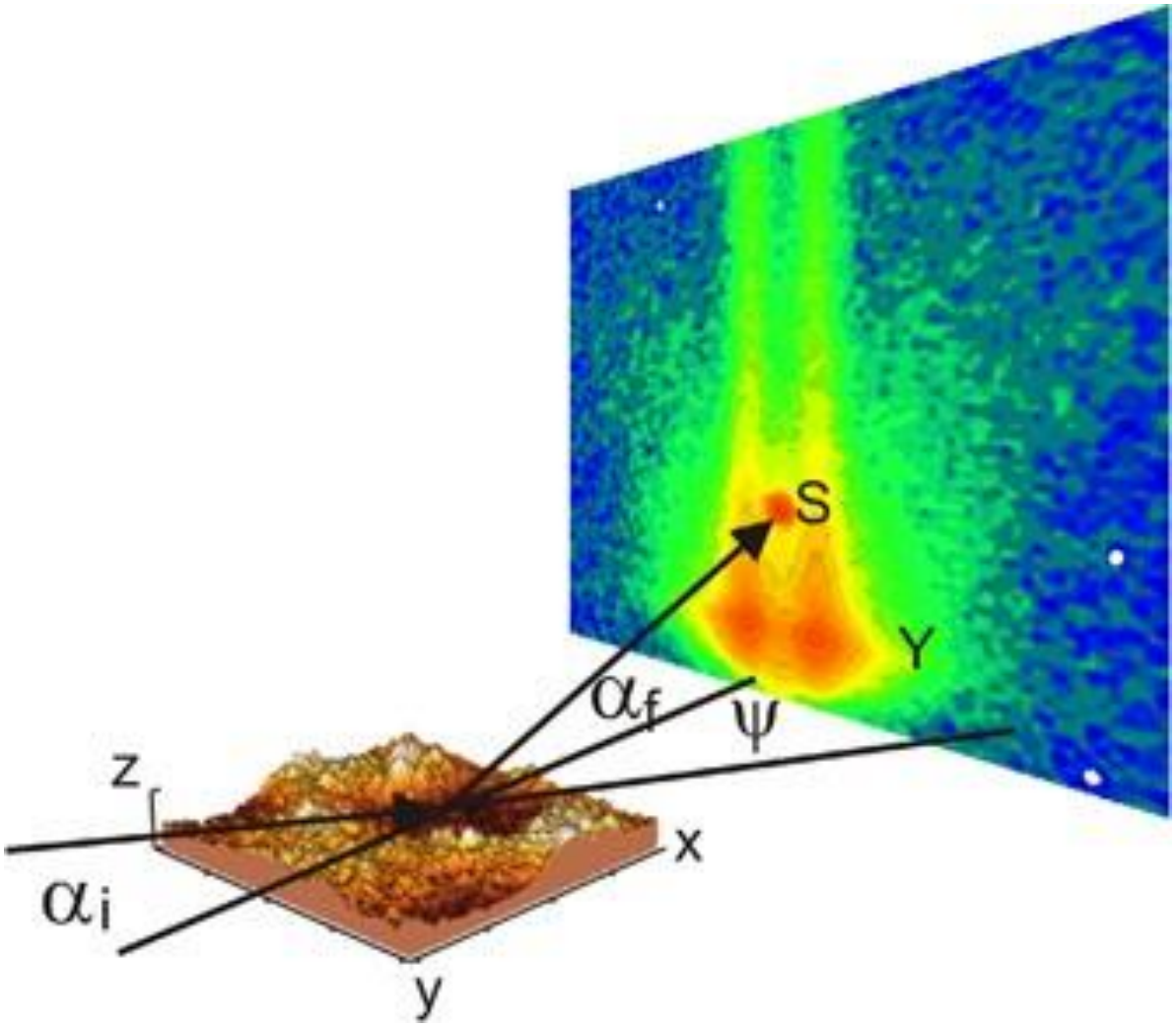

*P. Müller-Buschbaum, Polymer Journal **34** 892 (2013)*

Scattering from rough surfaces

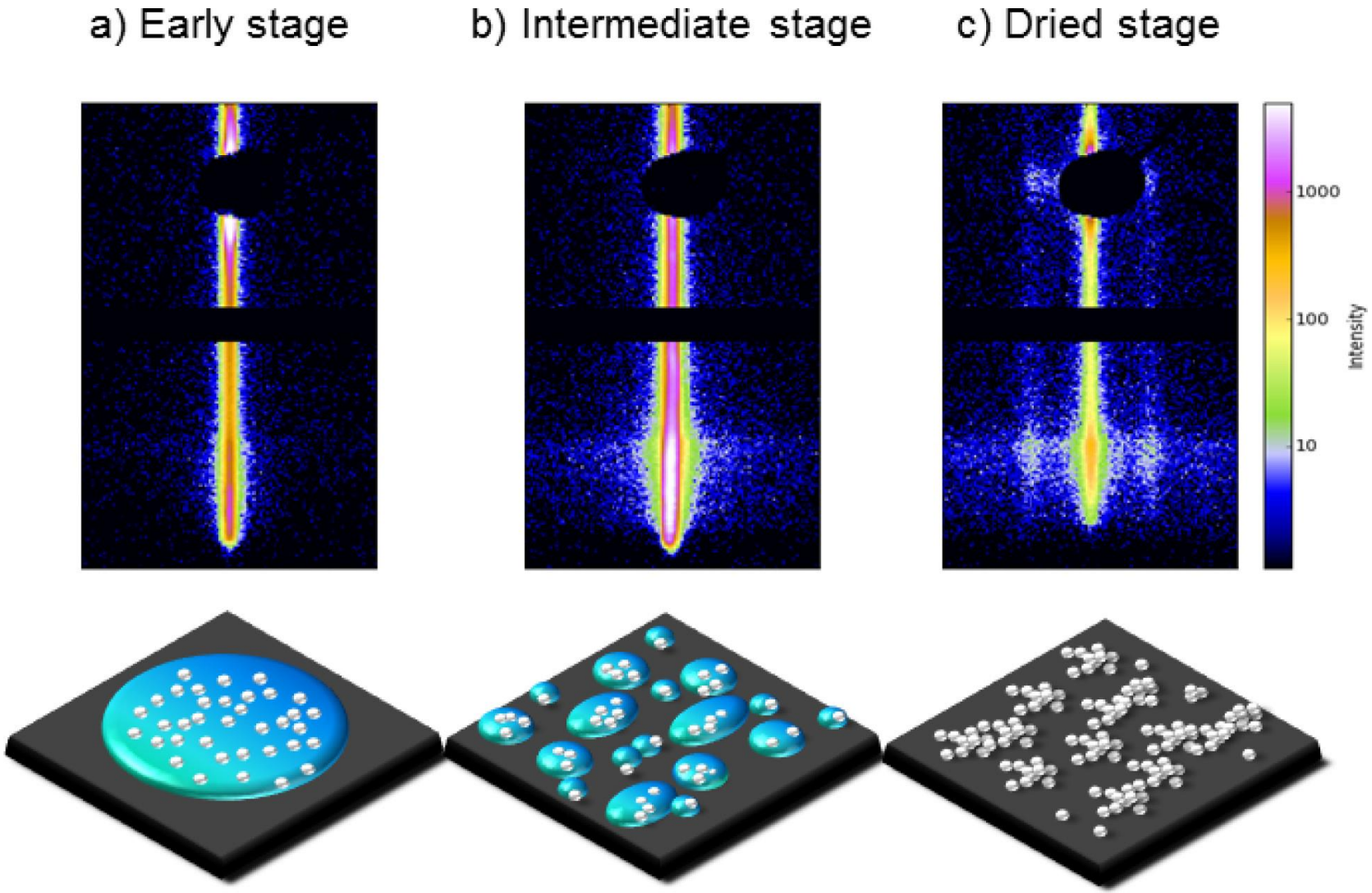

The spray deposition and subsequent self-assembly during drying of a polystyrene nanoparticle dispersion

*G. Herzog et al., Langmuir **29** 11260 (2013)*

Scattering from rough surfaces

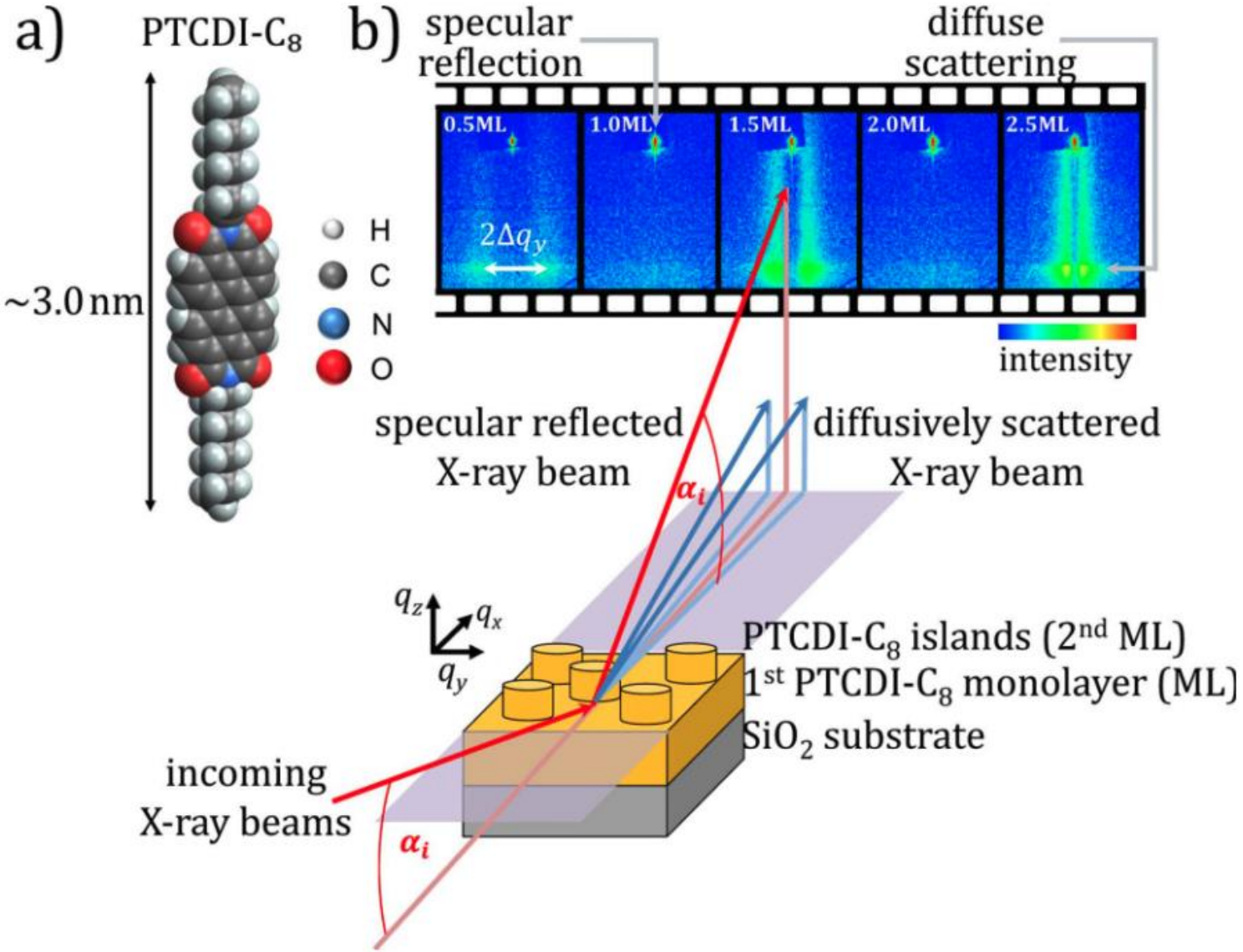

A. Zykov et al, J. Chem. Phys. ***146****, 052803 (2017)*

Absorption spectroscopy

Probe

System

Measured spectrum

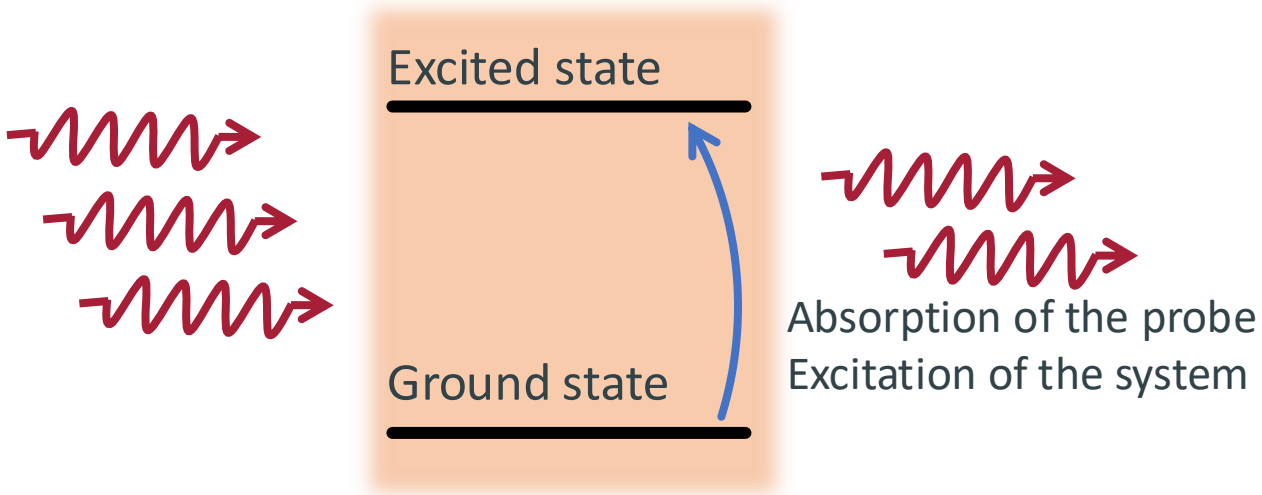

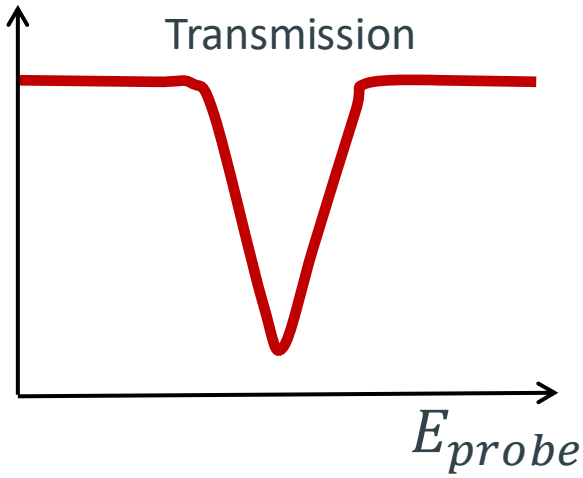

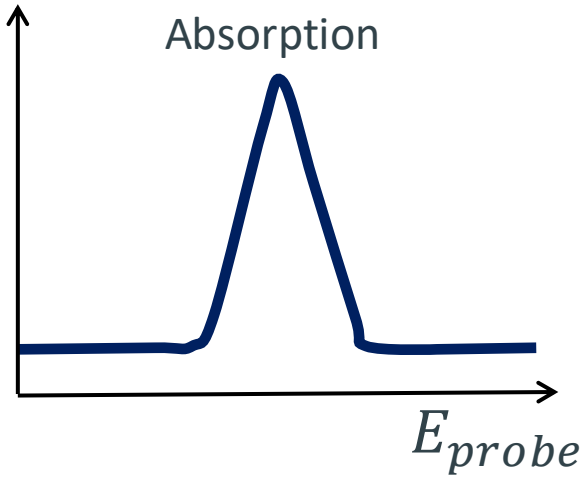

- Electromagnetic wave

Electromagnetic spectrum

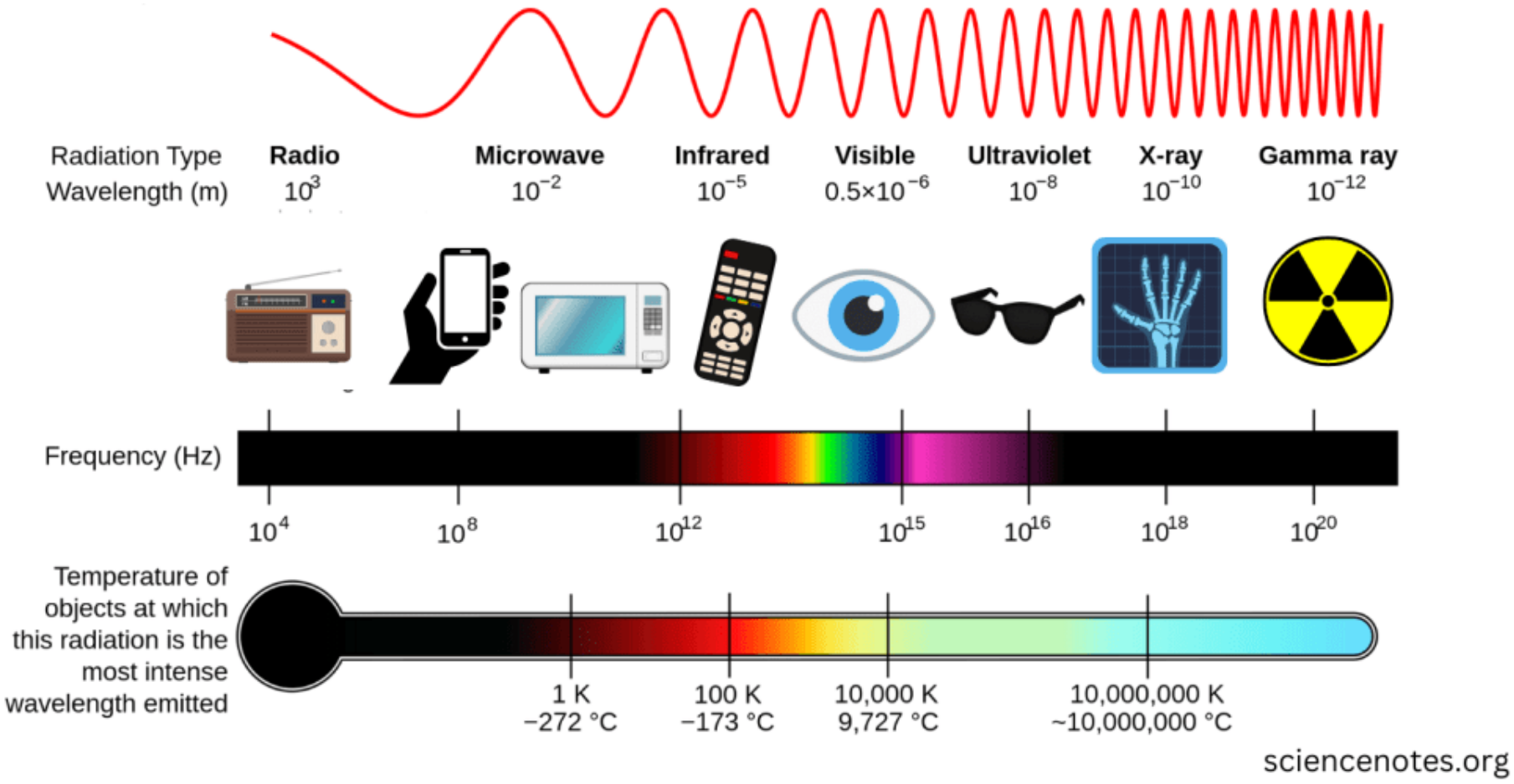

Characteristic time and length scales

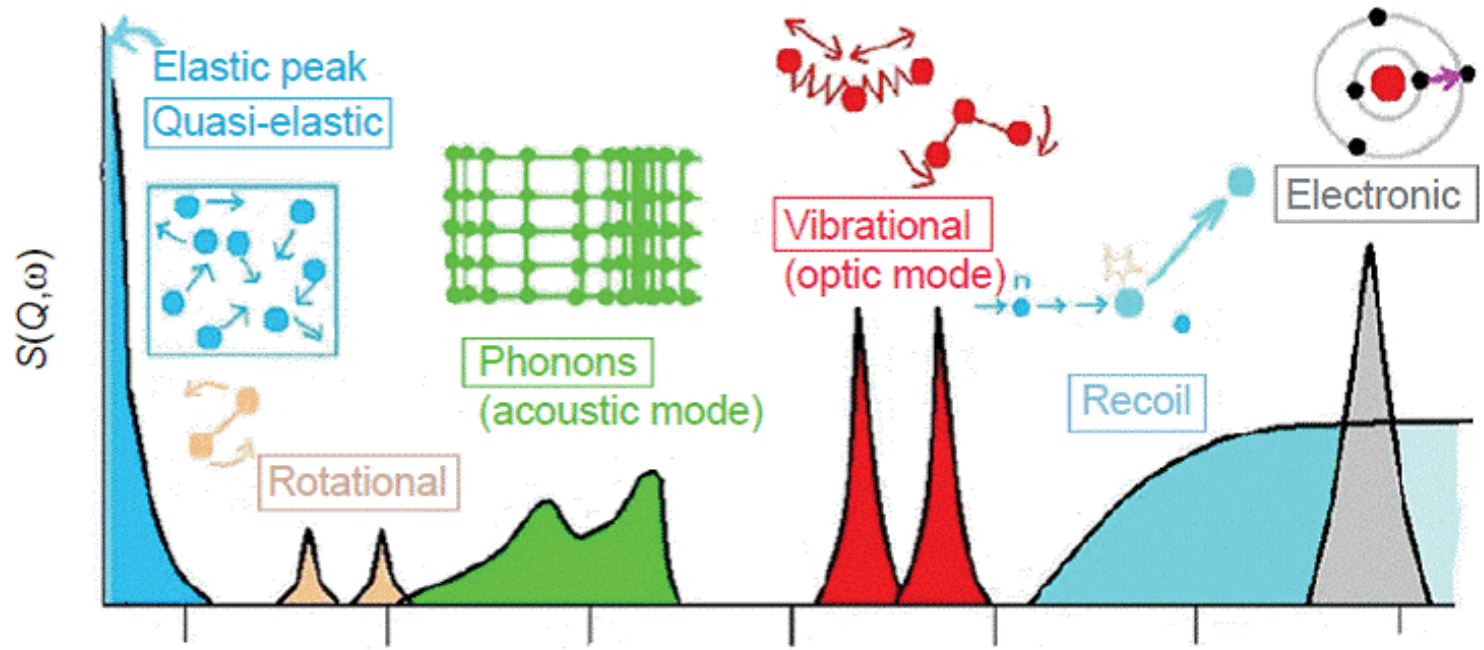

$\Delta E \Delta t \approx \hbar$

Energy transfer, ΔE(ev)	10^{-4}	10^{-3}	10^{-2}	10^{-1}	1	10	10^{2}
Timescale, Δt(sec)	10^{-7}–10^{-11}	10^{-12}	10^{-13}	10^{-14}	10^{-15}	10^{-16}	
Length probed, Å	>30	10	1	0.1	0.001	0.0001	0.00001

Molecular orbitals

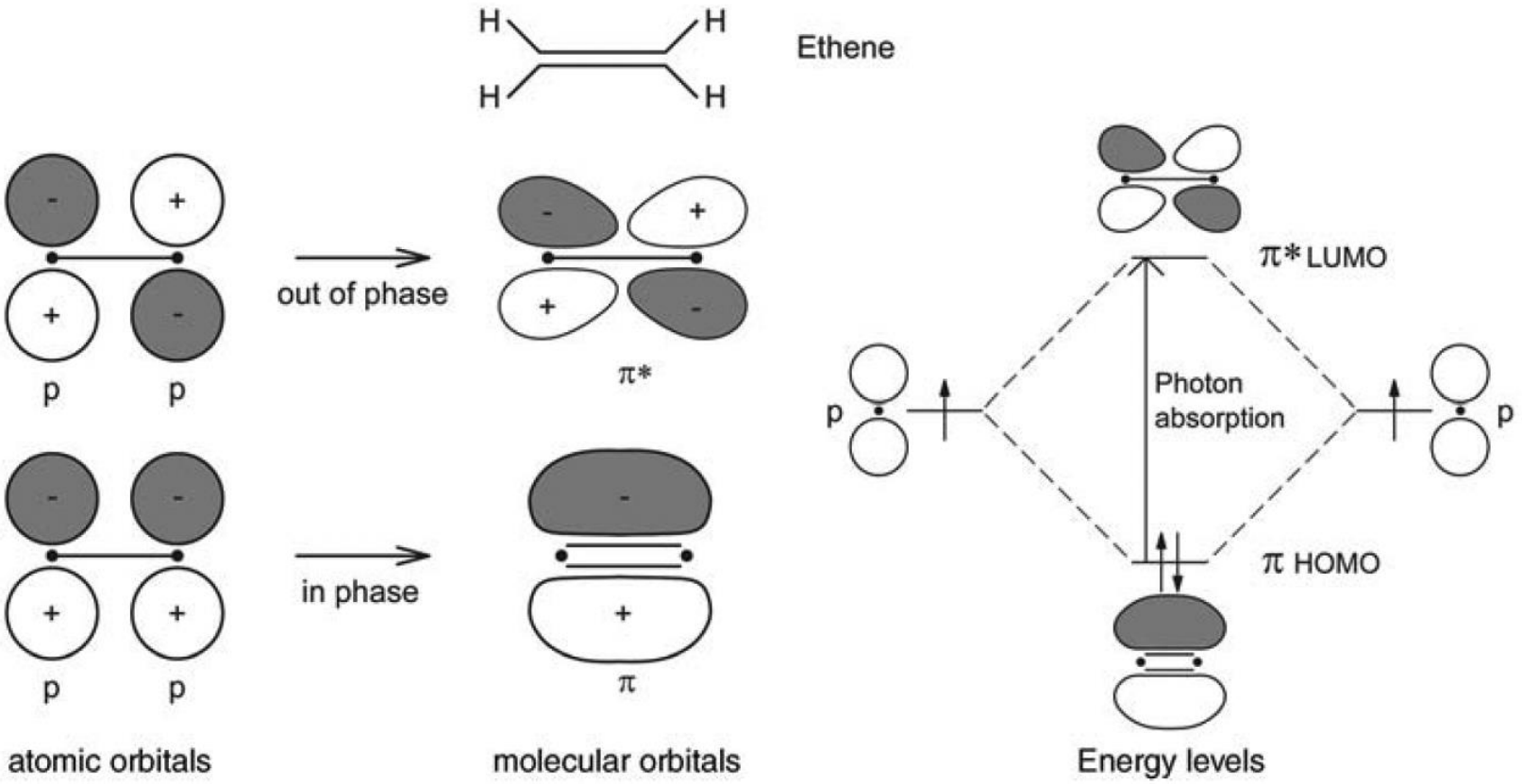

Figure 1.4 Schematic construction of bonding and antibonding molecular π-orbitals from atomic p-orbitals in the case of ethene.

P. J. Walla, *Modern Biophysical Chemistry* (2014)

Molecular orbitals

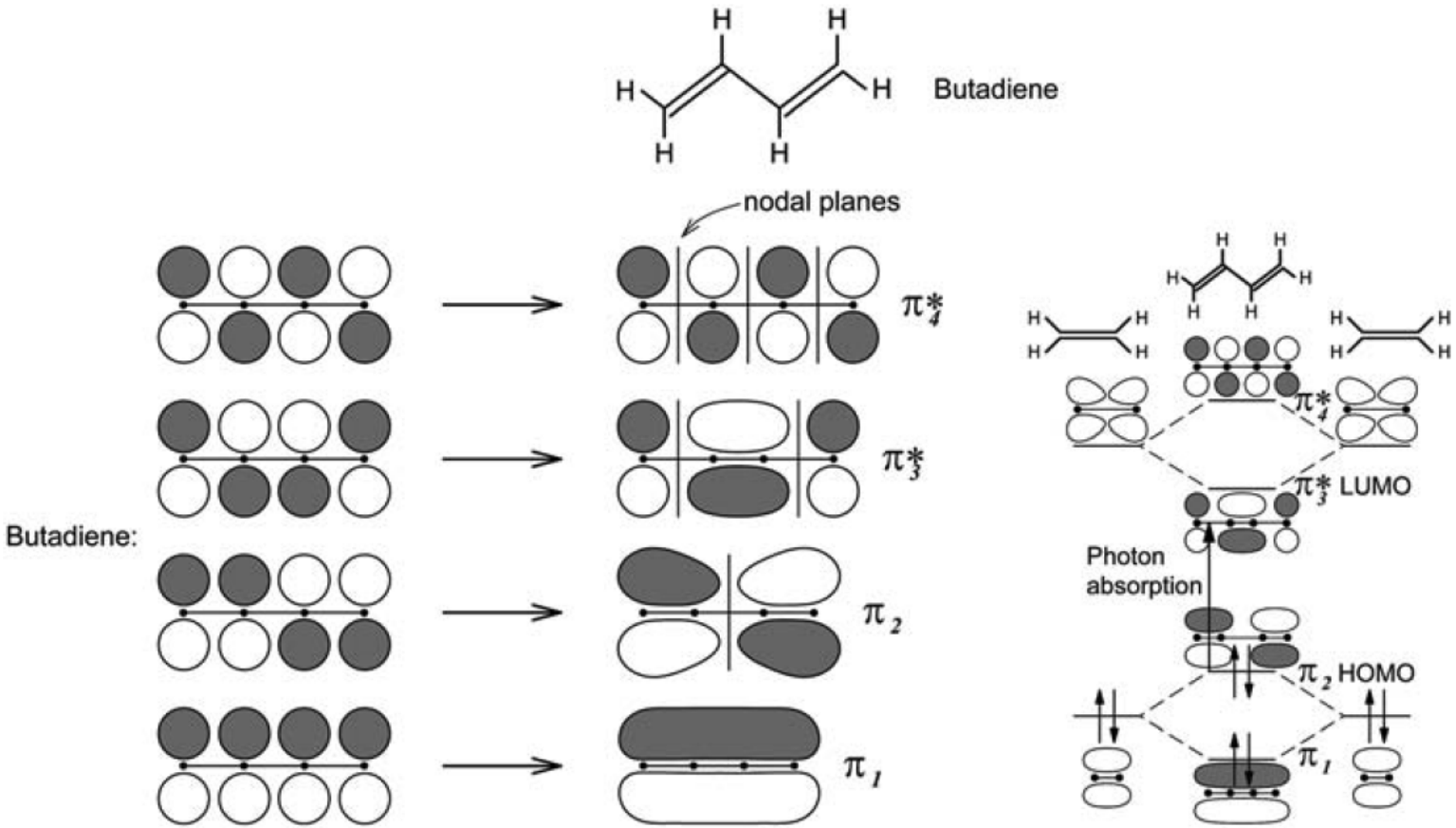

Figure 1.5 Schematic construction of an extended molecular π-orbital system from conjugated atomic p-orbitals. The example corresponds to butadiene. The HOMO and LUMO of butadiene correspond to the π_2 and π_3^* orbitals, respectively. The four molecular orbitals π_1, π_2, π_3^*, π_4^* of butadiene can also be thought of as being constructed from the two molecular orbitals, π, π*, of two ethene molecules. Direct comparison of the energy levels of the HOMO and LUMO of ethene with the HOMO and LUMO of butadiene shows that the energy gap of the latter is smaller.

P. J. Walla *Modern Biophysical Chemistry* (2014)

Light-matter interaction

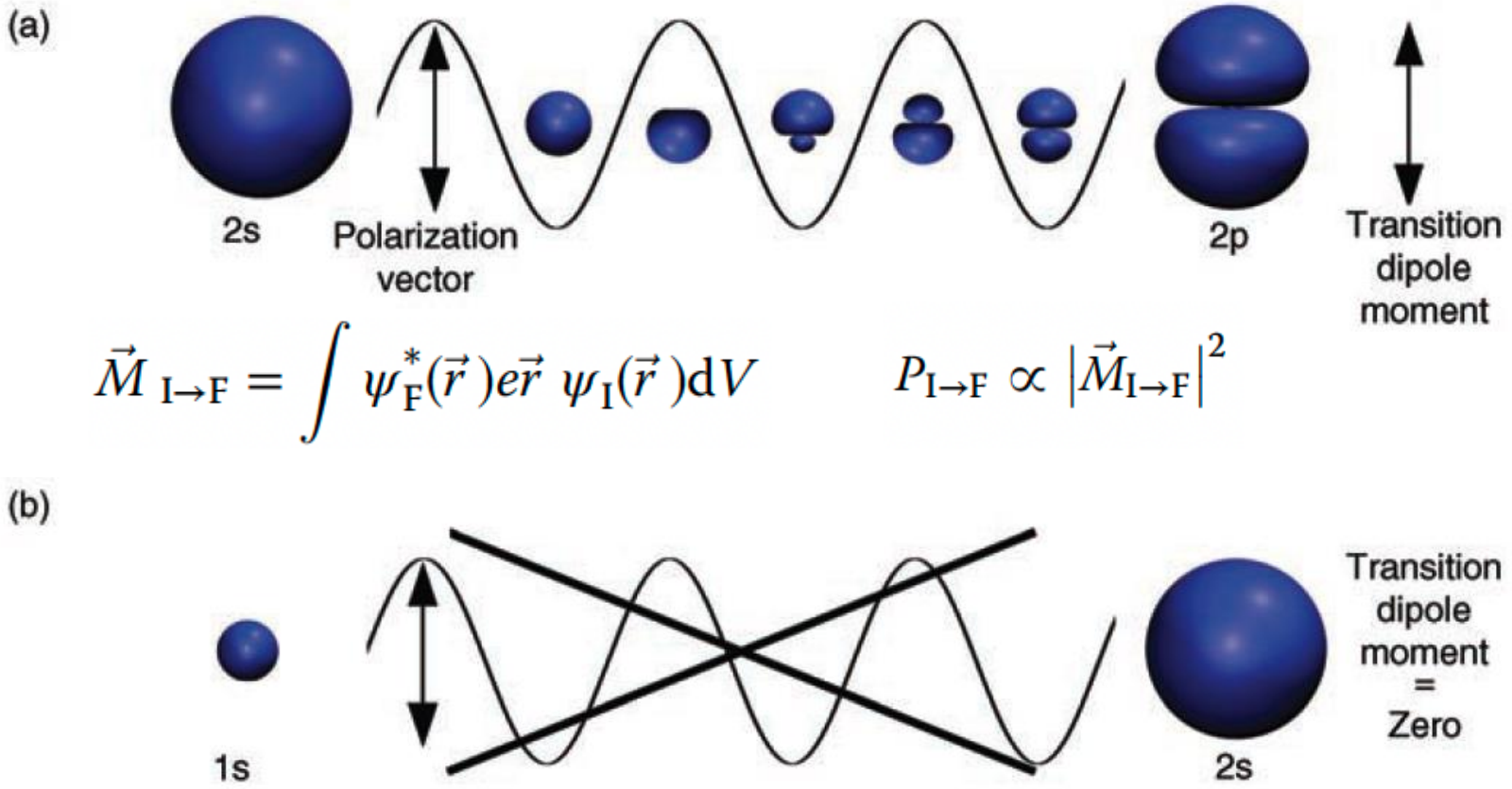

Figure 1.7 (a) The oscillating electric field component of light can induce a transition from an s to a p orbital when it has the correct polarization (direction of oscillating electric field component of light). Please note that here probability densities and not wave functions are visualized. The response of the electron probability densities to the oscillating electric field during the transition is also schematically illustrated. (b) In contrast, the oscillating electric-field component of light cannot induce a transition from one s-orbital to another s orbital. Figure created using VMD (see Bibliography for details).

P. J. Walla, *Modern Biophysical Chemistry* (2014)

Ultraviolet-visible spectroscopy

Probes electronic transitions; can be used for qualitive and quantitative analysis.

Example: determination of nanoparticle size by absorption and/or fluorescence

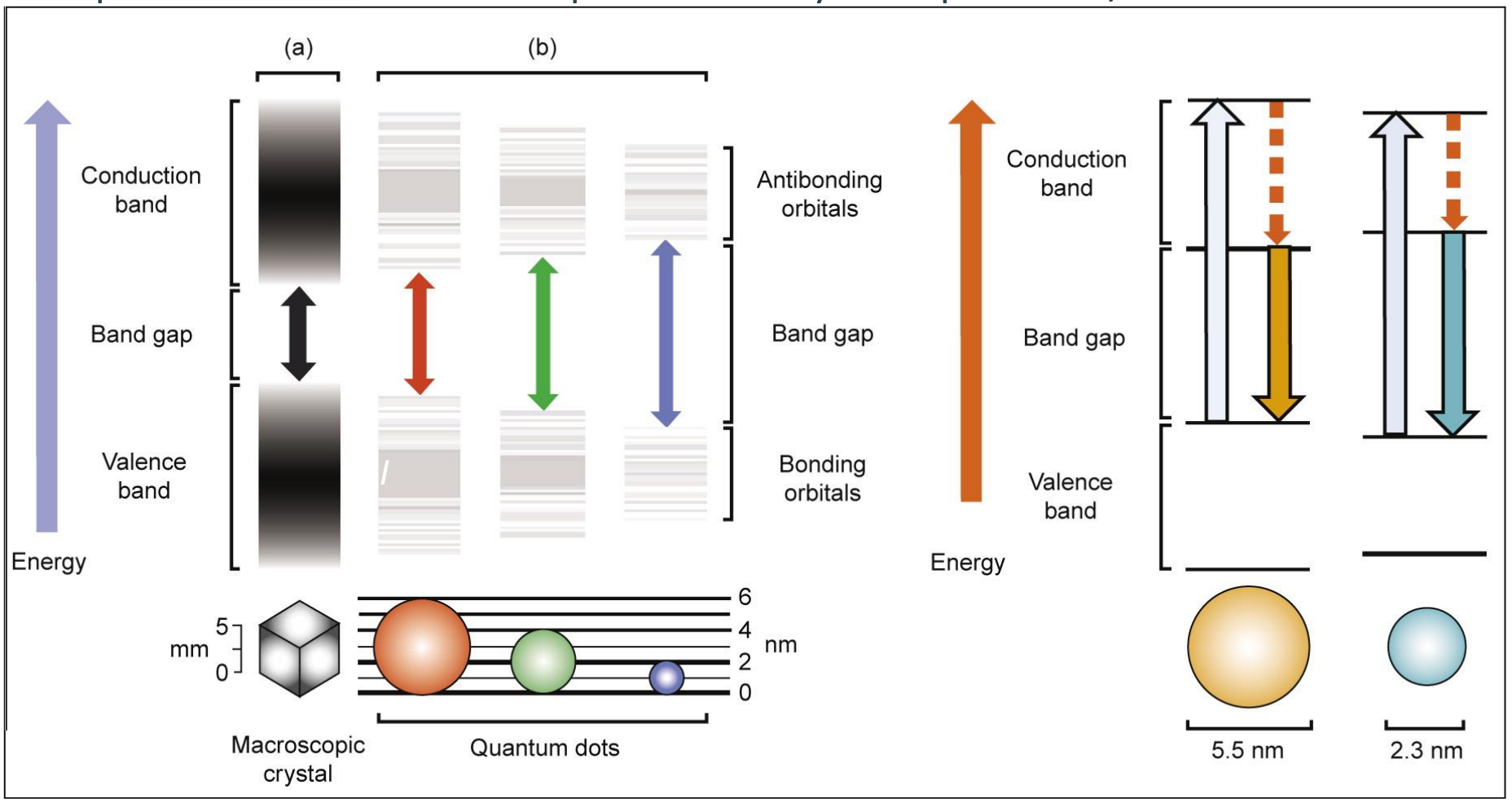

D. Ioannou and D. K. Griffin , *Nano Rev.*, **1** , 5117 (2010)

Ultraviolet-visible spectroscopy

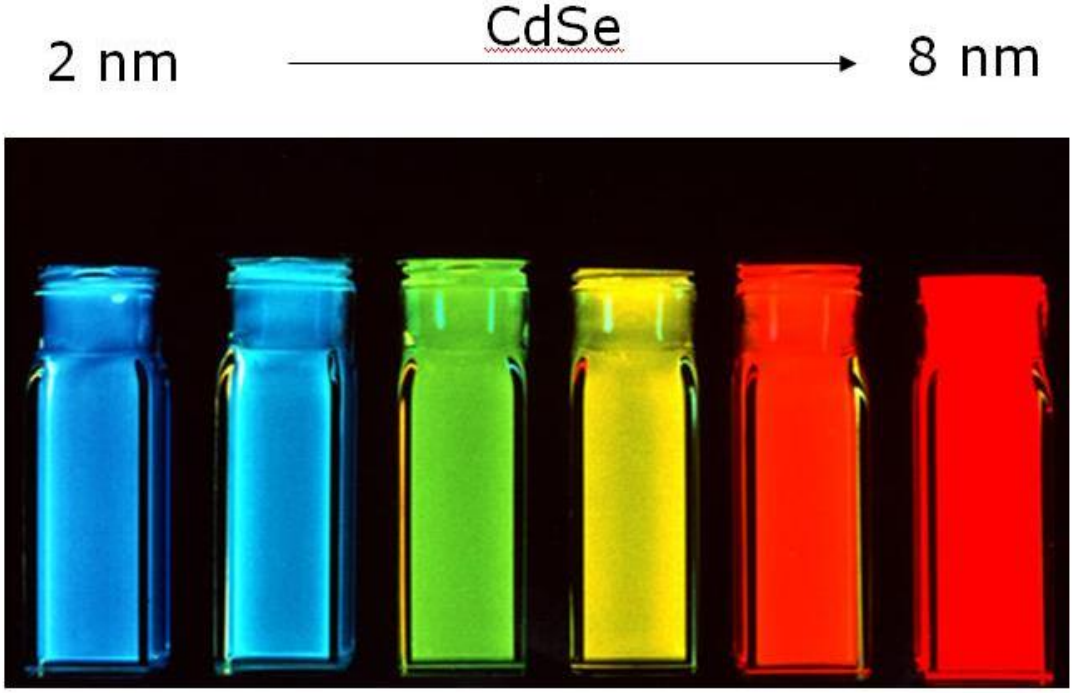

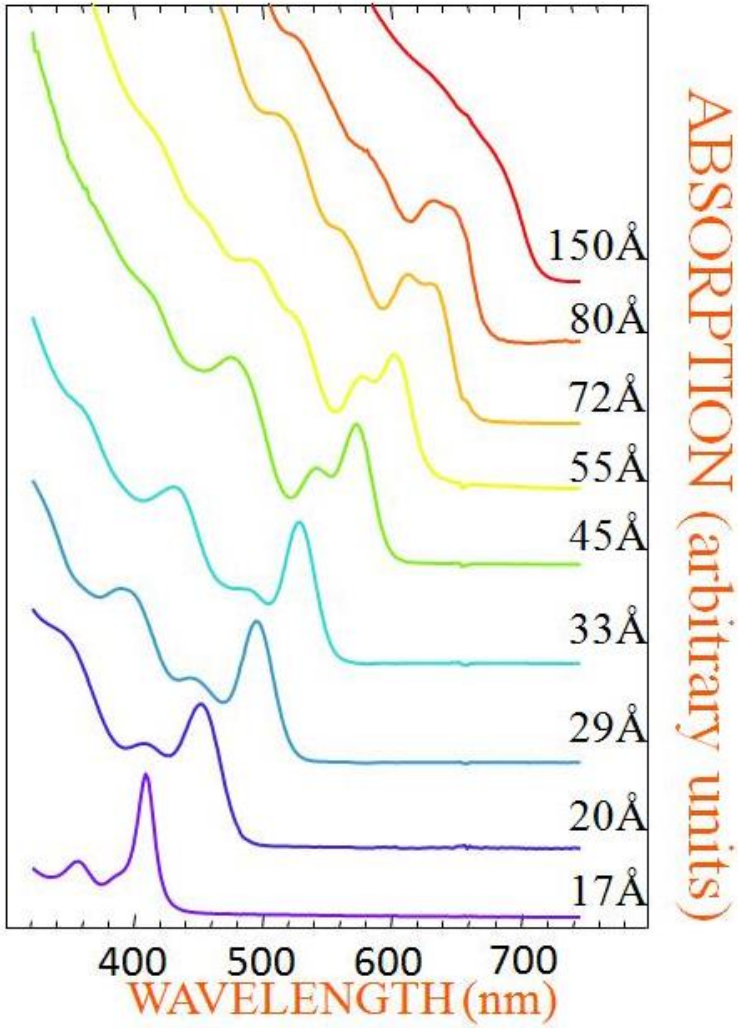

https://serc.carleton.edu/details/images/180093.html

Vibrational excitations and Franck–Condon principle

Equilibrium nuclear positions are the same for S_0 and S_1

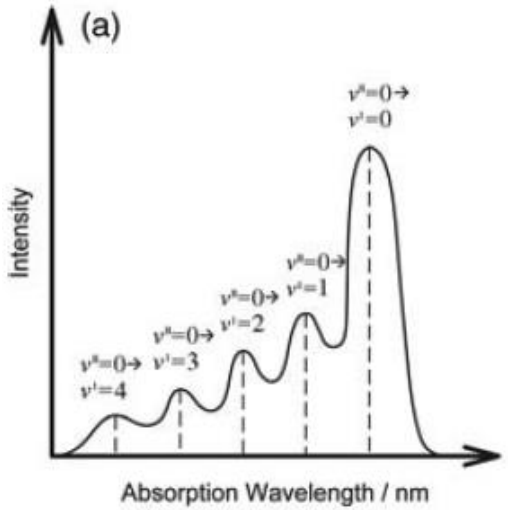

Equilibrium nuclear positions are different for S_0 and S_1

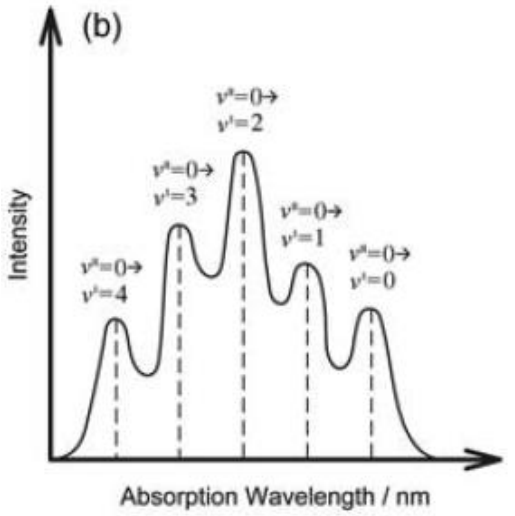

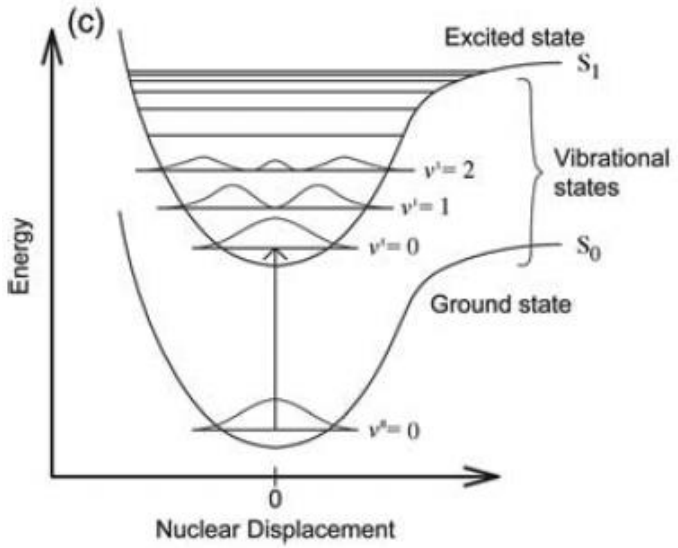

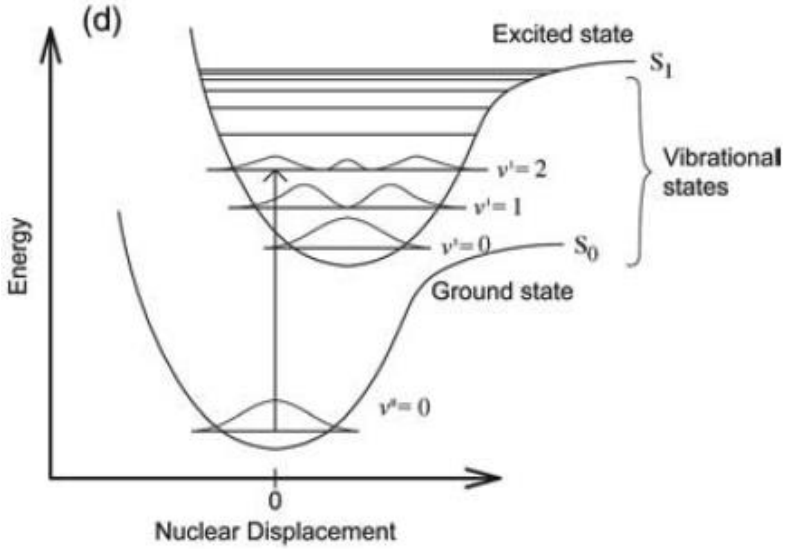

P. J. Walla, *Modern Biophysical Chemistry* (2014)

Infrared spectroscopy

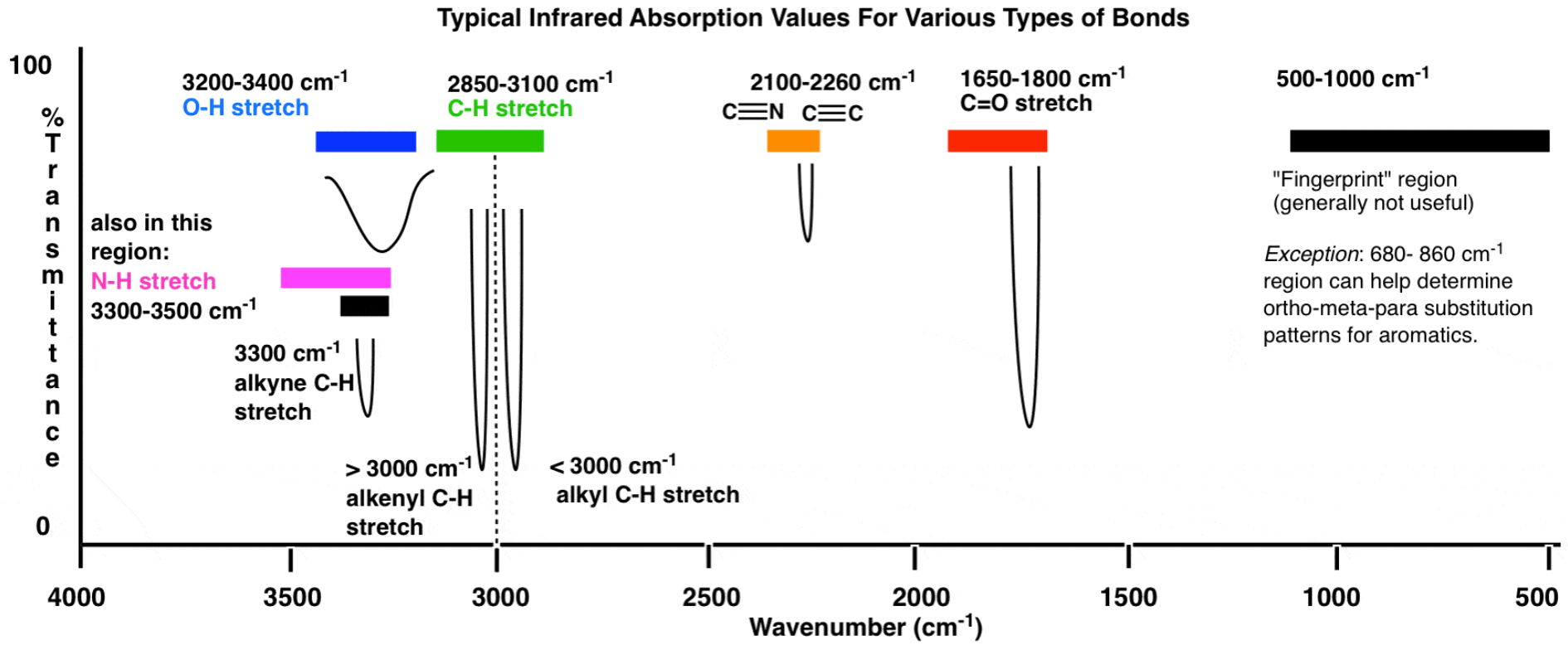

https://www.masterorganicchemistry.com/2016/11/23/quick_analysis_of_ir_spectra/

Infrared spectroscopy

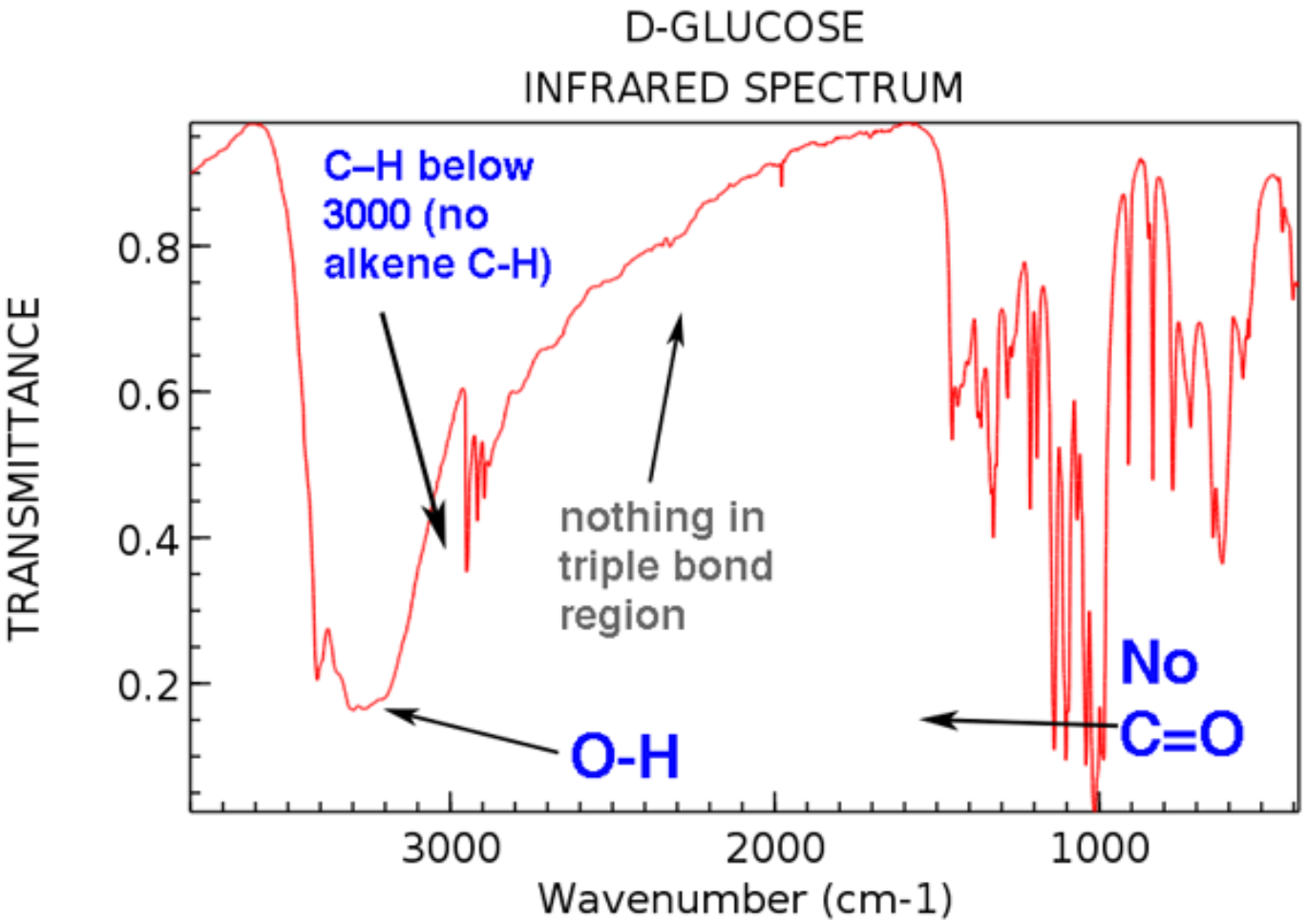

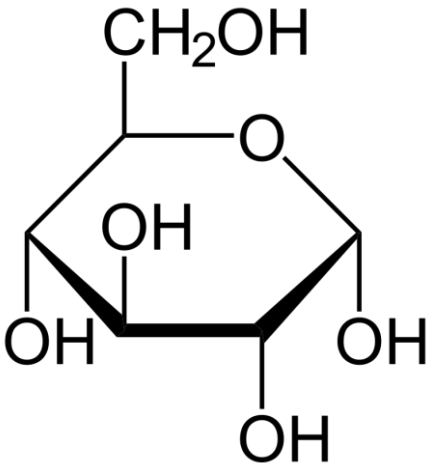

https://www.masterorganicchemistry.com/2016/11/23/quick_analysis_of_ir_spectra/

What happens after absorption?

Jablonski diagram

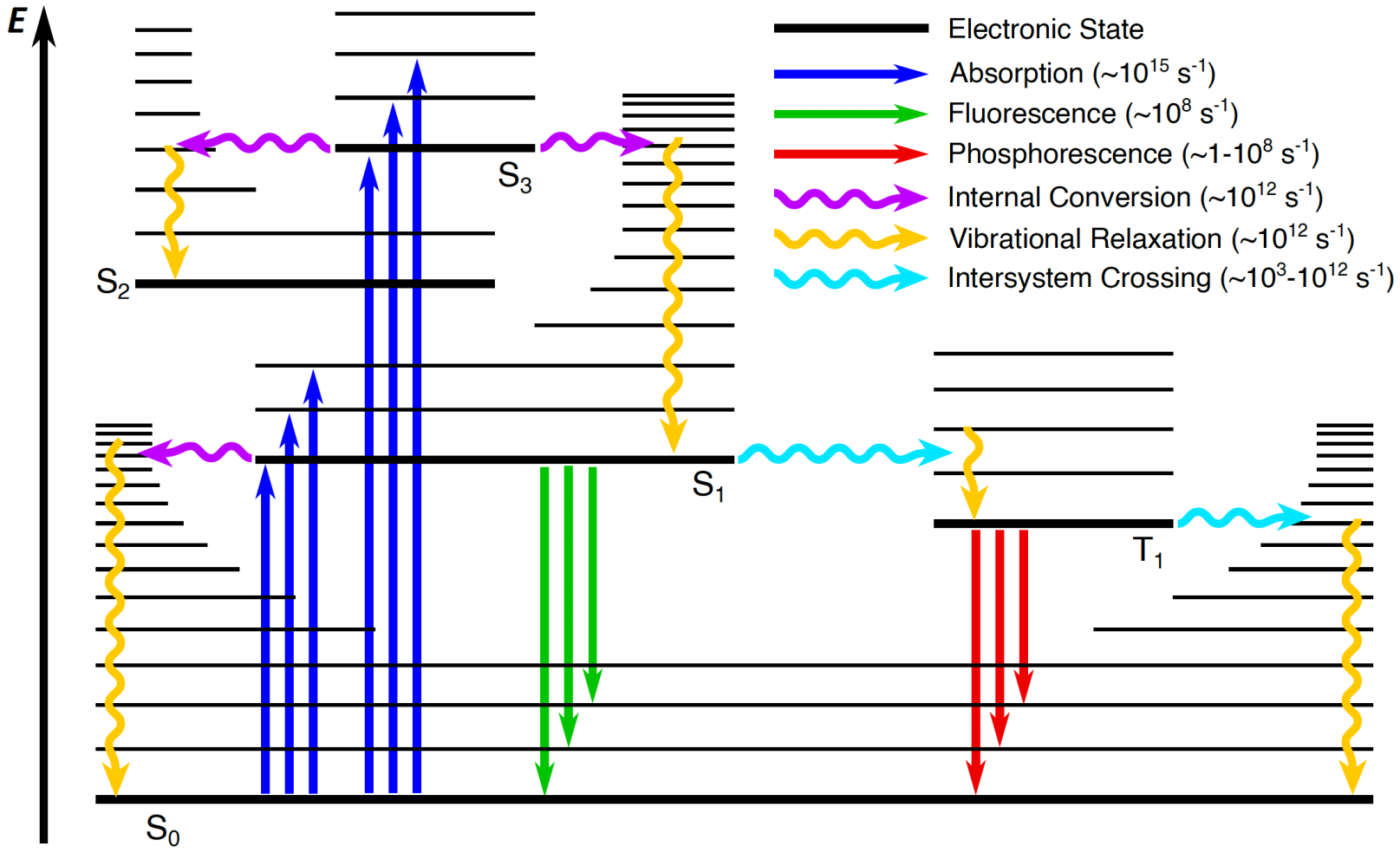

What happens after absorption?

Intersystem crossing and phosphorescence

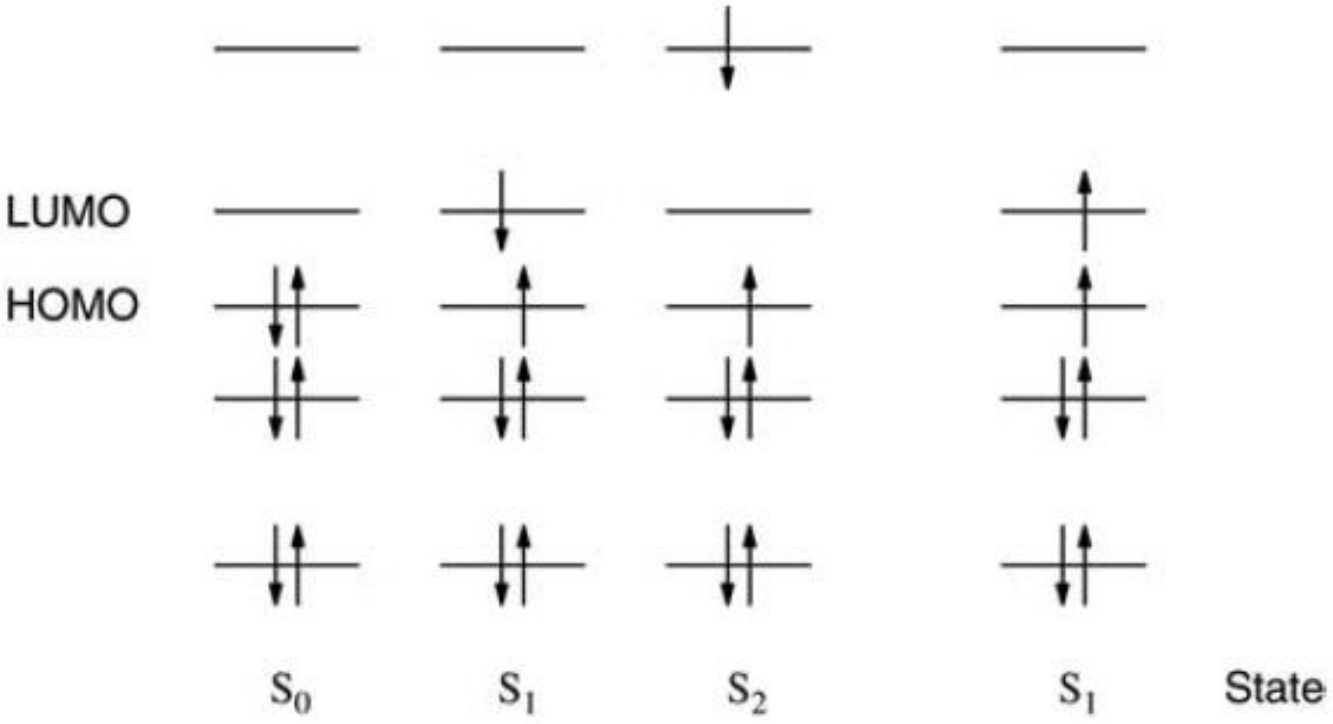

Figure 1.14 Possible excited-state configurations.

P. J. Walla, *Modern Biophysical Chemistry* (2014)

What happens after absorption?

Intersystem crossing and phosphorescence

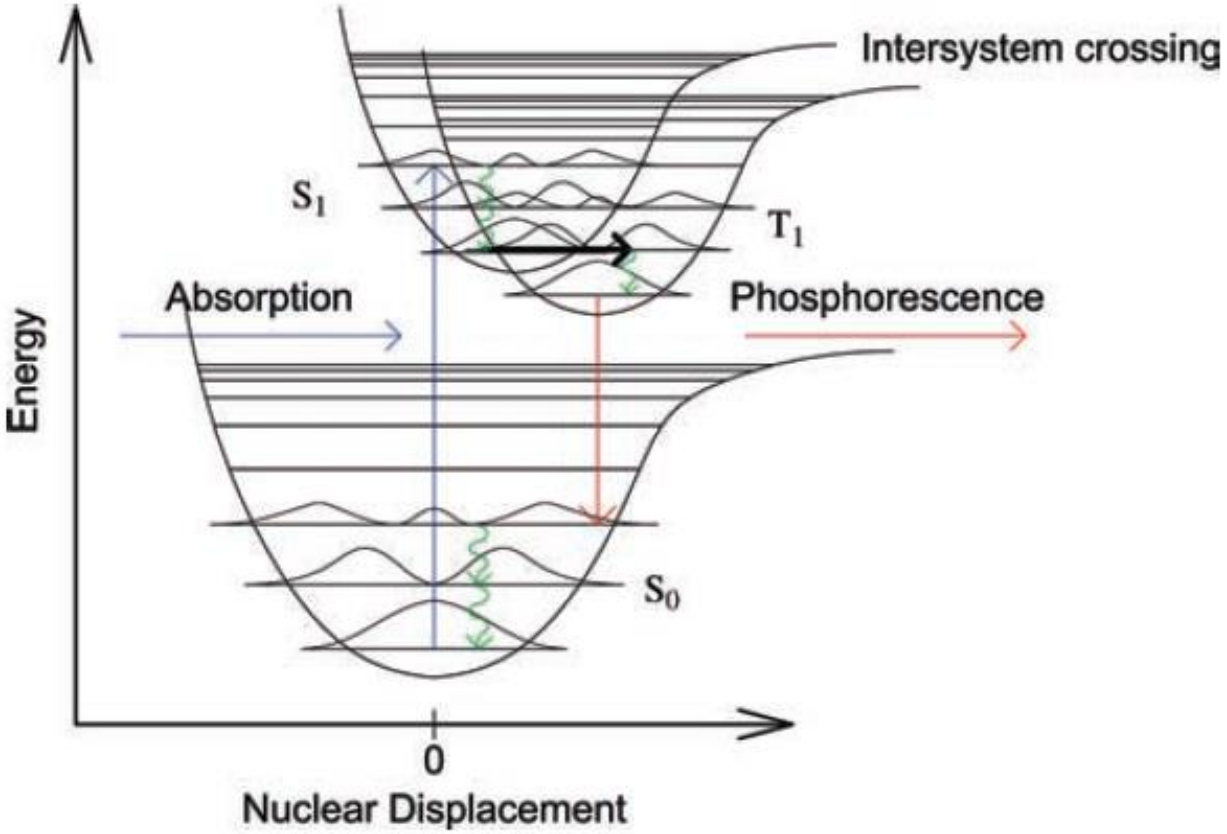

Figure 1.16 Visualization of triplet-state formation (intersystem crossing) and phosphorescence.

P. J. Walla, *Modern Biophysical Chemistry* (2014)

Emission spectroscopy

Probe

System

Measured spectrum

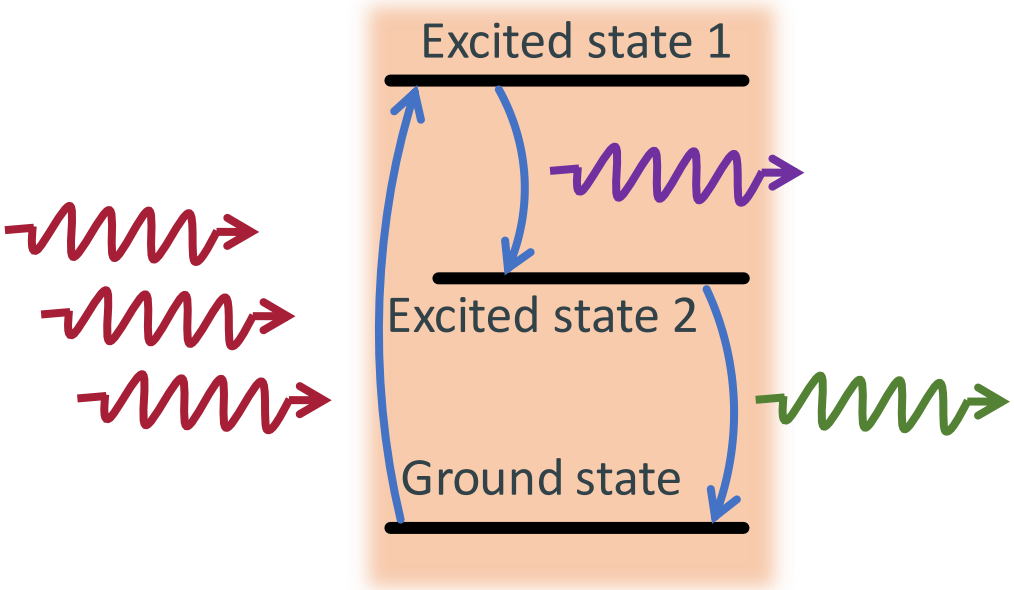

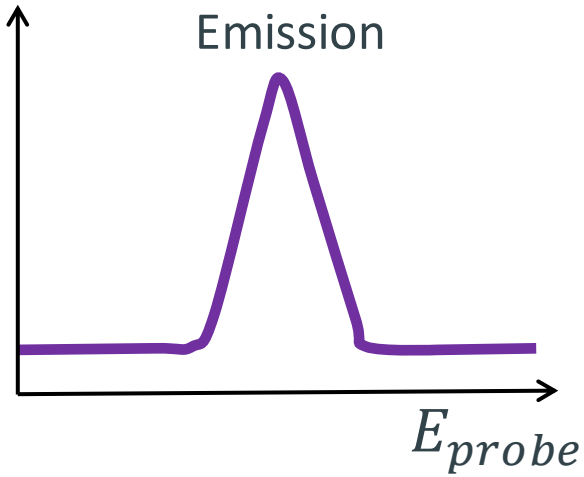

Emission is not necessary of the same nature as the probe.
For example, it can be:

- incoming probe: x-ray
- emission: photoelectron

Raman spectroscopy

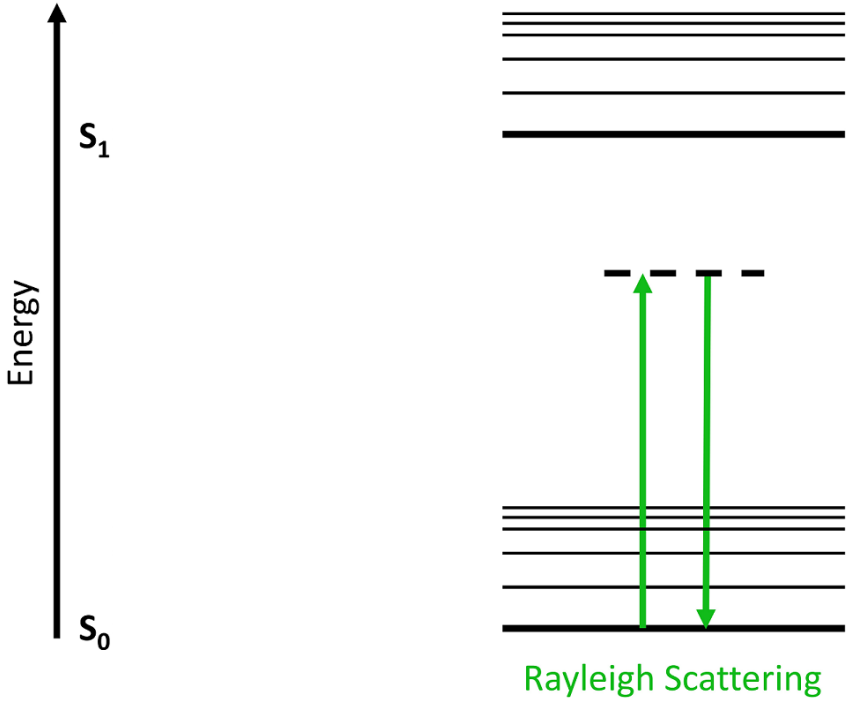

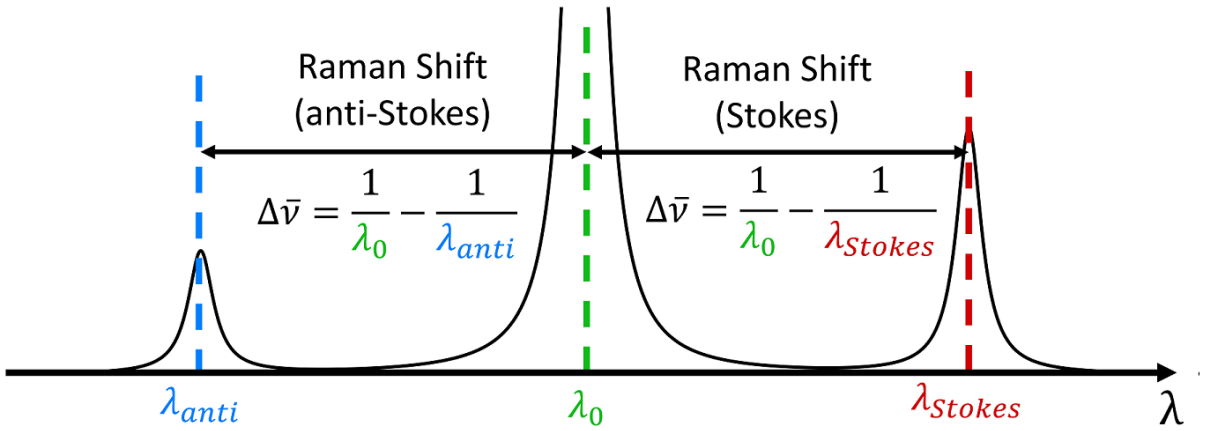

https://www.edinst.com/blog/what-is-raman-spectroscopy/

Raman spectroscopy

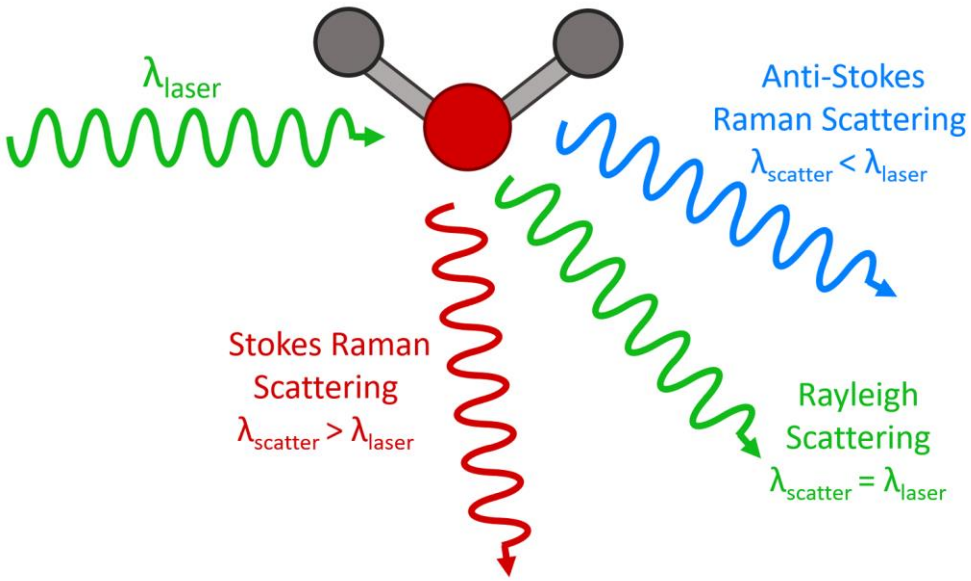

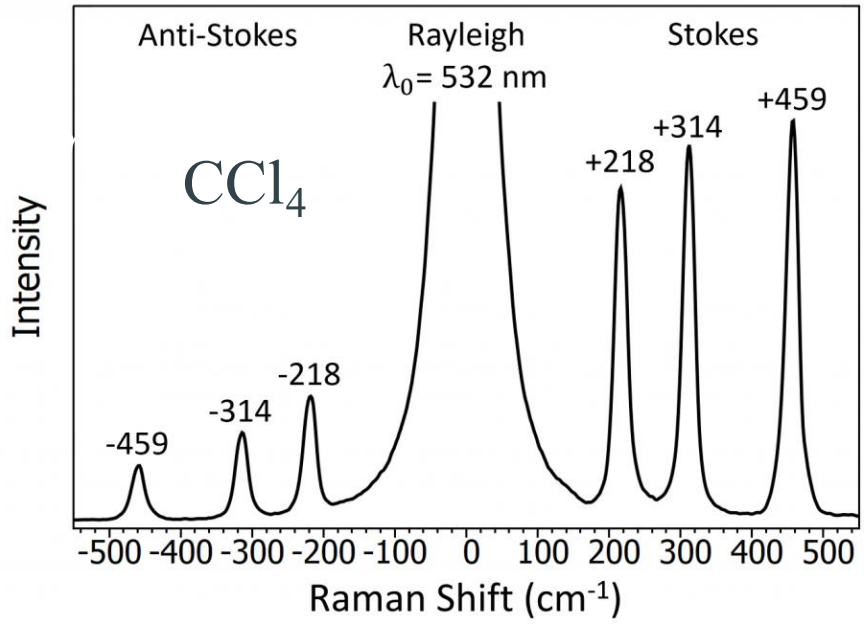

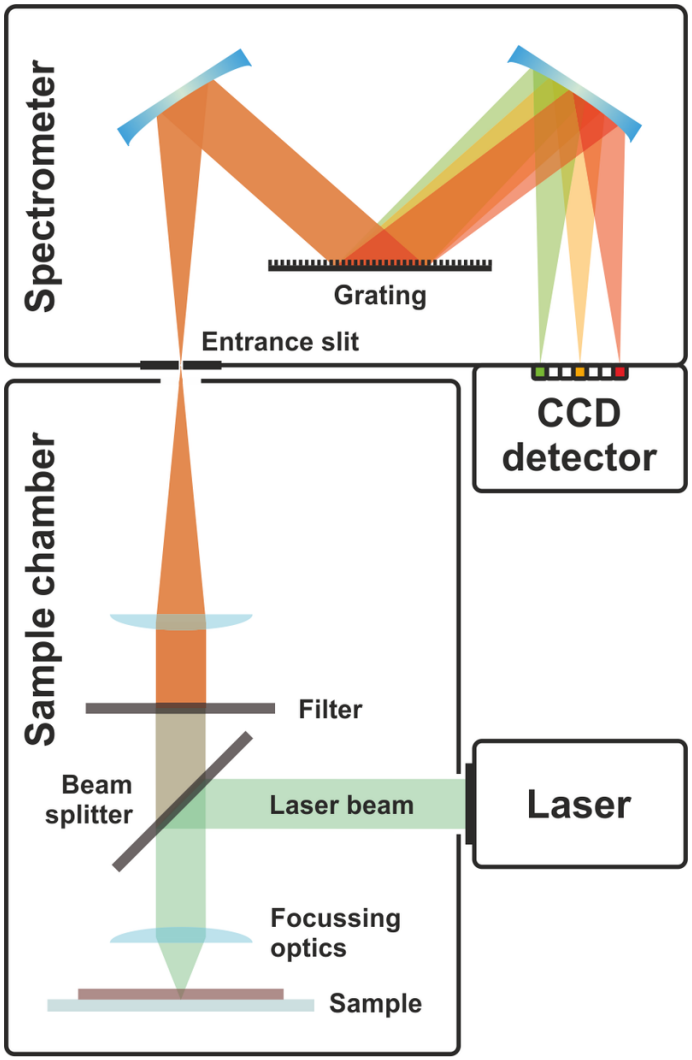

T. Schmidt, P. Dariz, Heritage **2** 1662 (2019)

Raman spectroscopy

Functional group	Raman Shift (cm^{-1})
O-H	3600-3000
N-H	3500-3100
C-H	3100-2800
C≡C	2200-2100
C=O	1750-1700
C=C	1675-1600
C-C	1300-700
Aromatic Ring	1000-900
O-O	900-800
C-Cl	850-650

Raman spectrum for TNT

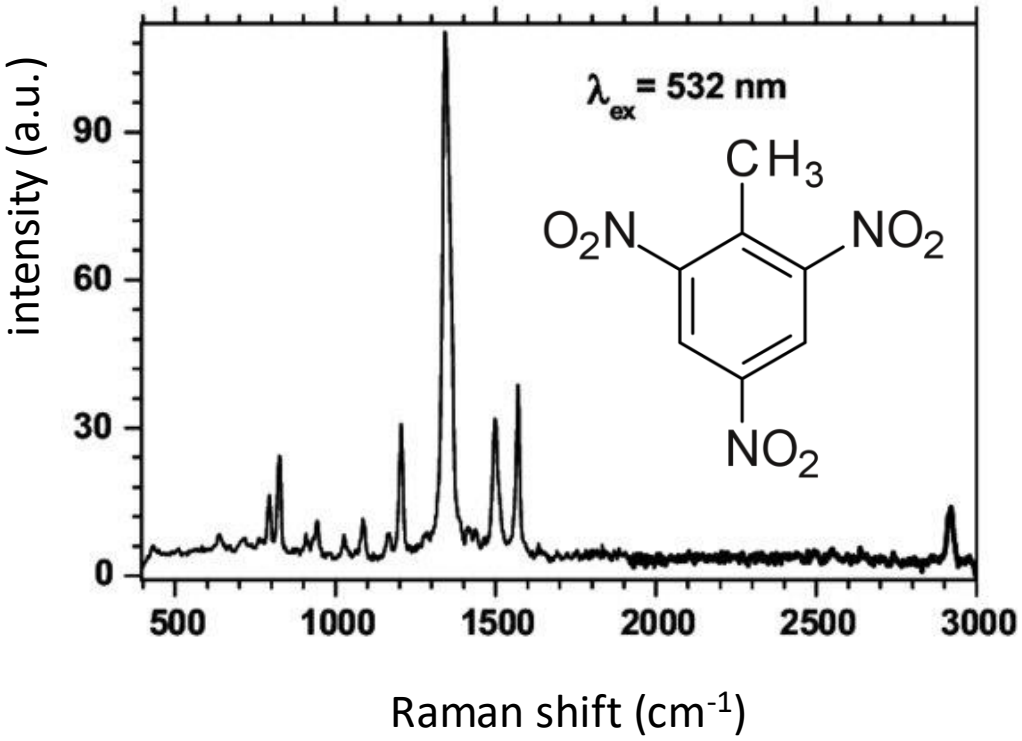

L. Nagli et al., Opt. Mater. **30** 1747 (2008)

X-ray fluorescence (XRF)

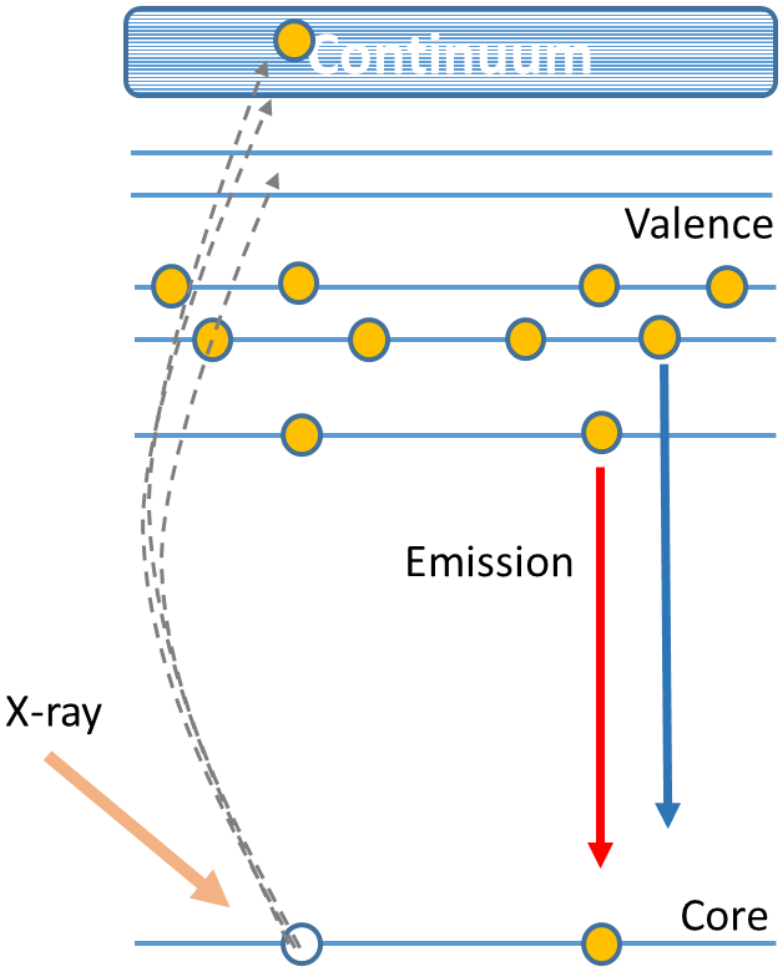

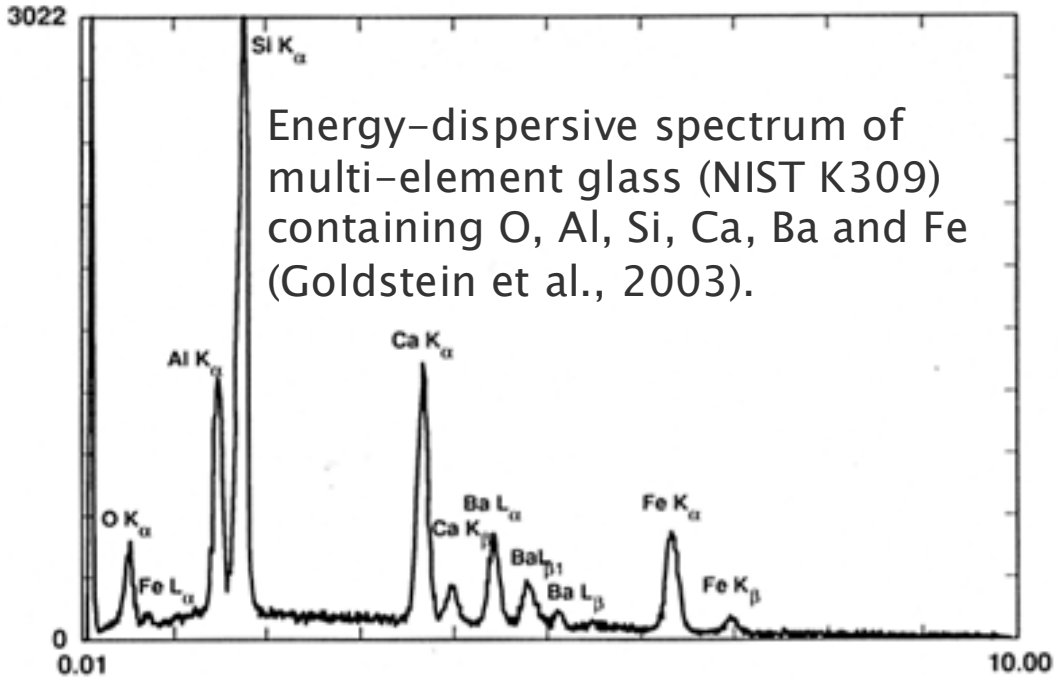

Energy-dispersive spectrum of multi-element glass (NIST K309) containing O, Al, Si, Ca, Ba and Fe (Goldstein et al., 2003).

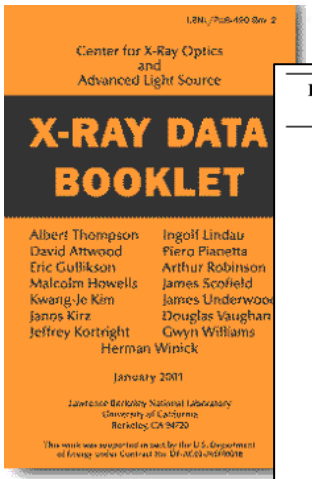

Energy (eV)	Element	Line	Relative intensity
54.3	3 Li	$K\alpha_{1,2}$	150
108.5	4 Be	$K\alpha_{1,2}$	150
183.3	5 B	$K\alpha_{1,2}$	151
277	6 C	$K\alpha_{1,2}$	147
348.3	21 Sc	Ll	21
392.4	7 N	$K\alpha_{1,2}$	150
395.3	22 Ti	Ll	46
395.4	21 Sc	$L\alpha_{1,2}$	111
399.6	21 Sc	$L\beta_1$	77
446.5	23 V	Ll	28
452.2	22 Ti	$L\alpha_{1,2}$	111
458.4	22 Ti	$L\beta_1$	79
500.3	24 Cr	Ll	17
511.3	23 V	$L\alpha_{1,2}$	111
519.2	23 V	$L\beta_1$	80

X-ray fluorescence (XRF)

Experiment at DORIS III

- Different paints contain different elements. For example, there is cobalt in «cobalt blue», mercury in «vermillion», antimony in «naples yellow», lead in «lead white».
- Using X-ray fluorescence one can measure the elemental map of a painting, and hence reconstruct the colors. Sometimes it reveals hidden pictures under the outer layer of the painting.

https://colourlex.com/project/x-ray-fluorescence/

X-ray fluorescence (XRF)

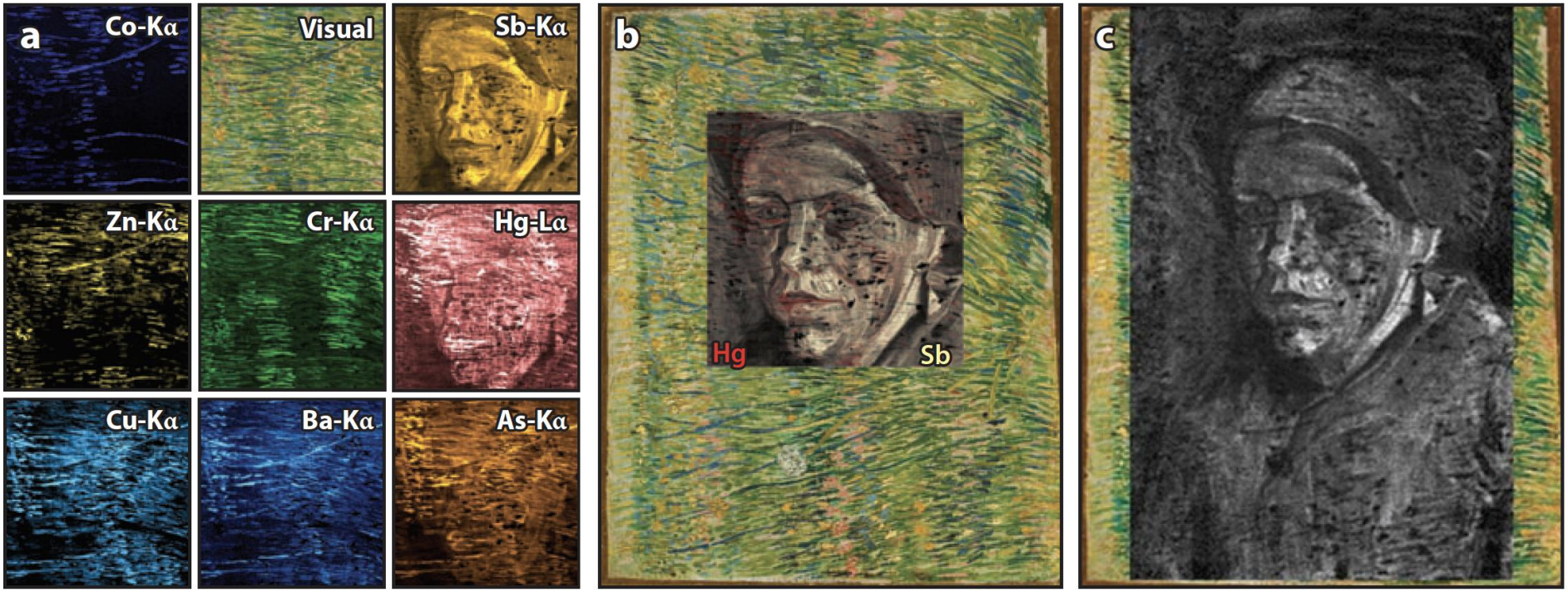

Figure 7

(*a*) Elemental maps recorded from Van Gogh's *Patch of Grass* (Kröller–Müller Museum, Otterlo, Netherlands) with macroscopic X-ray fluorescence (MA-XRF) scanning at beam line L (DORIS III synchrotron facility, Hamburg, Germany). (*b*) Reconstruction of the flesh tones of the hidden head of a woman, obtained by combining the Sb (*off-white*) and Hg (*red*) distributions mounted on a photograph of the painting. (*c*) Sb distribution obtained by mobile MA-XRF of (almost) the entire painting.

K. Janssens et al., Annual Review of Analytical Chemistry (2008) 6(1):399-425
J. Dik et al., *Anal. Chem.* 2008, 80, 16, 6436–6442

X-ray photoemission spectroscopy (XPS)

$$E_{kin}^{e} = \hbar\omega - E_{bind} - \varphi$$

E_{kin}^{e} - kinetic energy of an electron

$\hbar\omega$ – energy of an incident photon

E_{bind} - binding energy of an electron

φ – work function

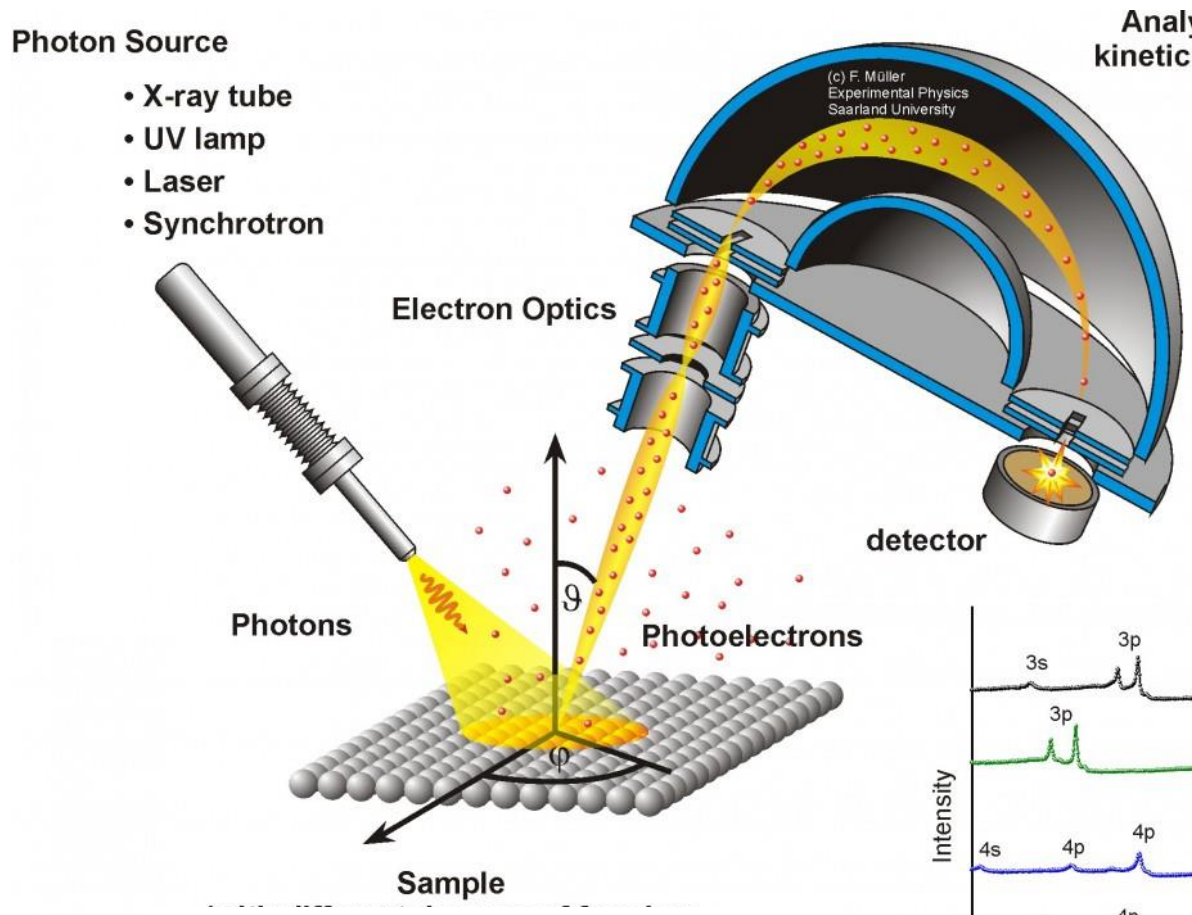

jacobs.physik.uni-saarland.de

Typical XPSpectra (of some metals)

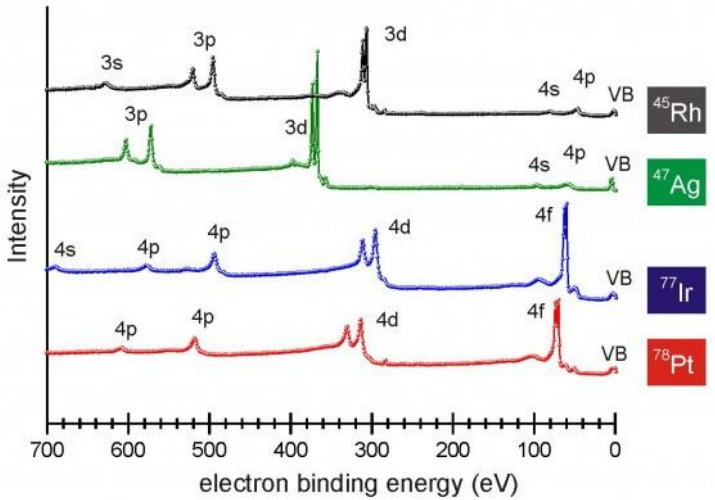

X-ray photoemission spectroscopy (XPS)

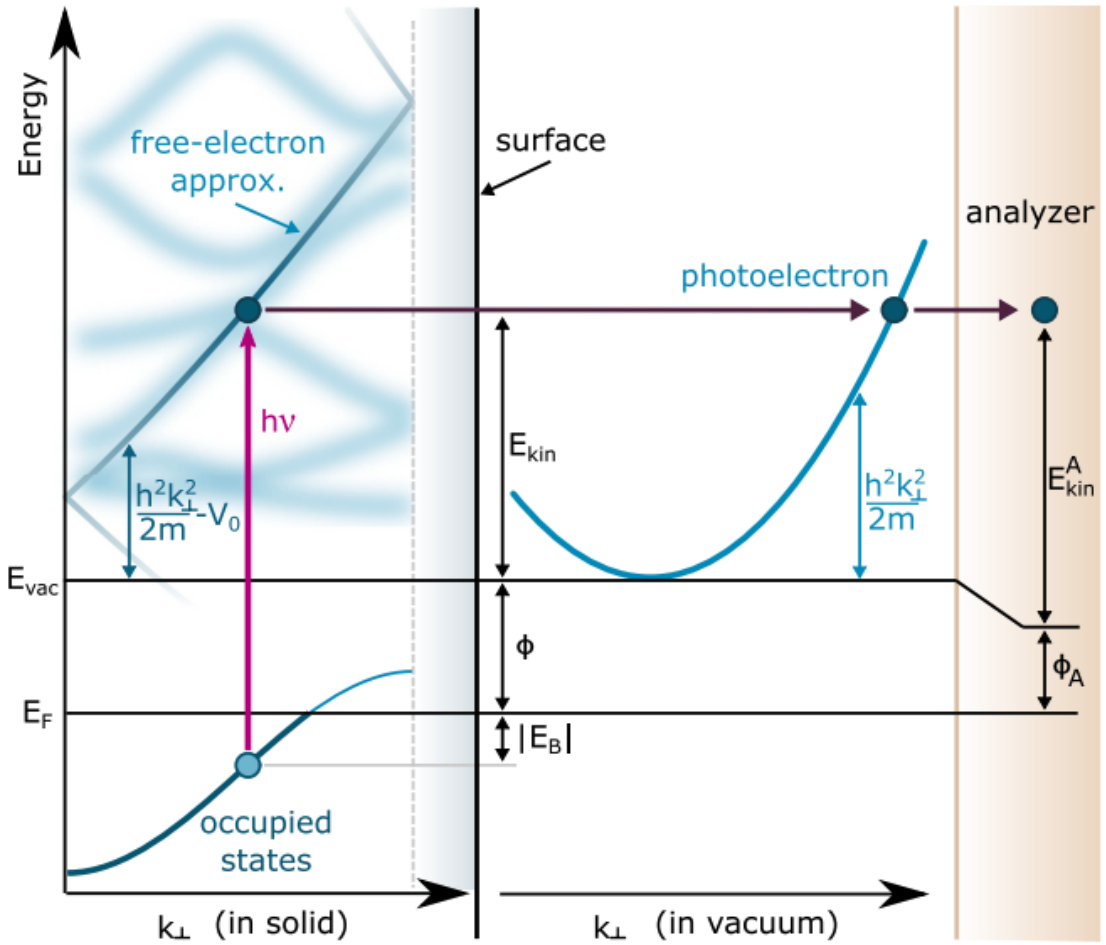

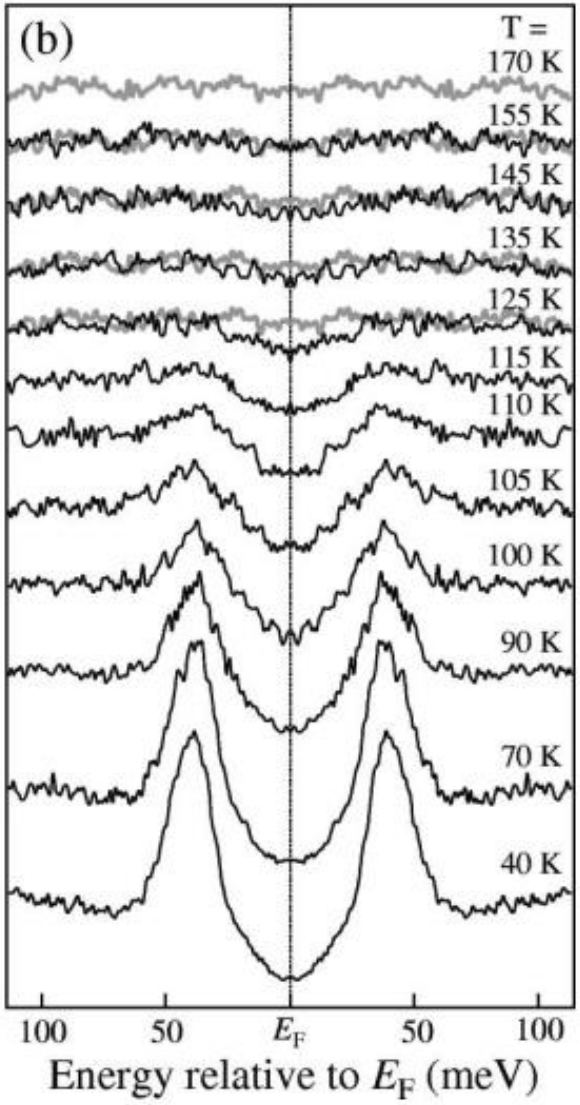

Damascelli, Hussein, Shen, Rev. Mod. Phys. **75**, 473 (2003)

Sobota, He, Shen, Rev. Mod. Phys. **93**, 025006 (2021)

Chemical shift

$$E_{kin}^{e} = \hbar\omega - E_{bind} - \varphi$$

It is possible to determine the oxidation state of the elements and even the type of chemical bonds.

E_{kin}^{e} - kinetic energy of an electron

$\hbar\omega$ – energy of an incident photon

E_{bind} - binding energy of an electron

φ – work function

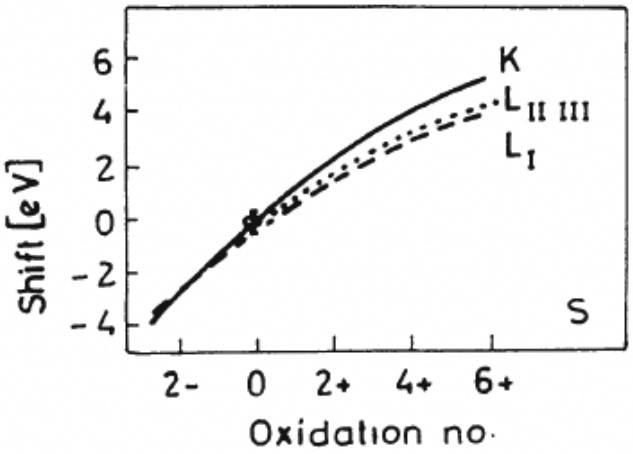

Chemical shifts of the K , L_1, $L_{2,3}$ levels of sulfur for different oxidation numbers, by photoelectron spectroscopy.

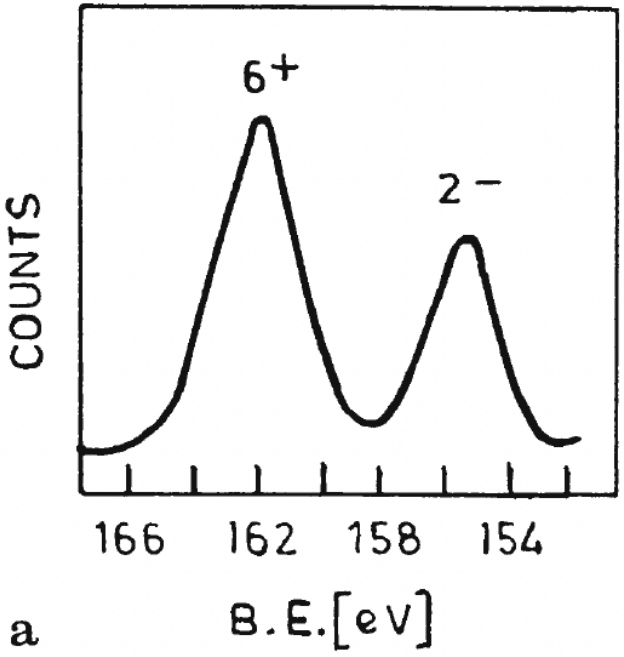

Sulphur spectrum from sodium thiosulphate by a photoelectron (2p level, Mg Kα line as source)

sodium thiosulphate

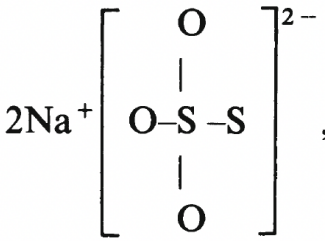

Agarwal, X-ray spectroscopy (1991)

Electron inelastic mean free path (IMFP)

$$I(d) = I_0 \exp\left(-\frac{d}{\lambda(E)}\right)$$

Decay of the electron intensity in the media due to inelastic scattering

$$\lambda[monolayers] = \frac{538}{E^2[eV^2]} + 0.41\sqrt{a[nm]E[eV]}$$

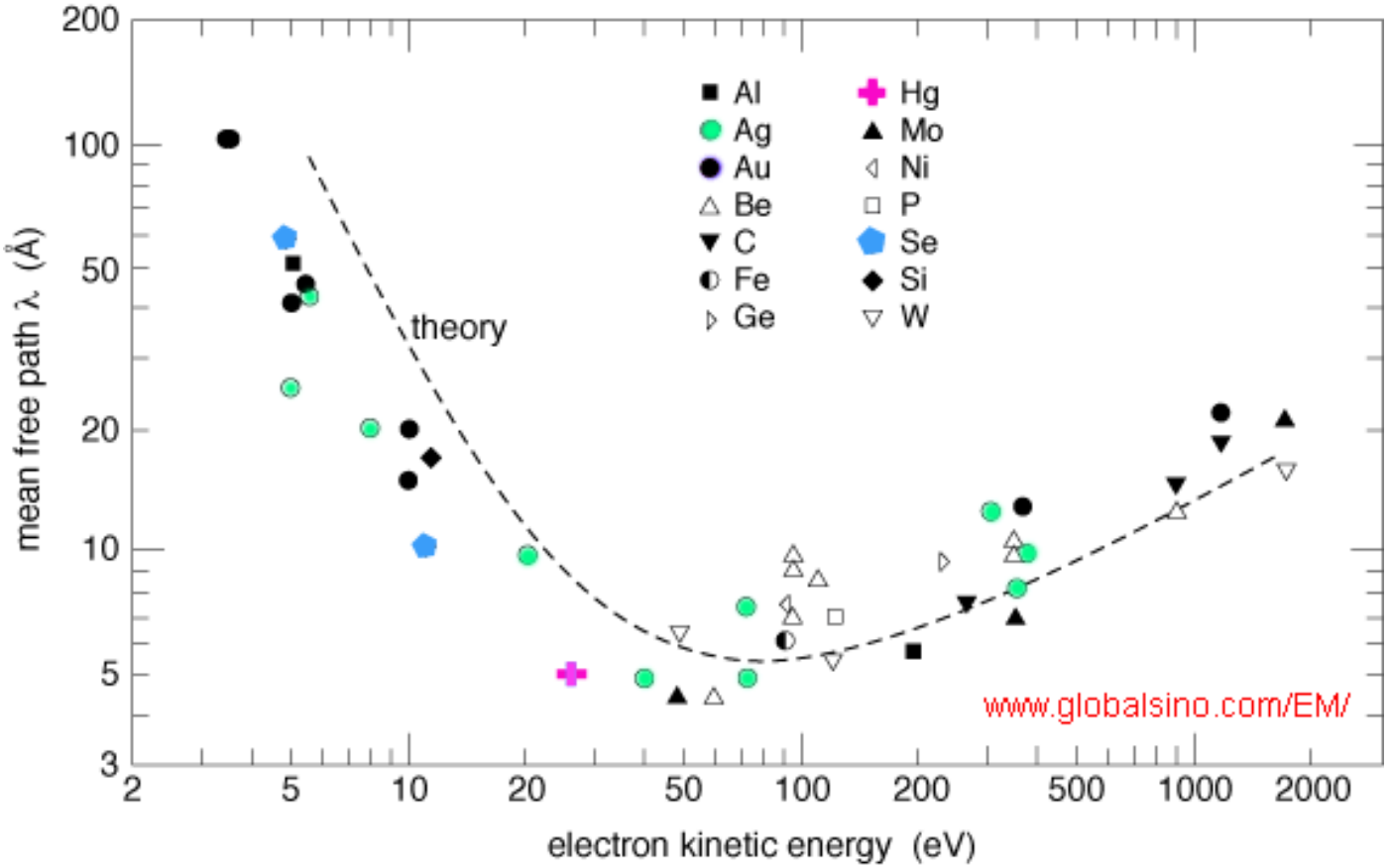

M. Seah and W. Dench, Surf. Interface Anal., **1** 2-11 (1979)

Angular-resolved photoelectron spectroscopy (ARPES)

- Both energy and momentum of photoelectron are measured
- One can reconstruct the band structure

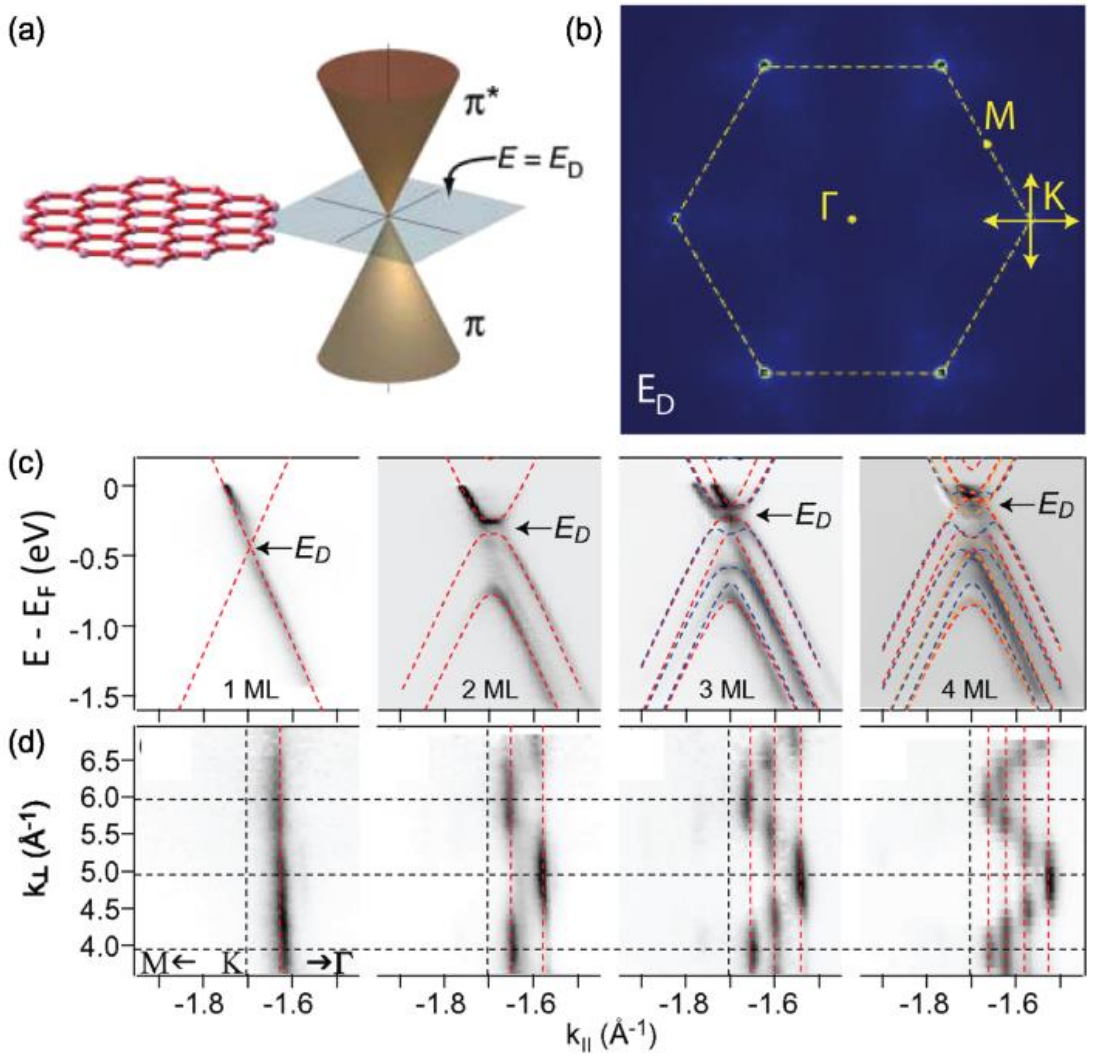

FIG. 31. Band structure of graphene. (a) Monolayer graphene and its computed Dirac cone band structure at the Brillouin zone corner. (b) Measured isoenergy contour at the Dirac point energy E_D of monolayer graphene. Adapted from Ohta *et al.*, 2006. (c) Band structure near the Dirac point and (d) $k_{||} - k_z$ Fermi surface maps for monolayer to four-layer graphene. Adapted from Ohta *et al.*, 2007.

Final remarks

Preparation:

- growth of thin films: statistical growth, layer-by-layer growth
- Formation of nanoclusters: islands (Wulff construction, diffusion-limited aggregation)
- Experimental techniques: PVD, CVD, lithography

Characterization:

- Scattering techniques: scattering from atomic layers of thin films, scattering from nanoparticles, scattering from surfaces and interfaces
- Microscopy: visible light, electron microscopy, SPM
- Spectroscopy: absorption & emission (VIS, UV, IR, X-ray)

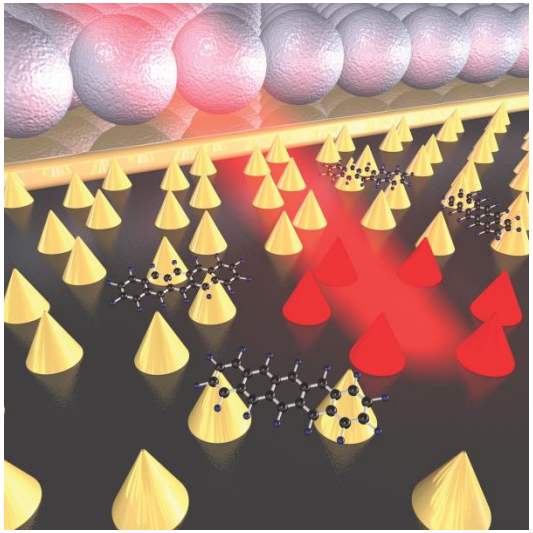

More on scattering in WiSe2026:

Advances topics in physics of condensed matter

Good luck at the exam!

Lectures: M. Fleischer, I. Zaluzhnyy; Exercises: R. Löffler